THE GEOLOGY, MINERALOGY AND CHEMISTRY OF THE GRAHAMSTOWN CLAY DEPOSITS

Thesis presented for the degree of
Master of Science in the
Department of Geology, Rhodes University

by JOHANN SMUTS
MARCH, 1983

Declaration

All work in this thesis is the original work of the author except where specific acknowledgement is made to the work of others.

Signed:

J. Smuts
'Evergreen'
Park Street
Boesmansriviermond 6190

March, 1983

Abstract

The Grahamstown clay deposits extend in a broad belt from $26^{o}23$ to $26°50$ East longitude and from $33^{o}15$ to $33^{o}22$ South latitude along two distinct geomorphological features, the Grahamstown Peneplane (650 m) and the Coastal Plain (520m). The clay deposits traverse four different lithologies including the Bokkeveld Shale, Witteberg Shale, Dwyka Tillite and Ecca Shale. The two planes invariably have a covering of silcrete which is also present over most of the clay deposits except where erosion has taken place.

X-ray fluorescence analysis shows that chemically there is a fairly wide variation between and within the deposits. The greatest variation is in the SiO_2/Al_2O_3 ratio which appears to be controlled by the parent lithology and to some extent by the amount of leaching. K_2O shows an increase in concentration with depth and therefore indicates the limits of hydrolysis and leaching and of the clay.

X-ray diffraction study shows the Peneplane and Coastal Plain deposits to be quite distinct. The Peneplane deposits consist of kaolinite, illite and quartz and the Coastal Plain deposits of kaolinite, illite, quartz and pyrophyllite. The presence of pyrophyllite is not fully understood as there is no indication of major faulting, metamorphism or pyrophyllite in the parent rock. The pyrophyllite most probably represents a transformation product of kaolinite.

The kaolinite from the various deposits shows a considerable variation in crystallinity in both the X-ray diffraction traces and electron photomicrographs. The most poorly crystalline kaolinites are from the Coastal Plain deposits and the difference in crystallinity is most probably due to differences in the degree of hydrolysis and the parent rock material in the case of the tillite.

Genetically all of the deposits are residual types generated by hydrolysis and subsequent leaching of micas and feldspars. The principal elements leached are silicon, iron and potassium. The hydrolysis and leaching took place over a long period of time in the flat lying areas of the Peneplane and Coastal Plain.

The deposits are exploited economically and the clay is used principally in the tile, pottery and whiteware industries with some usage in the paper, refractory and brickmaking industries. The price commanded by raw kaolin is not very high and as a result the clay industry in Grahamstown is not as viable economically as it could be.

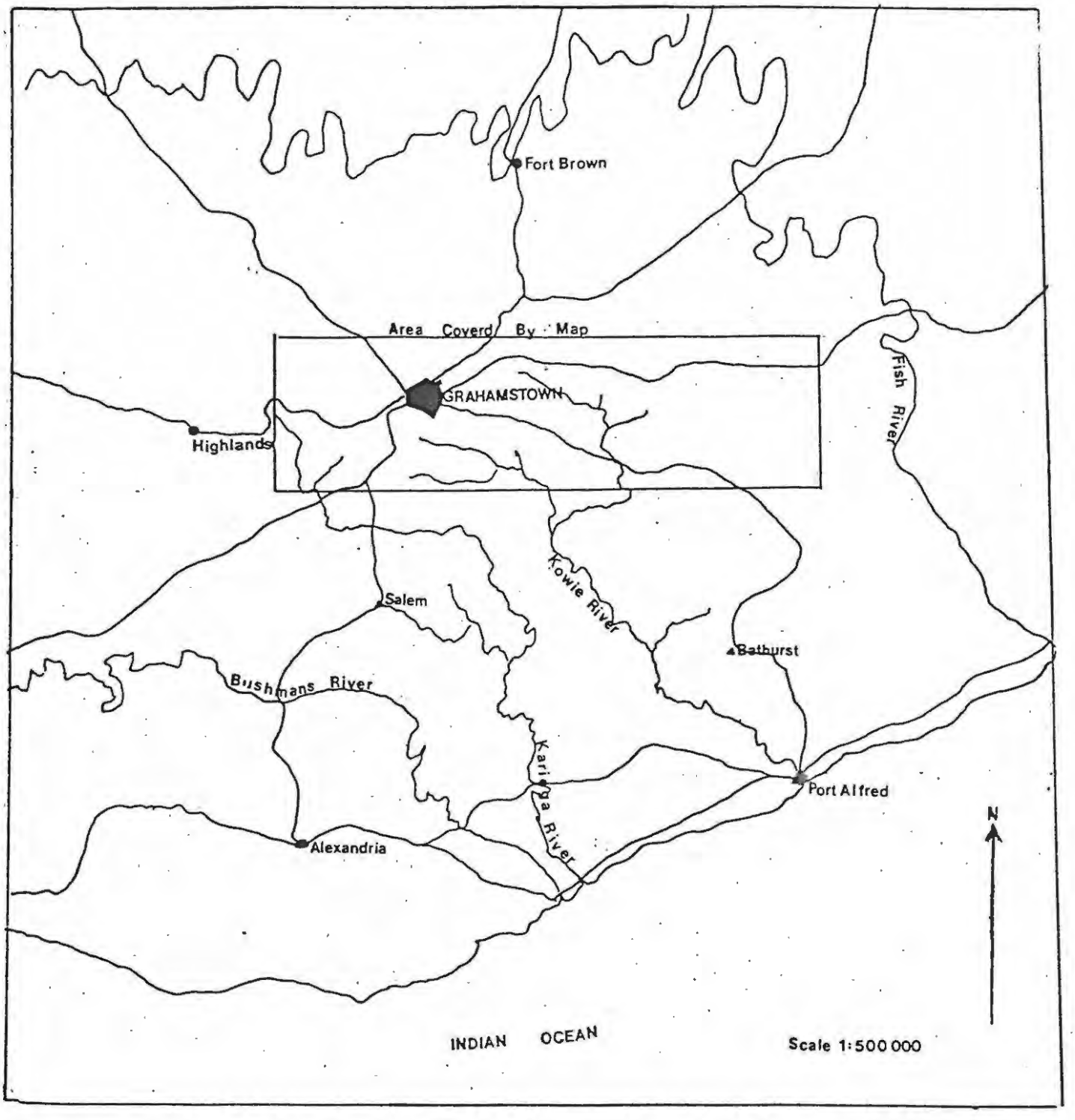

Figure 1.1 Locality Map showing the area covered by the geological map and overlay in the appendix.

CONTENTS

		Page No
ABSTRACT		
(1) INTRODUCTION		(1)
	General Geology	
	1) Physiography	1
	2) Stratigraphy	2
	3) Structure	5
	4) Previous Work	5
(2) DISTRIBUTION AND GENERAL FEATURES OF THE DEPOSITS		(8)
	Introduction	
	1) Avenue Park	8
	2) Melrose	10
	3) Crous	11
	4) Upper Gletwyn	13
	5) Wallace	13
	6) Strowan	14
	7) Palmer 1 and 2	15
	8) Other Deposits	17
		19
	Summary	
(3) CLAY MINERALS		(20)
	Introduction	
	1) Kaolinite	22
	2) Illite	24
	3) Pyrophyllite	26
(4) CHEMISTRY AND MINERALOGY		(28)
	1) Avenue Park	28
	2) Melrose	39
	3) Crous	43

4) Upper Gletwyn 47
5) Wallace 51
6) Strowan 52
7) Palmer 57

(5) DISCUSSION OF THE CHEMISTRY AND MINERALOGY (62)

Chemistry

1) Alkalis 62
2) Alkali-Earths 63
3) Iron 65
4) Trace Elements 67

Mineralogy 68

(6) GENESIS OF CLAY MINERALS (72)

1) Breakdown of Alumino Silicates 73
2) Mechanism of Breakdown 73
3) Solubility of the Elements 75
   (a) Alkalis and Alkali-Earths
   (b) Aluminium and Silicon
   (c) Iron
4) Neoformation or Transformation 78

(7) PYROPHYLLITE AND KAOLINITE STABILITY (80)

(8) GENESIS OF THE GRAHAMSTOWN CLAY DEPOSITS (83)

(9) ECONOMICS AND USES OF KAOLIN WITH REFERENCE TO THE GRAHAMSTOWN DEPOSITS (87)

1) XRF Techniques 89
(a) Sample Preparation
(b) Instrumental Conditions
(c) Standards and Correction Procedure
(d) Errors in Detection 91
2) Trace element determinations using XRF
(a) Sample preparation
(b) Instrument Conditions on Phillips PW 1410 X-Ray Spectrometer
(c) Standards and correction procedure
(d) Errors in detection
3) XRD Techniques 92
(a) Sample Preparation
(b) Instrumental Conditions
4) Electron Microscopy 93
(1) Morphology
(a) Sample preparation
(b) Instrument
(2) Electron Diffraction
5) Size Analysis 94

Acknowledgements 95

References cited 96

Map and Overlay

1. INTRODUCTION

The Grahamstown clay deposits are amongst the most extensive in South Africa. The deposits are strictly controlled by the topography and geomorphological history and traverse four different lithologies. All of the deposits are residual types and are similar in their mode of occurrence although differences do exist. The chemistry and mineralogy of these deposits distinguish them from any other known deposits in the country.

The aim of this thesis is to show the similarities and differences between the various deposits on the basis of their chemistry and mineralogy and to demonstrate the restraints placed on them by the topography and geology with the object of showing their genetic significance.

GENERAL GEOLOGY

1. Physiography

The city of Grahamstown lies approximately 130 km east of Port Elizabeth and some 40 km inland from the coast. The area in which the clay deposits were investigated extends from $26^{o}23'$ East to $26^{o}50'$ East and $33^{o}15'$ South to $33^{o}23'$ South.

Physiographically, Grahamstown is situated in a depression carved out of the Grahamstown Peneplane. The Peneplane forms a flat plain which is marked by the 650 m (2100-foot) contour and extends as a broad strip 8 km long and 2 km wide in an East-South-East to West-North-West direction. The plain is flanked on both the north and the south by prominent quartzite ridges and in the South East by the Coastal Plain which is marked by the Blaaukrantz and Botha's Rivers. These two rivers are both tributaries of the Kowie River, which flows in the Belmont Valley between the southern and northern ridges.

The southern ridge forms the escarpment between the Coastal Plain and the interior and extends from Highlands (730 m), through Mountain Drive (758 m), Signal Hill (738 m) and Stone's Hill (658 m) and is traversed by the Port Alfred road to Manley's Flats, which is at the level of the Coastal Plain. The ridge is dissected at one point by the Palmiet river which

forms Howieson's Poort.

The northern ridge extends from Botha's Hill (736 m) into the Kap River Mountains and Driver's Hill (864 m), on which the F.M. tower is situated, and is traced by the East London road. To the north-east of the Kap River Mountains is an extention of the Coastal Plain which slopes gently toward the Great Fish River in the east, where it is truncated by the Fish River Valley. Parts of the plain are capped by Fish River Silcrete. In the region of Driver's Hill the northern ridge forms the escarpment between the Coastal Plain and the Peneplane.

2. Stratigraphy

Grahamstown is situated along the contact between the Cape Supergroup and the Karoo Sequence with the Bokkeveld Group constituting the oldest group in the area and the Ecca Group the youngest. Large areas are overlain by silcrete which is much more recent.

The nomenclature of the stratigraphy in South Africa has recently been revised and boundaries of groups have been changed which has affected the area under review to a large extent. Previously, from the base were the Bokkeveld, Witteberg, Dwyka and Ecca Groups, in that order, with numerous subdivisions. The South African Committee for Stratigraphy (SACS),(1980) changed the nomenclature and divided each of the groups into a number of formations. The main changes are that the Bokkeveld Group has been divided into two subgroups, the lower Ceres and upper Traka consisting of six and three formations respectively. The boundary of the Bokkeveld and Witteberg Groups is controversial as it is difficult to define boundaries on a purely lithostratigraphic basis for areas as large as the Karoo Basin where there are lithologic variations from area to area at the same statigraphic horizon. Fossil evidence is apparently not abundant enough to be used effectively.

The Witteberg Group constitutes the uppermost group of the Cape Supergroup and is divided into the Weltevrede and Witpoort Formations at the base, and the Lake Mentz (3 formations) and the Kommadagga (4 formations) Subgroups towards the top. The Dwyka Formation, formerly the Dwyka Group, forms the contact between the Cape Supergroup and Karoo Sequence, (formerly the Karoo Supergroup). The Dwyka has been divided and the former Upper Dwyka Shales now form the base of the Ecca Group and

are named the Prince Albert Formation. The White Band which was previously regarded as the contact between the Dwyka and Ecca Groups is now called the White Hill Formation. The changes in the nomenclature are summerised in the table below, table 1.1.

The silcrete horizons, Grahamstown, Fish River and Coastal Plain silcretes are now grouped together as the Grahamstown Silcrete Formation although they represent different geomorphological horizons and very possibly different ages. This is another problem of over emphasis on lithostratigraphic classification.

The axis of greatest thickness for the Bokkeveld, Witteberg, Dwyka and Ecca all pass through Grahamstown. The Bokkeveld (750 m) which is lower Devonian in age is composed of alternating sandstones and shales and is conformably overlain by the Witteberg. The Witteberg (730 m) is Upper Devonian to Lower Carboniferous in age and consists predominantly of ortho-quartzites but becomes more argillaceous towards the top of the sequence. The Dwyka (450 m) is Permo-Carboriferous in age and is entirely composed of the tillite which is a massive blue-black rock which has a speckled appearance due to inclusions of allogenic fragments. The Ecca, primarily the Lower Ecca Prince Albert Formation is fine grained sediment which is conformable on the tillites and is overlain by the White Hill Formation, formaly the White Band, which typically weathers to a white colour and forms a very distinct marker horizon. The White Hill and overlying Collingham Formation are the uppermost formations of the Karoo Sequence which outcrop in the area under review.

The only other rock type which is considered in relation to the clay is silcrete, which is probably late Tertiary in age in the Coastal Plain regions and possibly Miocene in the Peneplane area although the age relationships are not known.

Table 1.1 Stratigraphy of the Grahamstown Area

Group	Subgroup	Formation	Previous Nomenclature
		Grahamstown Silcrete	
Ecca		Fort Brown (Sh)	Middle Ecca
		Ripon (Sst)	
		Collingham (Sh)	
		White Hill (Sh & Chert)	White Band
		Prince Albert (Sh)	Upper Dwyka Shale
		Dwyka (Tillite)	
Witteberg	Kommadagga	Dirkskraal (Sst)	
		Soutkloof (Sh)	Upper Witteberg
		Swartwaterpoort (Sst)	
		Miller Diamictite	
	Lake Mentz	Waaipoort (Sh)	
		Floriskraal (Sst)	
		Kweekvlei (Sh)	
		Witpoort (Sst)	Witteberg Quartzite
		Weltevrede (Sst & Sh)	Lower Witteberg
Bokkeveld	Traka	Sandpoort (Sh)	
		Adolphspoort (Silt St)	
		Karies (Sh)	
			Bokkeveld
	Ceres	Boplaas (Sst)	
		Tra-Tra (Sh)	
		Hex River (Sst)	
		Voorstehoek (Sh)	
		Gamka (Sst)	
		Gydo (Sh)	

Sh - Shale, Sst - Sandstone

3. Structure

A broad syncline underlies the Grahamstown area. The axis of the major syncline follows the general strike direction which is east- south-east to west-north-west. The two Witteberg Quartzite ridges previously mentioned form the limbs of the syncline and are both anticlinal structures themselves. The major syncline has a plunge towards West-North-West and the axis is traced by the outcrop of the Ecca Shale, Prince Albert Formation.

The northern limb of the syncline has a general dip of 10^{o} towards the south-west but locally the actual contact between the Witteberg Quartzite and the Shale is in the order of 60^{o}. The steeper dip is due to tighter folding which is localized along the contact. The southern limb has a steeper general dip resulting in narrower outcrops in that region.

All the folding in the area predates the formation of the Peneplane and represents expression of the Cape Folded Belt which had its origin in early Jurassic times. Very little major faulting is evident in the area.

4. Previous Work

Reference to the Grahamstown clay deposits was made by Schwarz (1919) in the paper entitled 'A Report on the Grahamstown Brickfields'. These deposits were, however, known for a long period before this time as there was already an extensive production of bricks by 1875 (Mountain, 1931). It has also been reported that the local Xhosa tribe has been using the local clay deposits since the early 1800's for cosmetic and decorative purposes.

The first work which was done on the deposits besides various analyses by independent brick companies was that by Blignaut (1928) in an unpublished M.Sc. thesis. The thesis embraces a description of the local geology and brickfields, two analyses of the brickfield clay and a report on the grain size, shrinkage on firing and plasticity of this clay. The mineralogy is described as being quartz, feldspar and mica with some amorphous material. The mica was thought to be of secondary origin and the clay genesis due to weathering of the Lower Dwyka Shales (Upper Witteberg Shales) and Dwyka Tillite.

Twenty-one major elements analyses were published by Mountain (1931), six of these having been done by Adams (1918) for a brick company. The analyses included one analysis of the 'black shale' underlying the clay deposit at the brickfields. An extreme weathering process was suggested as the cause of leaching which removed the soluble elements. This resulted in the formation of the clay material with silica being deposited at the surface in the form of surface quartzite.

Frankel and Kent (1937) published a paper dealing with the Grahamstown silcretes. They give some chemical considerations as to the formation of the silcrete and evidence that the silica is derived from the underlying rocks. The argument given for the solution of the silica is the presence of metal salts. The silica was transported in colloidal form and precipitated at the surface after capillary action had carried it there. The soluble elements were said to be leached during alternating wet and dry seasons. The presence of ferricrete lenses in the silcrete was used as supporting evidence of a silica hydrosol with a negative charge and a ferric oxide hydrosol with a positive charge. These two sols were then said to coprecipitate at the surface. Colloform structures in the silcrete were evidence of a rhythmic migration during the wet and dry seasons. NaCl, wind blown from the sea, was said to assist the precipitation of the silica in the surface soil.

Bosazza (1946) made several analyses of the tillite clay and the Dwyka Shale (Ecca Shale) clay and compared them to tillite from Natal. The genesis was reported to be due to 'quiescent leaching'. He proposed a scheme as follows:

Silcrete and Ferricrete Residual White Clay	migration by capillary action
Yellow Weathered Residual Clay Dwyka Tillite and Shales	hydrolysis and solution

A number of reports for SAPPI were written by Eales (1962-1975). Most of the reports are on the Upper Gletwyn Deposit and describe the grit content, whiteness and ore reserve estimates. The report by Eales (1975) includes chemical analyses of various size fractions of clay and grit, and a brief account of the mineralogy is also given.

Murray and Smith (1973) published an abstract on 'The Grahamstown Kaolin Deposit'. The abstract refers to the mineralogy of the tillite clay at the Palmer Quarry and also Liesegang rings which they refer to as root casts. The mineralogy is reported as kaolinite, degraded illite-muscovite, quartz and anatase. The illite showed slight expansion with ethylene glycol.

The National Building Research Institute has published a number of information sheets on the various Grahamstown clays. Included are the Wallace, Webber, Strowan, Palmer, Gletwyn and Blake's Deposits. Each information sheet has a listing on the chemistry, mineralogy and physical properties including thermal expansion, plasticity, casting, soluble salts, firing, colour and grain-size distribution.

Schmidt (1976) classified the various deposits into more plastic types containing organic material and less plastic ones. Included in the plastic types are the Wallace, Webber and Crous deposits. Less plastic types are Palmer's, Blake's, Gletwyn and Avenue Park deposits. He also describes the deposits as being dependent on the formation of the Grahamstown Peneplane and that they sometimes contain feldspar and pyrophyllite.

2. DISTRIBUTION AND GENERAL FEATURES OF THE DEPOSITS

The Grahamstown clay deposits are distributed in broad belts at specific altitudes. The deposits are similar in appearance although they traverse four different lithologies. In detail there are differences which are readily recognisable.

Silcrete is ubiquitously associated with the clay deposits but there are differences in both thickness and texture of the clay at the various localities. Broadly, the clays show textural, structural and colour similarities, but there can be large variations within and between the deposits which are due to stratal changes in the parent rock bodies. The amount and type of iron oxide staining and grit material within the deposits is greatly variable over short distrances. Within deposits colour can grade from white to grey to black and clay may be interbedded with shale and sandstone horizons.

1. Avenue Park Deposit 26°25 East 33°22 South

Avenue Park is situated 20 km to the west of Grahamstown and 3 km to the north of the Port Elizabeth road. The quarry is at the base of the Highlands ridge at an altitude of 495 m. The form of the deposit is that of a relict conical hill on the Coastal Plain with the quarry being excavated in the central part. The deposit borders on the contact between the Bokkeveld Group and the overlying Witteberg Group.

Blocks and boulders of Coastal Plain silcrete form part of the 1-metre overburden which covers the deposit. The silcrete has rounded boulders of Witteberg Quartzite up to 50 cm in diameter embedded in a siliceous matrix. Directly beneath the overburden is the clay body which is grey in colour and shows joint and bedding planes of the original rock body. There is heavy iron oxide staining along the parting planes but for the most part the staining is not penetrative. In the western part, however, there is a broad band of penetrative iron oxide staining which discolours the clay.

The band of discoloured clay is approximately 10 m thick and its position appears to be structurally controlled. Tight folding, kink folds and shears are exposed in the western part of the quarry in the region of a drainage channel. The iron oxide staining and structural features

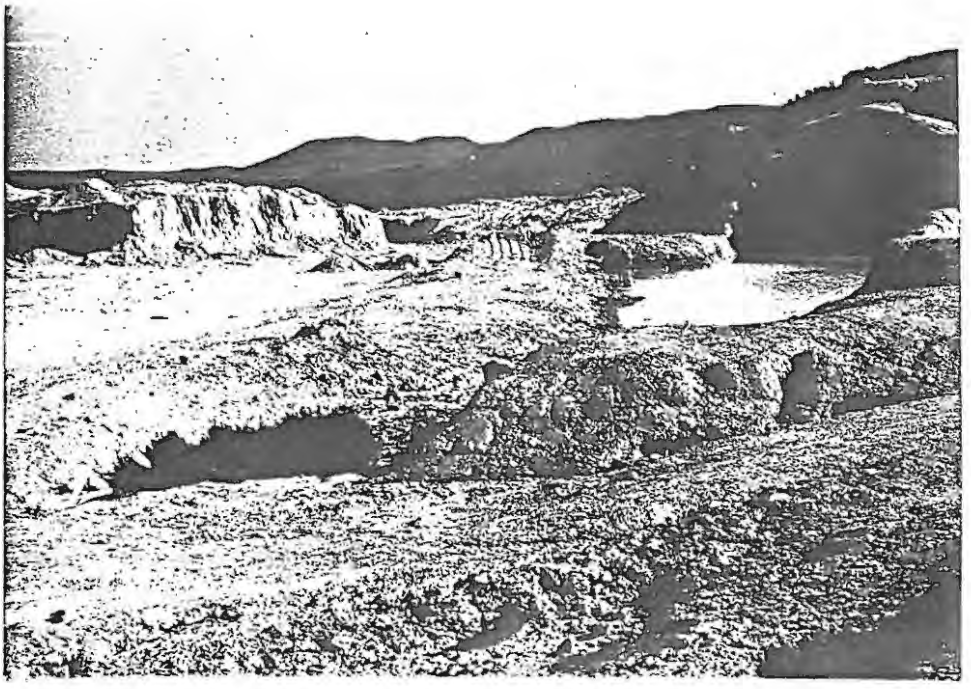

Plate 2.1 The Avenue Park deposit viewed from the east showing the Highlands ridge in the background. The anticlinal structure is shown just above the water.

Plate 2.2 Penetratively stained clay in the shear zone near the drainage channel. The tight folding and vein quartz are also evident.

can be traced along strike and are exposed in the southern area of the quarry. Vein quartz is associated with the shearing (see plate 2.2).

On the northern side of the quarry a broad anticline is exposed. The northern limb of the anticline forms the contact with the Witteberg Quartzite. The actual contact is 10 m behind the northern quarry face. There is a sharp contact between the clay and a friable siliceous and micaceous rock which has been deeply weathered and partially kaolinised (see plate 2.1).

In the southern region of the deposit in the proximity of a storage shed a number of prospecting pits were dug. Manganese staining which is dendritic in form and dark blue in colour is conspicuous in the clay in this region. The clay in the south is of an inferior quality at the surface but improves with depth.

In the central part of the quarry a prospecting pit was dug to a depth of 10 m below the present floor and the clay in the base of the pit appeared to be of good quality with regard to both colour and texture. The quarry floor is 7,5 m below the original surface which makes a total depth of at least 17 m for the deposit. The depth of the kaolinisation extends well below this level to approximately 25 m.

Two kilometers to the east of the deposit is a similar conical hill. On inspection this hill proved to be composed of the same friable rock to the north of the main deposit and probably represents the same lithological layer which is higher stratigraphically than the altered rock forming the clay body. Two other zones of kaolinisation are exposed in the area. One is in a road cutting on the Kenton-on-Sea road, 2 km from the junction with the Port Elizabeth road and the second is in a cutting 24 km west of Grahamstown on the Port Elizabeth road. Both of these exposures are of poor quality material.

2. Melrose Deposit $33^{o}20'$ South $26^{o}39'$ East

The Melrose deposit is 8 km South-East of Grahamstown and 3 km from the junction of the Manley's Flats and Port Alfred roads. A few metres to the east of the road is the Port Alfred railway line which follows the Belmont Valley. The deposit has not been exploited but is exposed along the road cutting.

The clay is situated close to the contact of the Witteberg Quartzite and the Witteberg Shales and is at the base of the Witteberg ridge which the Port Alfred road follows. The surface of the deposit is steeply inclined towards the railway line and has scattered boulders of typical Coastal Plain silcrete similar to that found at Avenue Park. The altitude of the deposit is between 510 m and 490 m.

The clay is dark grey in colour and has a soapy feeling. Thin beds of unaltered dark micaceous shale up to 2 cm in thickness are interbedded with the clay. Iron staining is apparent along the joint surfaces and bedding planes. Due to very poor exposure the structure is not very well defined but some folding is apparent. The extent of the deposit is difficult to discern in both depth and area but along strike it is exposed for a least 250 m. Generally speaking, although this clay appears to be similar to that of the Avenue Park deposit with regard to both colour and texture, it is of an inferior quality.

3 Crous Deposit $33^{o}16,5'$ South $26^{o}52,5'$East

The Crous deposit is located just north of the East London road, 24 km east of Grahamstown, on the high ground overlooking the Fish River Valley. The deposit is situated on a narrow synclinal infold of Witteberg Shale. The outcrop of the shale is only 60 m in width at surface and is truncated by a ravine in the north.

The deposit is capped by a 2 m layer of Fish River silcrete which is similar to the Coastal Plain silcrete and forms the main part of the overburden. Directly below the silcrete is a thin layer of lateritic material which grades into a hard brittle white clay which was found to be very siliceous. The siliceous material grades into a pure white, soft, grit-free clay. The clay shows iron oxide staining along the joint and bedding plane partings, but the staining is not penetrative. Cylindrical channels of red iron oxide staining up to 2 cm in diameter cut through the clay body in the northern section of the quarry. These channels are due to the penetration of roots from the plants on the surface and are what were described as root casts by Murray and Smith (1973).

The clay is easily mined in blocks formed by the intersection of the bedding and joint partings. This affords easy hand cobbing to remove the

Plate 2.3 The Crous deposit showing the bedding and joint surfaces with iron oxide staining.

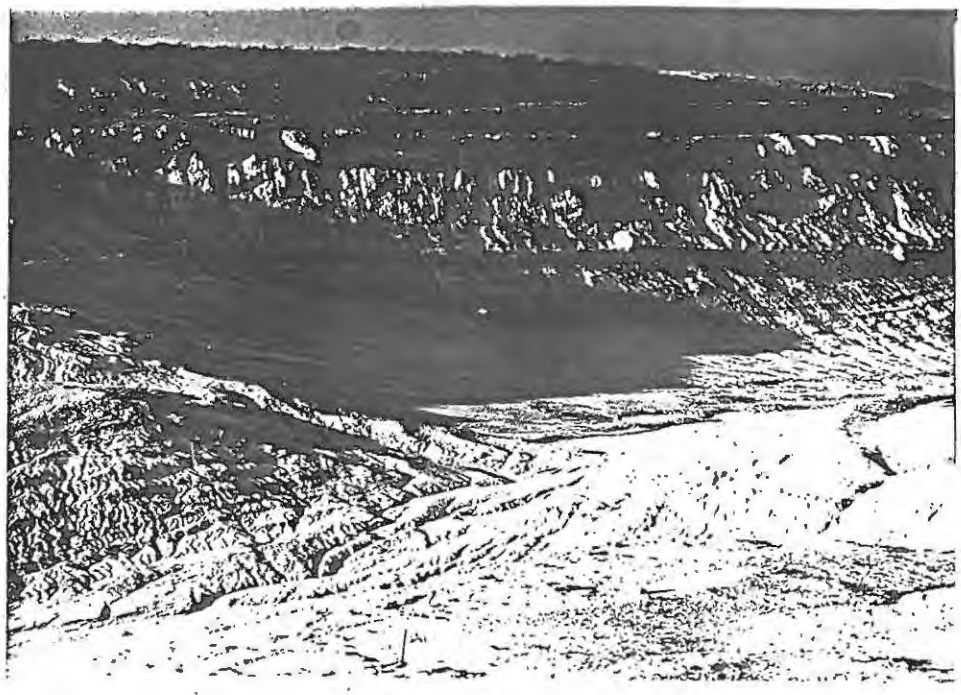

Plate 2.4 The Upper Gletwyn deposit showing the two distinct silcrete horizons on the eastern side of the quarry.

thin layers of iron oxide (see plate 2.3).

The deposit has not been fully evaluated, but it appears to extend for at least 800 m along strike and a drill hole put down in the central part of the quarry reputedly proved a depth of at least 40 m of clay material. Overall the clay in the Crous deposit is of good quality and grit-free in the whole of the working area.

4. Upper Gletwyn Deposit 33°16,5' South 26°36,5' East

The Upper Gletwyn deposit is 6 km to the east of Grahamstown and 1 km to the south of the East London road. The deposit is on the southern lip of the Grahamstown Peneplane on the edge of the Belmont Valley and is situated within Witteberg Shale. The altitude of the deposit is 630 m.

There are two distinct silcrete horizons exposed on the eastern quarry face. The upper silcrete is 1 m thick and lies directly beneath the soil cover. Below the upper silcrete lies a lateritic layer which grades into a layer of poor quality grey clay, 3-5 m thick. Below the clay layer is a silcrete terrace which is up to 2 m thick (see plate 4). The silcrete body is a massive unit at the top and grades into a blocky type which becomes nodular and pebbly towards the base and then grades into a cream-coloured clay which is hard, brittle and siliceous. The clay below this is the white soft clay of the main body. Towards the top of the clay body there are small, matchhead-sized grains of authigenic quartz which are absent at greater depth.

The Upper Gletwyn deposit is broadly anticlinal with an axial plane parallel to strike. The beds dip towards the west at an angle of 30-40°. The eastern limb is not exposed. There are lithological controls on the type of clay. In the western part of the quarry the clay is friable and micaceous and has a substantial quartz grit content. Thin beds of unkaolinised micaceous shale are exposed on the western side of the quarry and cross-cutting veins of quartz are evident. There is very little iron oxide apparent in the Gletwyn deposit. Generally speaking the clay has a good whiteness but does not appear to be as plastic as that of Crous' deposit.

5. Wallace Deposit 33°16´ South 26°36´ East

The Wallace deposit is 2 km north of the East London road and 6 km to

the east of Grahamstown on the farm Collingham which is now owned by Moss and Son. The deposit borders on the Botha's River and is situated on a lenticular synclinal infold of Witteberg Shale.

There is a thick overburden of silcrete to the south of the deposit. The clay is of three distinctive types. The statigraphically highest is a cream coloured friable type with a low grit content. This clay is also not as plastic as the other two types found in the deposit. The second clay type is a grey plastic type of clay which is grit-free. This clay also shows distinctive bedding planes. The third type of clay which is stratigraphically lowest is a black clay which is very plastic. The black colour is caused by a high content of organic matter.

The deposit has been mined in a haphazard fashion but generally along the strike direction east-south east to west-north-west. Open folds on a wavelength of $\pm$ 10 meters are apparent in the west of the quarry and a few smaller scale symmetrical folds are present. Thin beds of shale and quartzite are interbedded with the clay in places. Towards the base of the deposit is a bed of khaki-coloured clay.

The surface of the deposit is at an altitude of 630 m and is inclined to the Botha's River (600 m) to the north. The full extent of the deposit is not known because of the thick silcrete cover but it appears to be at least 300 m wide and extends for at least 1 km along strike. The clay has reputedly been proven to a depth of 35 m by drilling. The western edge of the clay extends into Webber property.

6. Strowan Deposit $33^{o}17'$ South $26^{o}29'$ East

The Strowan deposit is 3 km north of Grahamstown and 800 m to the west of the Cradock road. The deposit is in Ecca Shale, Prince Albert Formation (Upper Dwyka Shales) and approximately on the axis of the main synclinal structure which dominates the Grahamstown area. The width of the outcrop of Ecca Shale is approximately 600 m at this point.

The quarry is on the side of a slope which descends from the Cradock road to a small stream in the west, which forms the headwaters of the Palmiet River. Silcrete capping is evident only at the top of the deposit at the level of the Grahamstown Peneplane. For the most part the surface of the deposit has only a thin veneer of soil with scattered boulders of silcrete

(see plate 2.5.).

There is no evidence of tight folding or shearing in the deposit. Anticlinal and synclinal open folds are exposed on the northern face of the quarry. There does not appear to be any lithological control on the clay or any evidence of lithological variation. The clay is relatively grit-free except for vein quartz which cuts across the body.

Iron oxide is concentrated in pockets which facilitates easy selective mining. Orbicular concretions of manganese and iron oxides are scattered throughout the deposit.

The quarry is in the form of a series of ten benches which have been cut into the slope. The depth of the quarry is approximately 25 m and clay has been proven to a depth of 15 m below the quarry floor and extends for at least 400 m along strike. The Strowan deposit is the largest single quarry in the Grahamstown area and is adjacent to the Coronation and Blake's quarries.

7. Palmer 1 and 2 Deposits $33^{o}17,5'$ South $26^{o}36$ East

The Palmer deposits are on opposite sides of the Manley's Flats road, 2 km to the South East of Grahamstown on the farm Elandskloof. The Palmer deposits are both at an altitude of 620 m. The Palmer 1 deposit is on the edge of the peneplane and the Palmer 2 deposit is on an outlying remnant separated from the plane by a tributary of the Blaaukrantz River.

The deposits are both situated on Dwyka Tillite. There are no bedding features because of the massive nature of the parent rock. The clay bodies both have a distinctive silcrete capping which is 1 m thick. Directly below the silcrete is the white clay which is brittle and siliceous. Below this is the clay body which shows variations in colour according to the extent of the leaching and the presence of iron oxide. The clay often reflects the bluish tinge of Dwyka Tillite and this becomes more pronounced with increasing depth. The clay is gritty and shows relict structures of fragments of feldspar of the original tillite. The Palmer 1 deposit is highly fractured and the fractures are filled with pure, exceptionally white clay which is of secondary origin (see plate 2.6).

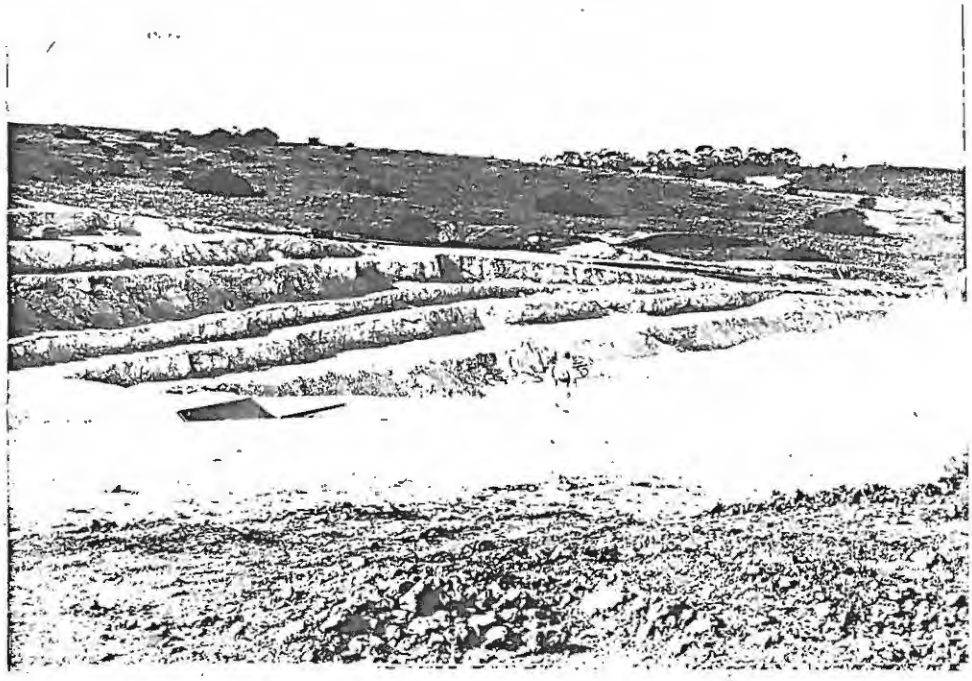

Plate 2.5 The Strowan deposit viewed along strike showing the extent of the mining operation and the Coronation deposit in the background.

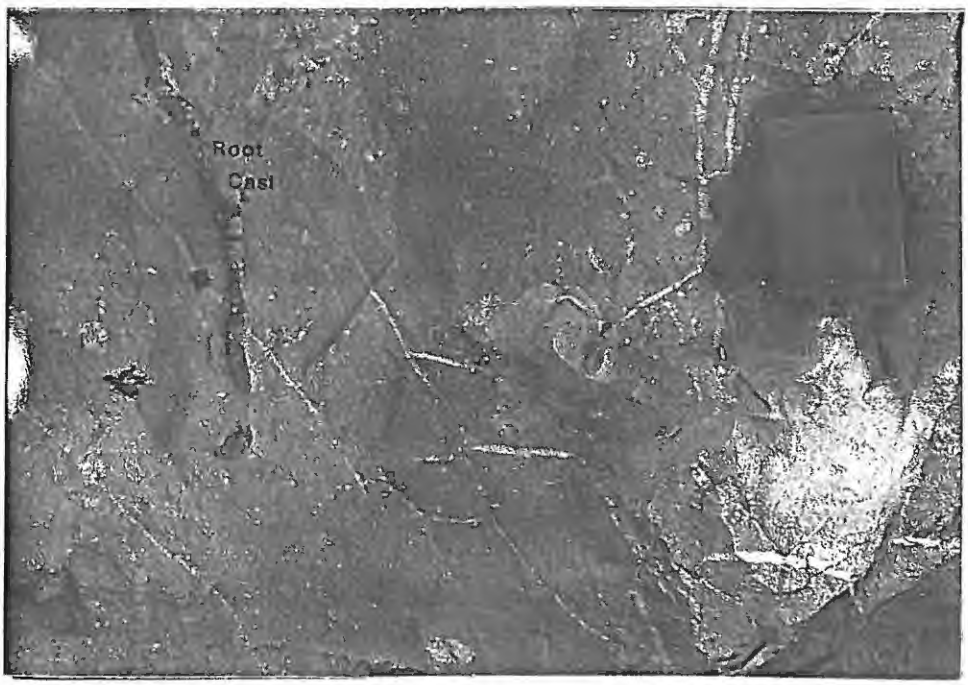

Plate 2.6 The Palmer clay showing the 'ghost' allogenic fragments and fracture fillings which are whiter in colour. Also note the root cast on the left side of the photograph.

Parting surfaces are coated with iron oxide, and Liesegang rings occur around cavities created by the penetration of roots which are prevalent in the deposits. Some fragments of Witteberg quartzite are also present in the clay. The clay body is at least 30 m thick but with increasing depth the clay reflects the colour of the parent rock to a greater extent.

The quality of the Palmer clay, in terms of whiteness, is probably the best in the Grahamstown area but it is necessary for it to be washed before use because of high grit content.

The extent of the Palmer deposits is considerable and a large number of prospecting pits have been dug in the surrounding area on the edge of the peneplane. The actual extent of the deposits to the north is difficult to discern because of the considerable silcrete cover.

8. Other Deposits

There are several other deposits in the Grahamstown area. The Webber deposit, which has been previously mentioned, is in close proximity to the Wallace deposit and is very similar in most respects to the statigaphically lower Wallace clay. The deposit has not been worked as extensively as the Wallace deposit and the part which is exposed appears to be a good quality ballclay type. The Webber deposit has the disadvantage of having a very thick, massive, silcrete covering which makes mining difficult (see plate 2.7). Very fine bedding structures can be seen in the clay and small iron oxide spots are evident.

Two other deposits in the vicinity of Strowan quarry are Burnt Kraal, which is on the opposite side of the Bedford Road and situated on Dwyka Tillite, and the Coronation deposit which is along strike from Strowan, and very similar in character to it.

The only other clay occurrence which is of interest in the present study is that just below P J Olivier School. This is probably the oldest working in the area but is almost completely worked out. The deposit is anomalous in that is is at an altitude of 570 m which does not correlate with any of the other major deposits.

The deposits described are not the only ones present in the area. Kaolinisation is almost continuous along the 630 m and 500 m contours

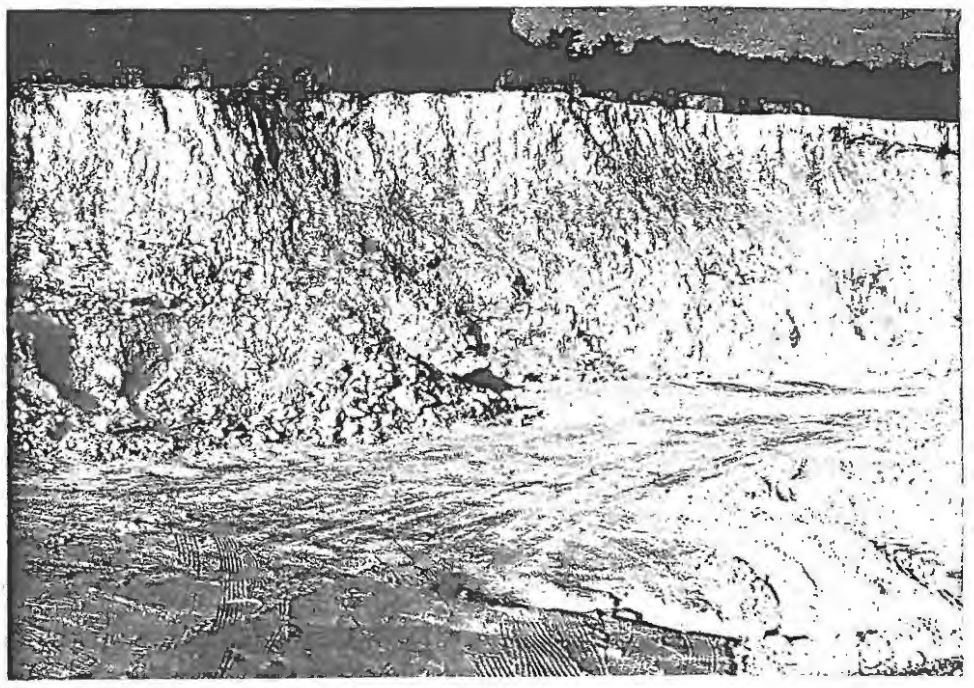

Plate 2.7 The Webber deposit viewed towards the east and showing the 2 m - thick silcrete layer overlying the clay.

Plate 2.8 The textural variety of clay found in the Webber and Wallace deposits. Note the fine bedding and the small spots which are due to iron oxide staining.

except where the rock type does not afford alteration of aluminium silicates, i.e. Witteberg Quartzite.

Summary

1. The kaolin deposits in the area are not stratabound. Their occurrence appears to bear no relationship to the structure and folding of the sedimentary assemblages.
2. The deposits are related to the two geomorphological features in the region, the Grahamstown peneplane and the Coastal plain which are at altitudes of 600-630 m and 500-530 m respectively.
3. The surfaces of the deposits are all capped by silcrete except where the silcrete has been removed by erosion.
4. The depth of kaolinsation is more or less uniform in all of the deposits to a depth of 45 m although the clay which is usable may not extend to this depth.
5. The lithology of the original rock appears to have the greatest control over the quality and uniformity of the deposits.

3. CLAY MINERALS

The structure, chemistry and crystallinity of clay minerals which occur in the Grahamstown area will be discussed to afford better understanding of alteration processes which occur in weathering and the genesis of clays.

Introduction

Clay minerals in general show variations in their chemistry because of limited substitution and absorption of ions. They hardly, if ever, show the ideal chemistry for any one particular mineral. Clays almost always occur as mixtures which increases the difficulty of finding pure mineral species. The degree of crystal perfection, size and habit are widely variable in the clay mineral group.

Clay minerals are layer silicates with basic structural sheets of tetrahedra and octahedra. The building blocks of the tetrahedral sheets are silica $(SiO_4)^{-2}$ tetrahedra which are connected at 3 corners in the same plane to form a hexagonal network. The fourth coigns of the silica tetrahedra all point in the same direction. The octahedral sheet is formed by two layers of hydroxyl ions which octahedrally co-ordinate a plane of cations, usually Al^{3+}. The apical oxygens of the tetrahedral sheet project into the lower hydroxyl layer and replace 2/3 of the hydroxyl ions thus combining the tetrahedral and octahedral sheets (see figures 3.1, 3.2 and 3.3)

The tetrahedral and octahedral sheets can combine in different ways and ratios to form different clay minerals. The clays are therefore classsified or grouped on the basis of the ratio of tetrahedral to octahedral sheets.

A 1:1 clay mineral, i.e. 1 tetrahedral and 1 octahedral sheet has a d 001 of approximately 7 Å whereas a 2:1 clay mineral, i.e. 2 tetrahedral to 1 octahedral sheet has a d 001 of 10 Å. The two major basic groups can be subdivided on whether the octahedral sheet contains 2 cations per 1/2 unit cell, i.e. dioctahedral or whether there are 3 cations per 1/2 unit cell, i.e. trioctahedral.

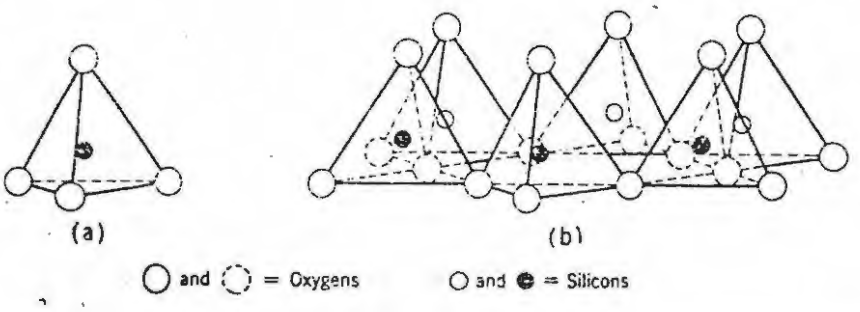

Figure 3.1 Diagrammatic sketch showing (a) a single silica tetrahedron and (b) the sheet structure of silica tetrahedra arranged in a hexagonal network (After Grim, 1968).

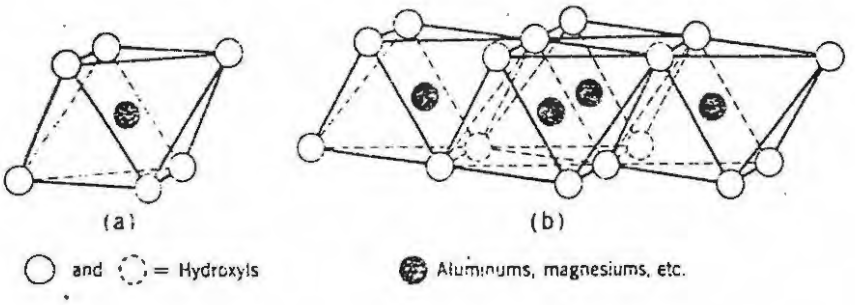

Figure 3.2 Diagrammatic sketch showing (a) a single octahedral unit and (b) the sheet structure of the octahedral units (After Grim, 1968).

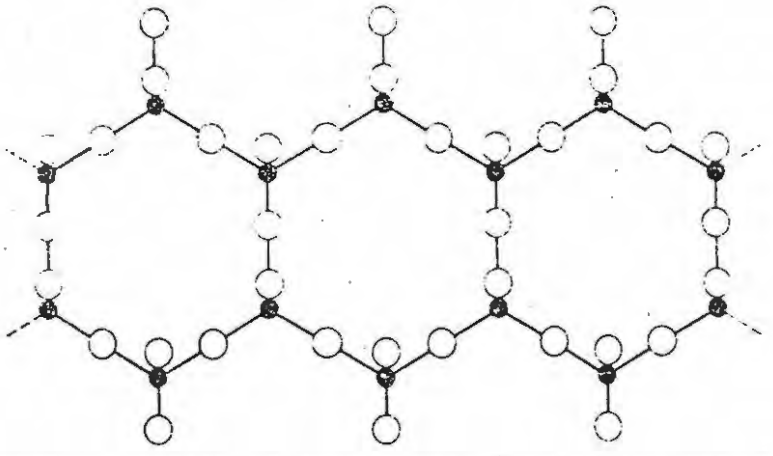

Figure 3.3 Diagrammatic sketch of double chains of silica tetrahedrons as in the structure of clay minerals (After Grim, 1968).

distinctions can also be made on the manner of stacking of the combined octa-tetrahedral sheets on one another. Further distrinctions can be made on the amount of isomorphous replacement within the structure (see figure 3.4.)

1. Kaolinite

Kaolinite is a 1:1 clay mineral and is dioctahedral. The structure is shown in figure 3.5. The ideal formula of this structure is $Al_4 Si_4O_{10} (OH)_8$ or if expressed as oxide weight percent, SiO_2 46,5% Al_2O_3 39,5%, H_2O 14%, but rarely if ever do kaolinites analyse as above. A comparison of the ideal composition and that of 4 U.S. kaolinites (Deer, Howie and Zussman, 1962) is:

Table 3.1

	Ideal	U.S.
SiO_2	46,5	45,8
TiO_2	0,0	0,2
Al_2O_3	39,5	39,1
Fe_2O_3	0,0	0,3
MgO	0,0	0,1
CaO	0,0	0,3
Na_2O	0,0	0,2
K_2O	0,0	0,3
H_2O^+	14,0	13,7
	100,0	100,0

Ti and Fe are almost always present in small amounts and Ca, Mg, Na and K may be adsorbed or structurally incorporated to a limited extent. The percentage of these cations is usually governed by the environment in which the clay has formed and, in the case of residual clays, the starting material. Anatase is almost universal in kaolin (Grim, 1968) and excess Al or Si may be present due to defects in the structure or may occur in the free ionic state (Weaver and Pollard, 1973).

Kaolinites vary in their crystallinity. A number of crystallinity indices have been formulated by Hinkley (1965) and Range et al. (1969), but these are empirical methods and many problems are involved with their

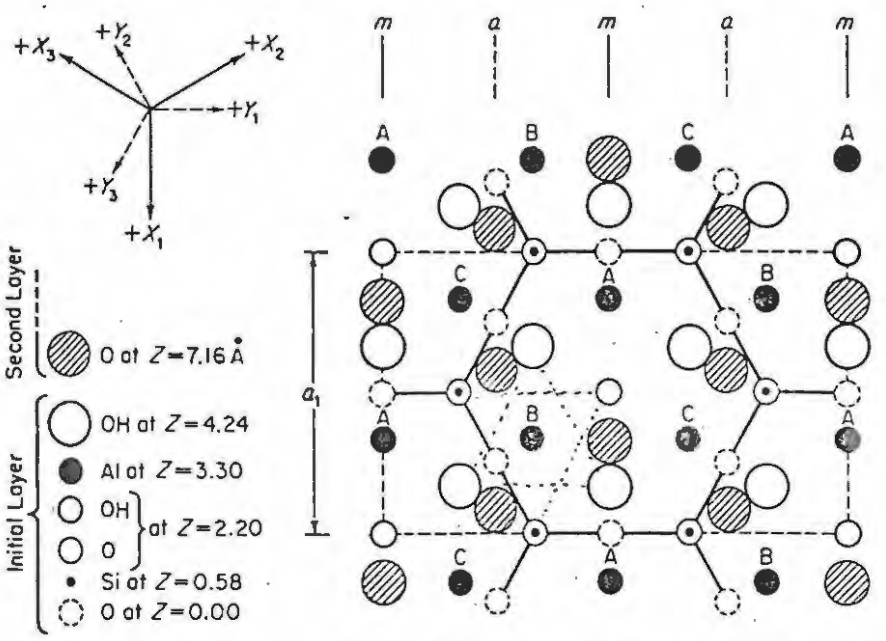

Figure 3.4 A normal projection onto 001 of a 7Å layer of 1:1 clay. The 3 possible octahedral sites only 2 of which are occupied in the kaolins are labelled A, B and C. The second layer has been shifted by 1/3a as in kaolinite to provide hydrogen bonds between the paired OH and O atoms at the layer interface. (After Bailey, 1963)

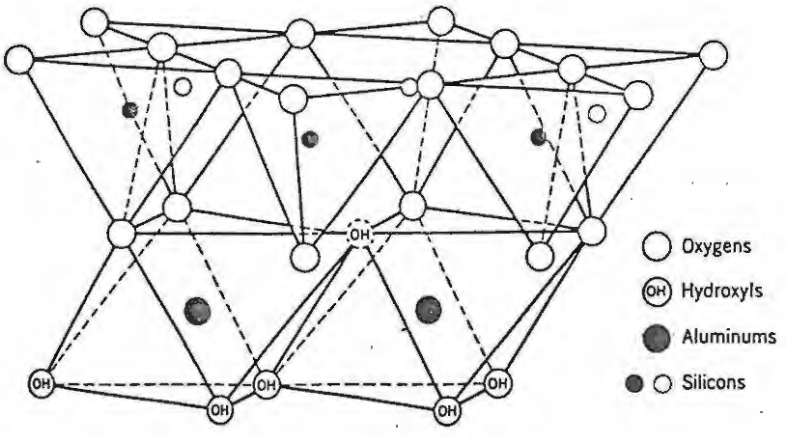

Figure 3.5 Diagramtic sketch of the structure of the 1:1 layer of kaolinite. (After Gruner, 1932)

use. They mostly use the ratios between the 111, 021 and 110 diffraction reflections. These are hardly ever used by ceramic firms in the classification of various types of kaolinite. The degree of crystallinity is most easily assessed by the broadening of peaks and the disappearance of reflections (Brindley and Robinson, 1946)(see figure 3.6). In poorly crystalline kaolinite, hkl reflections with k indices not 3 or multiples of 3 are weak or absent, whereas if k equals 3 or multiples of 3, reflections are largely unaffected i.e. 131, 161, 231 would not be affected whereas 121, 141, 111 would (Brindley, 1951). This is interpreted as a layer displacement parallel to the b axis. In ideal structures of kaolinite the hydroxyl groups lie parallel to the b axis at intervals of b/3 and therefore displacement parallel to b by 3nb/3 does not alter the OH-O bonds between the adjacent layers. The Al and Si atoms occupy a number of positions statistically in the average unit cell (Grim, 1968). This results in disorder.

In poorly crystalline kaolinites a hkl band is seen for 021, 111 and 110 reflections whereas 021 and 111 reflections will be distinct for well crystallised kaolinite (Bailey, 1963). Poorly crystalline kaolinites occur as less distinct hexagonal flake aggregates (Grim, 1962). The average grain size is usually smaller and the crystals are not well formed. The smaller size and poor perfection are probably due to the result of structural stress not allowing continued growth in the a and b direction. Substitutions of Fe or Ti for Al in the octahedral sites may be the cause of this in some cases (Brindley, 1951).

2. Illite

Illite is a 2:1 clay mineral. Both dioctahedral and trioctahedral illites are found, but the dioctahedral type predominates (Weaver and Pollard, 1973). The structure of illite is that of micas. The basic structure is two tetrahedral silica sheets with a central octahedral sheet. The tips of the tetrahedra in each of the tetrahedral sheets point towards the central octahedral sheet and replace the OH groups thus combining the 3 sheets into a unit. Some of the silicon ions are replaced by aluminium ions and the charge deficiency is balanced by potassium ions which are between the layers (see figure 3.7.)

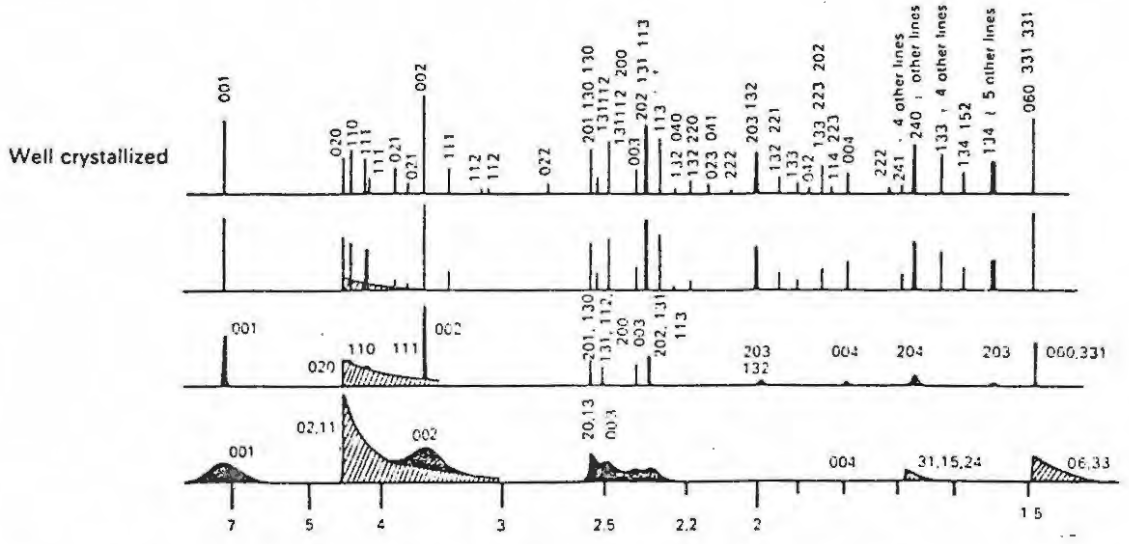

Figure 3.6 A diagram showing the tendency of broadening of peaks and a disappearance of others with degree of crystallinity. (After Brindley and Robinson, 1946).

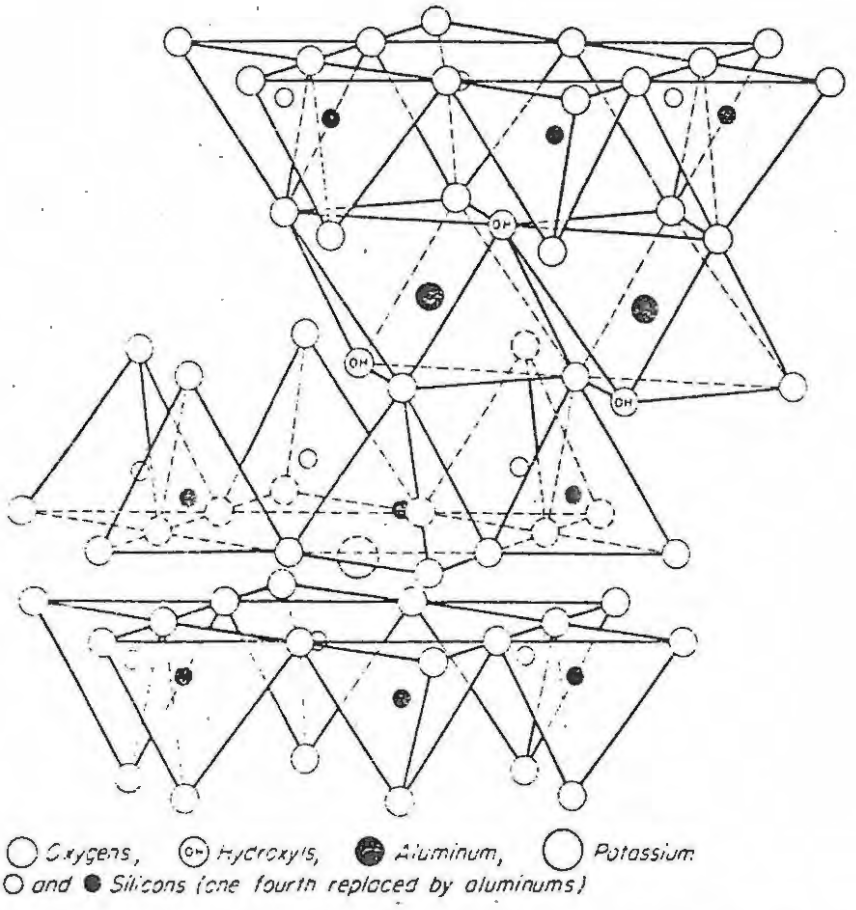

Figure 3.7 Diagramatic sketch showing the 2:1 structure of illite and muscovite. Pyrophyllite has a similar structure except that the large K^+ ion in between the two tetrahedral sheets is removed.

The average of 7 Fithian Illites (type illite) (Grim et al., 1937) is given below:

Table 3.2

SiO_2	56,91
TiO_2	0,81
Al_2O_3	18,50
$Fe_2)_3$	5,25
MgO	2,70
CaO	1,59
Na_2O	0,43
K_2O	5,86
H_2O	2,86
	99,50

In illites there is less substitution of Al^{3+} for Si^{4+} than in the well crystallized micas where 1/4 of Si^{4+} is replaced. In illites the substitution is in the region of 1/6. The K^+ may be replaced by Ca^+, Mg 2^+ or H^+. There is randomness in the stacking of the layers in the c direction and this results in small crystal sizes which are typical of illites as opposed to muscovite which often occurs as large sheets. hkl reflections are weak or absent in dioctahedral illite and Al may be replaced by Fe or Mg with K as the chief balancing cation of illites (Grim, 1968). Illites may be hydrolised to a greater extent by the replacement of K^+ by H^+.

3. Pyrophyllite

Strictly speaking pyrophyllite is not a true clay mineral, but is a 2:1 mineral and is grouped with the micas. It has a similar structure to illite with an octahedral layer sandwiched in between two tetrahedral layers. The octahedrally co-ordinated cation is Al and 2/3 of the octahedral sites are occupied by Al making pyrophyllite dioctahedral.

Pyrophyllite shows little deviation from the ideal chemistry but there may be small replacement of Si^{4+} by Al^{3+} by Mg^{2+} and Fe^{2+}. Minor Ca, Na and K may be present. The ideal chemistry is $Al_4Si_8O_{20}(OH)_4$. Pyrophyllite does not have a cation between the layers as in illite. The layers are held together by van der Waal's forces.

Pyrophyllite is found in three different forms. It may occur as fine grained foliate lamellae with a platy appearance, radiating crystals and needles or as massive, compact, spherulitic aggregates (Deer, Howie and Zussman, 1971).

4. CHEMISTRY AND MINERALOGY

The seven deposits that are actively worked in the area under review were sampled. Samples were taken at different levels in the respective quarries and then analysed by X-ray fluorescence and X-ray diffraction methods to establish their chemistry and mineralogy. Grain size determinations were done and the samples were also examined by transmission electron microscopy to determine the crystal morphology, and by electron diffraction to investigate their structure.

The aim of the investigation was to determine variations in the chemistry and mineralogy with absolute altitude and depth below surface and to establish the bulk chemistry and mineralogy of each deposit and to show differences according to lithology. The methods of analysis and sample preparation are given in the appendix.

4.1 Avenue Park

4.1.1 Experimental Data

The deposit was extensively sampled in view of the superior quality of the material mined and used in tile manufacture. Samples were taken from all of the quarry walls and from exploration pits in the southern, central and northern part of the deposit. Places showing excessive iron oxide staining were avoided particularly in the western 'shear zone' of the quarry. Two samples of Bokkeveld shale were taken along strike from the deposit for comparative purposes. The average composition of the clay, grit free clay and Bokkeveld shale are given in Table 4.1.

The Barth Standard cell is a calculated unit based on 160 (O + OH). Both calculated examples and general experimentation have shown that on average rocks contain 160 (O + OH) per 100 cations. For weathered rocks the number of oxygens is slightly larger and in addition more OH is present. Geological oxidation prevails at the surface and leaching removes cations from crystal lattices which are substituted by H^+. This results in relative oxygen enrichment.

The fact that the number of (O + OH) ions based on 100 cations varies only slightly can now be used for arriving at equal-volume calculated units. The units can be for assessing of material balances and weathering transformations without volume changes.

Table 4.1 Analyses of the Avenue Park Clay and related parent rock

	Bkv-ave	AP-ave	Ap-gf	Ap-5	AP-6	AP-7	AP-8
SiO_2	57,38	62,81	56,41	66,21	63,50	63,45	62,29
TiO_2	1,02	1,21	1,12	1,12	1,13	1,72	1,02
Al_2O_3	21,39	26,23	31,03	23,84	25,37	25,67	26,54
*Fe_2O_3	7,39	0,52	0,58	0,40	0,72	0,71	0,50
MnO	0,01	0,02	0,00	0,00	0,00	0,01	0,00
MgO	1,38	0,31	0,32	0,17	0,34	0,37	0,38
CaO	0,21	0,01	0,00	0,00	0,00	0,01	0,00
Na_2O	0,47	0,83	0,80	0,77	0,82	0,82	0,74
K_2O	4,67	2,95	3,02	1,99	3,47	3,48	3,09
P_2O_5	0,20	0,12	0,09	0,08	0,08	0,10	0,07
** LOI	5,30	5,27	6,66	5,21	5,15	5,06	5,42
	99,42	100,28	100,03	99,79	100,59	101,40	100,05

	AP-9	AP-10	AP-11	AP-12	AP-13	AP-14	AP-15
SiO_2	62,49	62,13	56,41	64,21	61,59	61,07	62,14
TiO_2	1,14	1,11	1,12	0,96	0,93	1,19	0,94
Al_2O_3	26,54	26,60	31,03	24,40	26,62	27,07	27,01
*Fe_2O_3	0,57	0,59	0,58	0,56	0,47	0,54	0,42
MnO	0,00	0,00	0,00	0,01	0,00	0,01	0,00
MgO	0,38	0,38	0,32	0,31	0,31	0,39	0,27
CaO	0,07	0,00	0,00	0,00	0,01	0,04	0,01
Na_2O	0,88	0,85	0,80	0,73	0,69	1,00	0,81
K_2O	4,04	3,27	3,08	3,79	3,59	3,15	2,18
P_2O_5	0,09	0,12	0,09	0,10	0,13	0,17	0,08
** LOI	4,30	5,28	6,66	4,94	5,81	5,18	6,10
	100,50	100,33	100,07	100,01	100,15	99,81	99,95

	AP-16	AP-17	AP-18	AP-19	AP-20	AP-21	AP-22
SiO_2	54,39	61,40	64,51	62,51	63,57	65,59	59,32
TiO_2	1,34	1,10	1,06	1,17	1,06	1,17	1,01
Al_2O_3	24,77	28,20	24,72	25,45	25,08	24,24	28,69
*Fe_2O_3	0,56	0,48	0,50	0,56	0,53	0,49	0,46
MnO	0,00	0,00	0,00	0,00	0,00	0,01	0,00
MgO	0 37	0,26	0,32	0,39	0,33	0,26	0,23
CaO	0,04	0,01	0,00	0,07	0,01	0,01	0,01
Na_2O	0,92	0,87	0,91	0,84	0,81	0,84	0,85
K_2O	3,49	2,65	2,92	3,52	3,94	2,60	2,65
P_2O_5	0,31	0,14	0,08	0,16	0,10	0,13	0,12
**LOI	3,95	5,27	4,73	4,72	4,75	4,74	6,32
	100,14	100,38	99,75	99,39	100,19	100,08	99,66

	AP-23	AP-24	AP-25	AP-26	AP-27	AP-28	AP-29	AP-30
SiO_2	60,69	61,05	64,59	61,77	62,58	63,18	66,12	65,88
TiO_2	1,07	1,07	1,10	1,01	1,05	1,14	1,19	1,17
Al_2O_3	27,36	27,04	26,64	27,60	26,45	26,35	26,63	24,21
*Fe_2O_3	0,39	0,40	0,47	0,45	0,48	0,65	0,67	0,54
MnO	0,00	0,00	0,00	0,01	0,01	0,00	0,00	0,00
MgO	0,21	0,52	0,22	0,50	0,21	0,21	0,25	0,24
CaO	0,03	0,00	0,00	0,00	0,00	0,00	0,00	0,00
Na_2O	0,80	0,88	0,85	0,81	0,84	0,80	0,80	0,84
K_2O	2,36	2,69	2,47	2,35	2,35	2,59	2,55	2,52
P_2O_5	0,11	0,11	0,11	0,09	0,12	0,13	0,11	0,09
** LOI	6,35	5,72	4,20	6,02	5,62	5,58	4,93	5,12
	99,37	99,48	100,65	100,61	99,71	100,63	101,24	100.61

* All iron is quoted as Fe_2O_3

** LOI is loss on ignition and taken as the loss on heating at 1000°C for 10 hrs. Where total Fe is low, the increase in mass of the sample due to FeO - Fe_2O_3 is small by contrast with LOI.

In Table 4.1, all Fe is quoted as Fe_2O_3, Bkv is the average of two duplicate analyses of Bokkeveld Shales, AP-ave is the average of 26 duplicate analyses of Avenue Park clay and AP-gf is an analysis of the -325 mesh fraction of Avenue Park clay.

Samples AP5-AP9 were taken at 1,5 m intervals from the quarry floor to ground height in the northern section of the quarry, (AP5 at the base). AP20-AP28 were taken at the same locality but at 1 m intervals and from a pit dug into the quarry floor, (AP20 at base). AP10-AP11 are from the southern wall and AP13 and AP14 and AP15 were taken to the south of the quarry at 1 m intervals (AP13 at base) and AP18 and AP19 from the eastern wall of the quarry. AP29 and AP30 are two samples of weathered Bokkeveld Shale.

The analyses were plotted on graphs by three different methods to show the relative loss or gain of elements in the weathering process and to avoid any bias. The three different methods were Barth Standard cell cation percentages, normalised cation percentages and a loss-gain diagram of Garrels and Mc Kenzie (1971).

In the Barth Standard cell plots, the standard cell cation percentages were calculated from the weight percentages of the oxides and plotted against the aluminium cation percentage values to show the variation in the chemistry of the original shale, clay and grit-free clay on an equal volume basis in figures 4.1 and 4.2.

Normalised cation percentages are calculated from the weight percent of oxide of the major elements normalised to the Al cation percentage of the original shale. The values for the various cations obtained are plotted against the cation percentage of Al in the clay. The basic assumption is made that no Al has come into the system and the apparent increase in Al is purely due to removal of other cations in the weathered material. If this assumption is accepted the increases or losses of the various elements are correctly represented. In this type of plot H_2O^+ is not taken into account and the degree of loss or gain is exaggerated to some extent.

The loss-gain diagram of Garrels and Mc Kenzie (1971) is constructed by taking the weight percentage of oxide of the original shale and dividing it by the weight percentage in the residual or altered rock. This type of diagram makes no assumptions and graphically illustrates gains and losses.

The diagrams for the Avenue Park deposit are shown in figures 4.1, 4.2, and 4.3.

Diffraction traces of the Avenue Park clay show that the clay consists of quartz, kaolinite, pyrophyllite and illite. No additional minerals were detected when different sample preparation methods were used. Methods used were the standard back mounting technique, powder press method and suction-onto-membrane filter method (see appendix for explanation of methods). The kaolinite 001 and 002 reflections are strong, as would be expected with a clay mineral with a perfect basal cleavage and thus preferred orientation. The 020 reflection is poorly developed and the 110,

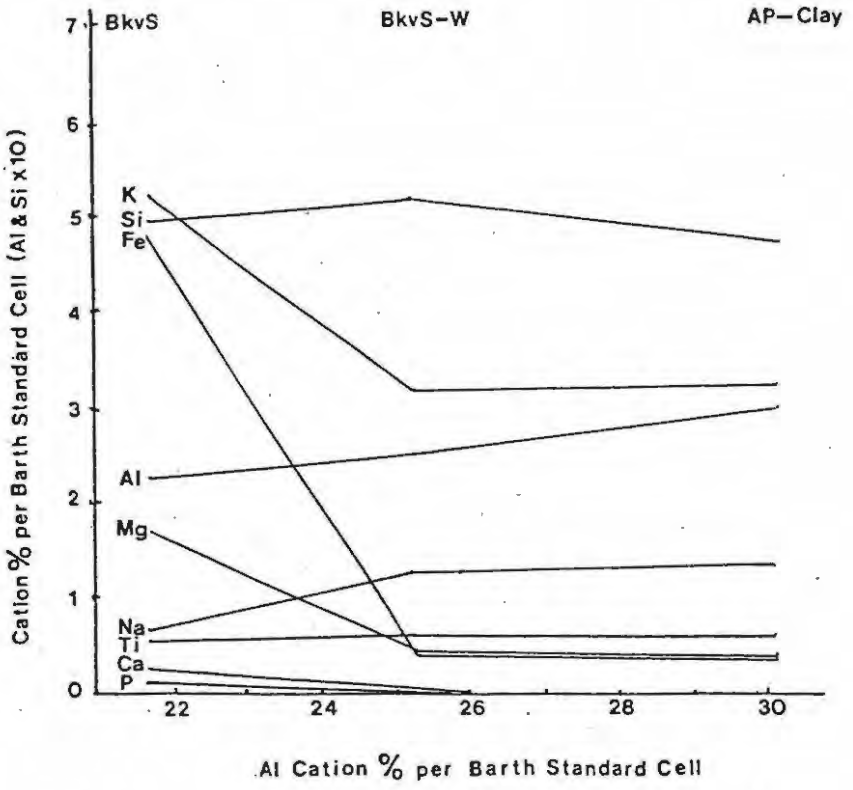

Figure 4.1 Barth Plot of the Avenue Park Clay deposit.

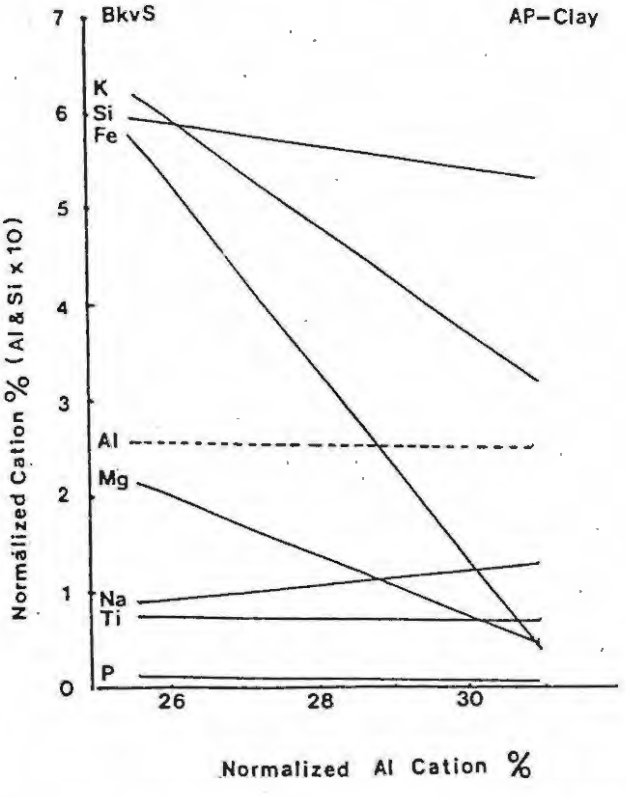

Figure 4.2 Normalized cation % plot of the Avenue Park clay.

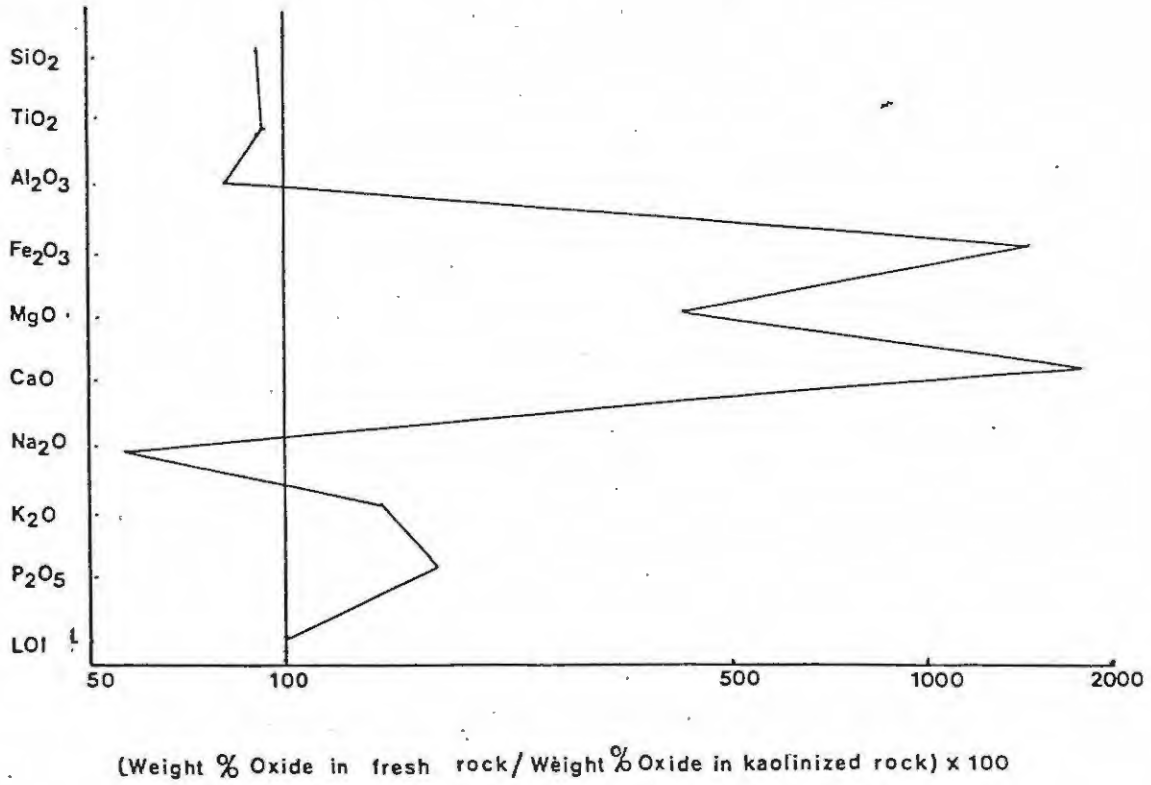

Figure 4.3 Loss/Gain diagram showing the relative enrichment or depletion of oxides. AP-ave and Bkv-ave are the analyses used.

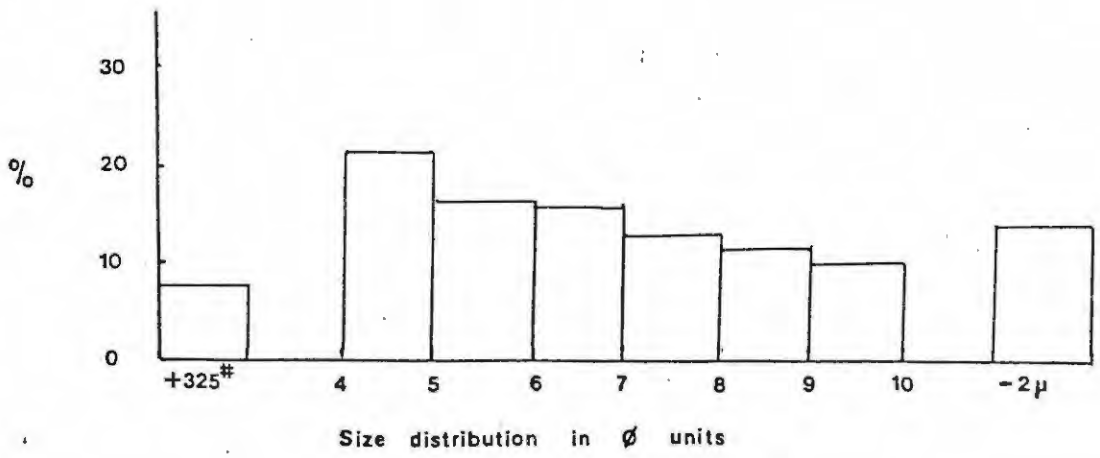

Figure 4.4 A histogram of the Avenue park clay showing the size distribution, grit content and -2 micron fraction weight percentage fractions.

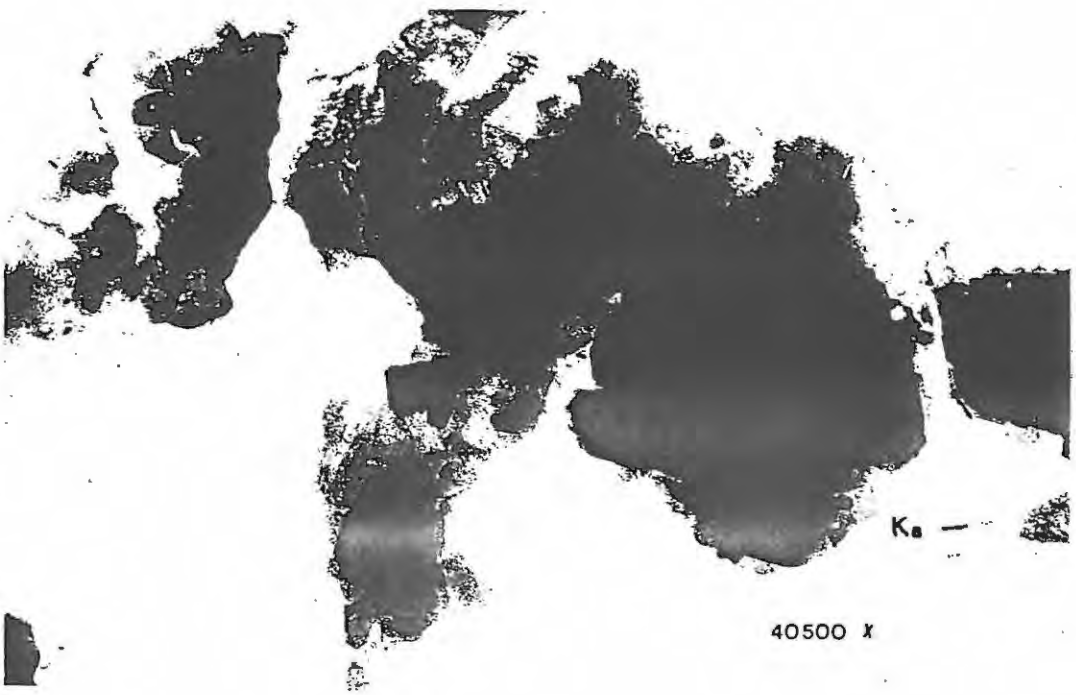

Plate 4.1 Electron photomicrograph of the Avenue Park clay. Note the poorly formed kaolinite crystals which form aggregates. Outlines of individual crystals can be seen and are characterised by the internal angles of 120^{0}

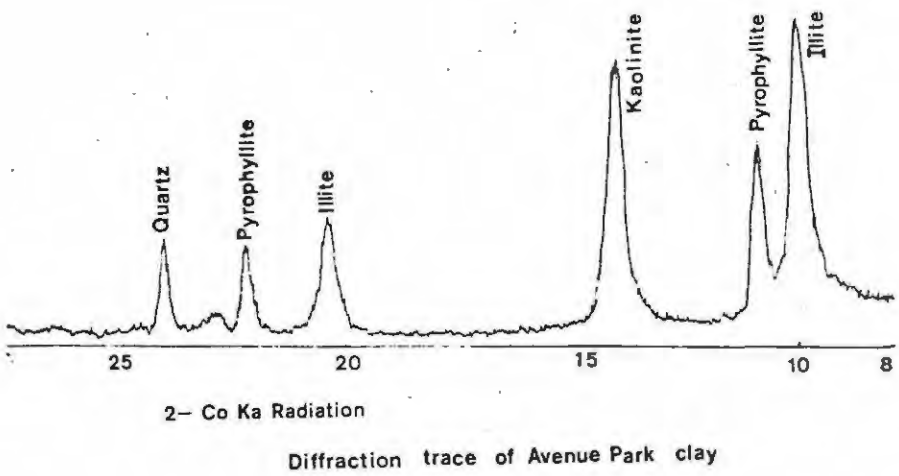

Diffraction trace of Avenue Park clay

Figure 4.4a

111 and 11$\bar{1}$ are absent which is indicative of b axis disorder in the kaolinite (Brindley and Robinson, 1964). A comparison of the XRD traces of sample P3 from the Palmer quarry, Fig. 44A, prepared in the same way, and which has similar chemistry and quartz content shows the differences in crystallinity distinctly in the 23-25^{o} 2θ Co Radiation area even although there is a slight interference by the pyrophyllite 01D reflection in this region.

Transmission electron microscopy (TEM) micrographs show the kaolinite to be indistinct aggregates of small crystals. The typical 120^{o} angle formed by the outline of individual crystals can be seen in the micrograph. Details of sample preparation are given in the appendix.

Electron diffraction studies were done on a number of crystals in the sample and all showed the crystals to be kaolinite. The sample was prepared from a suspension fraction after deflocculation and settling time to give material of 2 micron $\pm$ which is classified as the definition of clay by Folk (1968). The electron diffraction micrograph shows a double reflection with a rotation of a few degrees between the two sets of spots. This is because a second crystal is beneath the one observed although the crystal examined is almost transparent to the electron beam because it is so thin. The beam current of the electron microscope had to be turned down to see some of the crystals. The feature of multiple reflections is characteristic of the kaolinites which were shown to be disordered by XRD methods.

4.1.2 Discussion of Data

The Barth type plot shows a gain in Si and Na and the normalised cation percentage plot only shows an increase in Na for the clay relative to the parent rock. Although the Barth type diagram is a truer reflection of the elemental variations it does not illustrate them as well as a normalised cation percentage or a loss-gain diagram especially when the differences in the oxide percentages are very low. The loss-gain diagram has the disadvantage of overemphasising relative losses or gains for elements in concentrations of less than 1%. It can, however, easily be seen that the greatest loss in the clay relative to the parent rock is Fe, K and Mg. The normalised cation plot also shows a relative loss with respect to Si.

The grain size analysis of the Avenue Park clay showed a mean of 6,6 ϕ for the -325 mesh fraction and a grit content of 7,2%. 14,5% of the clay is finer than 10 microns. The grain size analysis cannot be considered to be very accurate because of the tendency for the clay to form aggregates of particles as is illustrated in the electron micrograph (see plate 4.4).

Attempts at quantifying the mineral proportions of the Avenue Park clay were made by using the mica convention of Griffiths and Radford (1965), a computer mixing program, and the peak intensities of the diffraction traces.

The mixing program is a general purpose least squares approximation routine which is normally used for calculating petrographic mixing equations. The program is a modification of the program 'Mixer F4' written at the Centre for Volcanology, University of Oregon and based on the program 'LSPX' written by Bryan et al. (1969). In essence the compositions of the mineral phases are mixed in proportions according to a least squares approximation routine to fit the composition of the whole rock. The mineral phases are then expressed as percentages of the whole rock. The reliability of the mixing program is dependent on the accuracy with which the chemical composition of the mineral phases is known. Often the chemistry of clay minerals is not known accurately, but maximum and minimum limits are often known and in the case of kaolinite and pyrophyllite their composition is not very variable. Good approximations of clay mineral chemistry can be found in Deer et al. (1962).

More recently a program 'STM 2' has been developed by Pearson (1978) which is suited to clay minerals. The program makes use of simultaneous equations which are solved to give clay mineral abundances. The only drawback of this method is that the quartz percentage has to be determined by XRD methods of Till and Spears (1969). This method was not attempted as the program was not available.

Quantitative mineralogical analyses of clays by XRD methods often produce poor results. Reasons for poor results are numerous and include inconsistent sample preparation techniques, variable crystallinity of the clay, instrumental design and geometry besides matrix differences and associated problems of X-ray methods.

Sample preparation is probably the single most influential parameter leading to poor results. Grain size differences affect the intensity of peaks even if there is no preferred orientation (Alexander and Klug, 1954), but this can be largely overcome by consistency in grinding. The method of sample mounting is critical and various internal standards have been used by authors for determining the degree of preferred orientation, (Thompson, 1970). Internal standards in themselves tend to cause problems because of dilution effects, peak interferences and inhomogeneity within the sample besides affecting the matrix. Of all the methods of sample preparation including pipette-onto slide, smear-on-glass, sedimentation, suction-onto-tile, suction-onto-membrane filter and powder press methods the powder press technique appears to be one of the least variable and shows good peak to background ratios (Cubitt, 1975). The variation in crystallinity is a considerable problem and unless clays can be matched for crystallinity results can be classed as estimates or at best semi-quantitative.

The method used to estimate mineral proportions by XRD methods was to use a relatively pure kaolinite from the Palmer clay, sample P5A. The sample was diluted with quartz to give five calibration points in the range of 10 to 50% quartz. The calibration points were made by measuring the peak intensities of the kaolinite 7,16 A^{o} peak and quartz 4,26 A^{o} peak. Illite was taken to be the balance in the clays where it was present and a third crude calibration curve constructed from the data derived . Pyrophyllite was taken as the balance of the clay in estimation of the Coastal Plain deposits. The results were therefore subject to large errors, firstly, because of the difference in crystallinity between the clays and secondly because of the multiplication of error caused because of the unavailability of pure illite or pyrophyllite from the deposits. Another source of error is that peak intensity was read as peak height minus background where peak areas are safer to measure. Yet another problem was that the excitation radiation had to be filtered which reduced the intensity of the peaks considerably.

The most correct procedure would be to separate out pure members of the minerals from the clay to be analysed. These minerals would then be mixed in known ratios with an internal orienting standard of 5% molybdenum sulphide. The peak areas of the kaolinite 7,16 A peak, pyrophyllite 9,9 A peak would be measured and molybdenum sulphide 6,16 A peak would be read as a monitor of the degree of prefered orientation. Peak

intensities would be corrected for matrix effects and quartz percentages would be calculated by measuring the 4,26 A after heating to 950°C to destroy interfering clay mineral peaks which is the method of Till and Spears (1969). Obviously this is impractical in the present study and at least very tedious even if done on a routine basis. It is for this reason why other methods of quantifying mineral proportions in clay bearing rocks have been attempted.

Table 4.2 Estimates of mineral abundences in the Avenue Park Clay

Mica Convention		Mixing Program		Diffraction Estimates
Kmica	25,01	Illite	20,50	29
Namica	10,18	Pyrophyllite	27,59	19
Clay	31,79	Kaolinite	21,49	26
Quartz	31,91	Quartz	30,49	25
	98,89		100,00	99

From the above data we can see that there is poor agreement between the various methods.

2. Melrose Deposit

Two samples of the Melrose clay were taken from separate prospecting trenches alongside the Manley's Flats road cutting. The samples taken were relatively free of iron staining. A sample of Witteberg Shale was also taken along strike from the deposit. Analyses of the Witteberg Shale, mean of the two raw clay samples and the -325 mesh fraction are given below:

Table 4.3 Analyses of the Melrose clay and associated rock

	Wts	M-ave	M-gf	M1	M2
SiO_2	67,34	63,74	59,23	57,73	69,70
TiO_2	0,77	0,94	1,06	1,06	0,81
Al_2O_3	15,73	24,88	27,68	28,70	21,06
Fe_2O_3	5,26	0,51	0,58	0,60	0,41
MnO	0,04	0,00	0,00	0,00	0,00
MgO	1,48	0,33	0,40	0,41	0,25
CaO	0,37	0,07	0,06	0,07	0,06
Na_2O	1,22	1,29	1,14	1,40	1,19
K_2O	2,65	3,10	3,57	3,68	2,53
P_2O_5	0,16	0,13	0,07	0,16	0,10
LOI	3,91	5,92	6,11	5,99	4,41
	98,93	100,91	99,90	99,80	100,52

Wts - Witteberg Shale; M-ave - average of M-1 and M2, M-gf - Minus 325 fraction, M-1 and M-2 two samples of the Melrose clay.

The analyses were plotted on a loss-gain diagram and a normalised cation percentage diagram. The tendencies shown on these two diagrams are very similar to the Avenue Park plots. Again Fe and Mg show the greatest relative losses.

The electron micrograph of the Melrose clay shows very poorly defined crystals kaolinite. The kaolinite particles are very difficult to define because of the extremely fine grained nature in the clay and the tendency to form aggregates. The typical 120^{o} angles formed by the outlines of the clay particles can be seen.

Diffraction patterns of the Melrose clay show illite, pyrophyllite and quartz peaks. The 111, $11\bar{1}$ and 021 peaks for kaolinite are absent and peak broadening on the 002 and 001 is apparent. The diffraction trace shows strong broad peaks for illite at 001 and 002. The diffraction trace is very similar to that of the Avenue Park clay (see appendix for the trace).

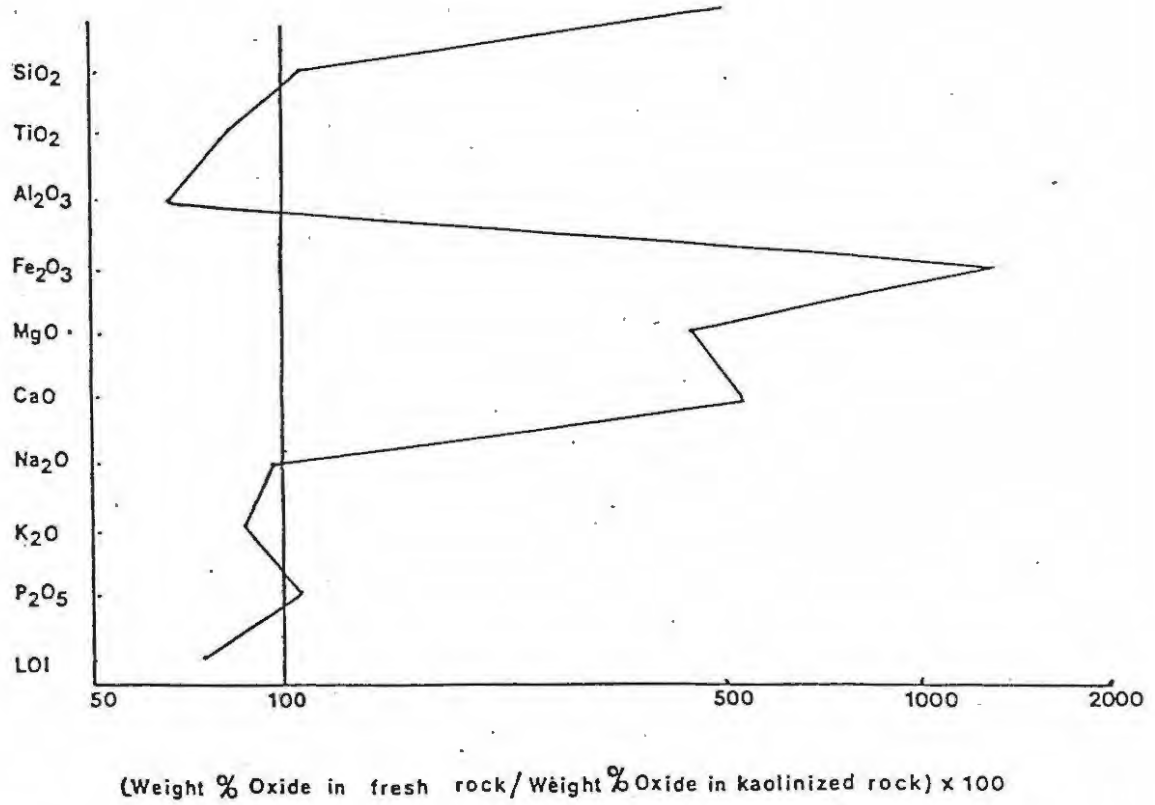

Figure 4.5 Loss/Gain diagram of the Melrose clay showing the relative movement of elements.

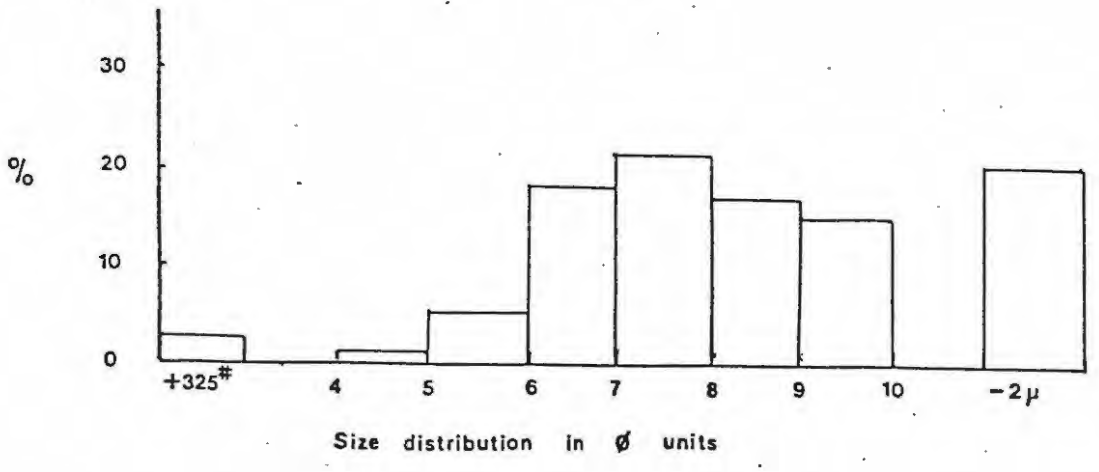

Figure 4.6 A histogram of the Melrose clay showing the size distribution.

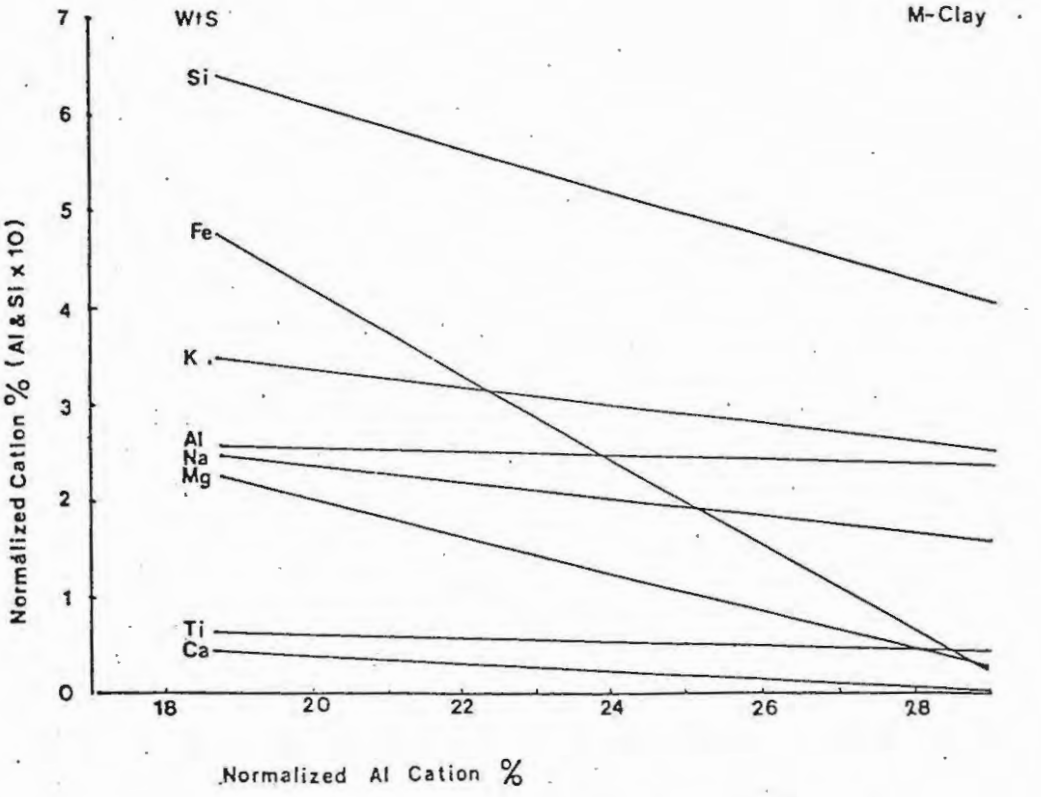

Figure 4.7 Normalized cation % plot for the Melrose clay
Wts - Witteberg Shale, M - Melrose clay.

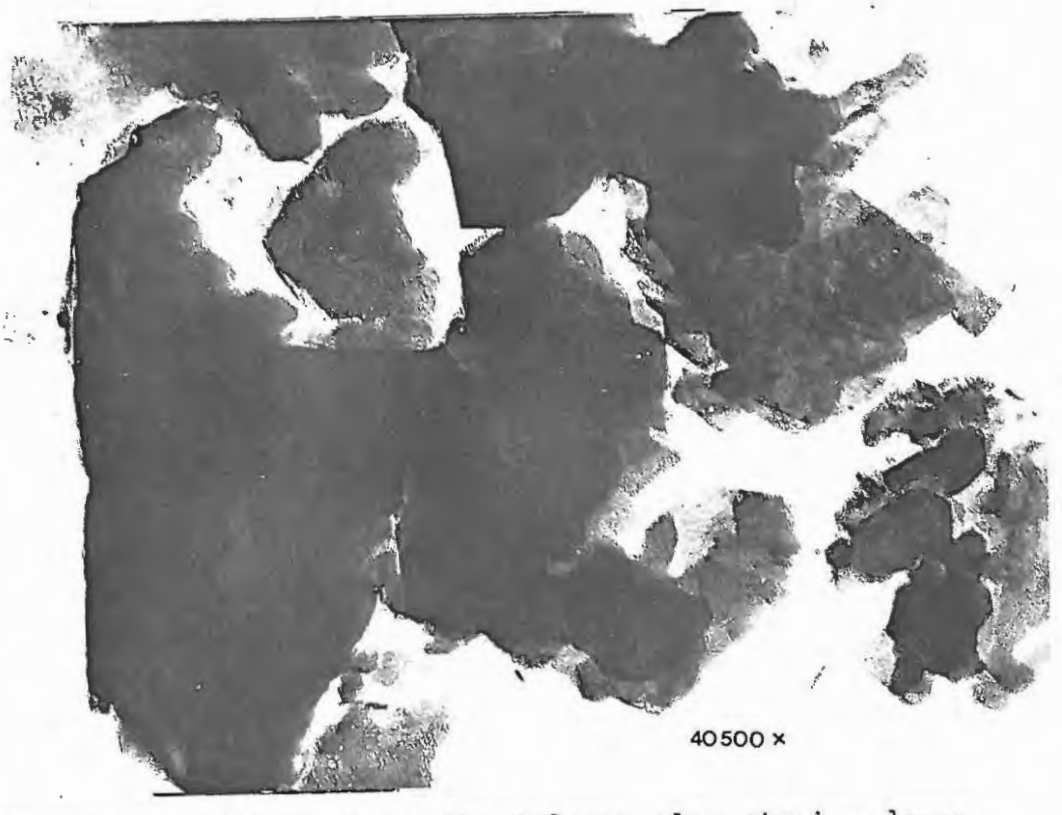

Plate 4.2 An electron micrograph of the Melrose clay showing large irregular plates of illite and some poorly defined aggregates of kaolinite

A histogram of the grain size of the Melrose clay is given in figure 4.9. The arithmetic mean grain size of the Melrose clay is 8 Ø which is considerably finer than the Avenue Park clay. The grit content is 2,1% and consists almost wholly of fragments of unweathered shale. 20% of the material is finer than 10 Ø which is also reflected in the electron micrograph.

Quantitive estimates of the minerals were made by the mica convention and by estimates of peak intensities of the diffraction traces. These estimates are given in the table below:

Table 4.4 Estimates of mineral proportions for Melrose Clay

Mica Convention		Diffraction Estimate	
Kmica	26,29	Illite	35
Namica	15,95	Kaolinite	25
Clay	21,30	Quartz	30
Quartz	34,49	Pyrophyllite	10
	98,03		100

3. Crous Deposit

Three samples were taken from the Crous deposit. C-1 was taken just below the silcrete, a second sample C-2, 5 m below the surface and a third C-3 sample at the base of the quarry. The samples taken were free of visible iron oxide. The average of the three analyses, an analysis of the -325 mesh fraction and an analysis of the Witteberg Shales are given below:

Table 4.5 Analyses of Crous Clay

	Wts	C-ave	C-gf	C-1	C-2	C-3
SiO_2	67,34	61,79	59,10	61,54	59,10	64,74
TiO_2	0,77	0,72	0,75	0,71	0,75	0,72
Al_2O_3	15,73	26,88	28,94	27,08	28,94	24,64
Fe_2O_3	6,26	0,65	0,63	0,77	0,63	0,54
MnO	0,04	0,00	0,00	0,00	0,00	0,00
MgO	1,48	0,28	0,27	0,32	0,27	0,25
Cao	0,37	0,04	0,05	0,06	0,05	0,02
Na_2O	1,22	0,78	0,74	0,75	0,74	0,85
K_2O	2,65	2,54	2,61	2,46	2,61	2,55
P_2O_5	0,16	0,11	0,15	0,11	0,15	0,06
LOI	3,91	6,64	7,17	6,78	7,17	5,98
	99,93	100,43	100,41	100,58	100,41	100,35

Wts - Witteberg Shale, C-ave - average of C1-C3, C-gf - 325 mesh.

The Crous analyses were plotted on a cation percentage (fig. 4.10) and a loss/gain diagram (fig 4.8). The greatest relative losses are Si, Fe, Mg and K with a large relative gain for aluminium. Electron microscopy of the Crous clay shows aggregates of hexagonal plates of kaolinite (Plate 4.3).

Diffraction traces of the Crous clay shows that the clay consists of kaolinite, illite, pyrophyllite and quartz. There are no distinct peaks in the 111, $11\bar{1}$ and 021 regions of the diffraction trace. This and the evidence from the electron micrograph show that the Crous clay is poorly crystallised. Again the diffraction trace is similar to Avenue Park. (See Appendix Fig. 2 for comparative XRD trace).

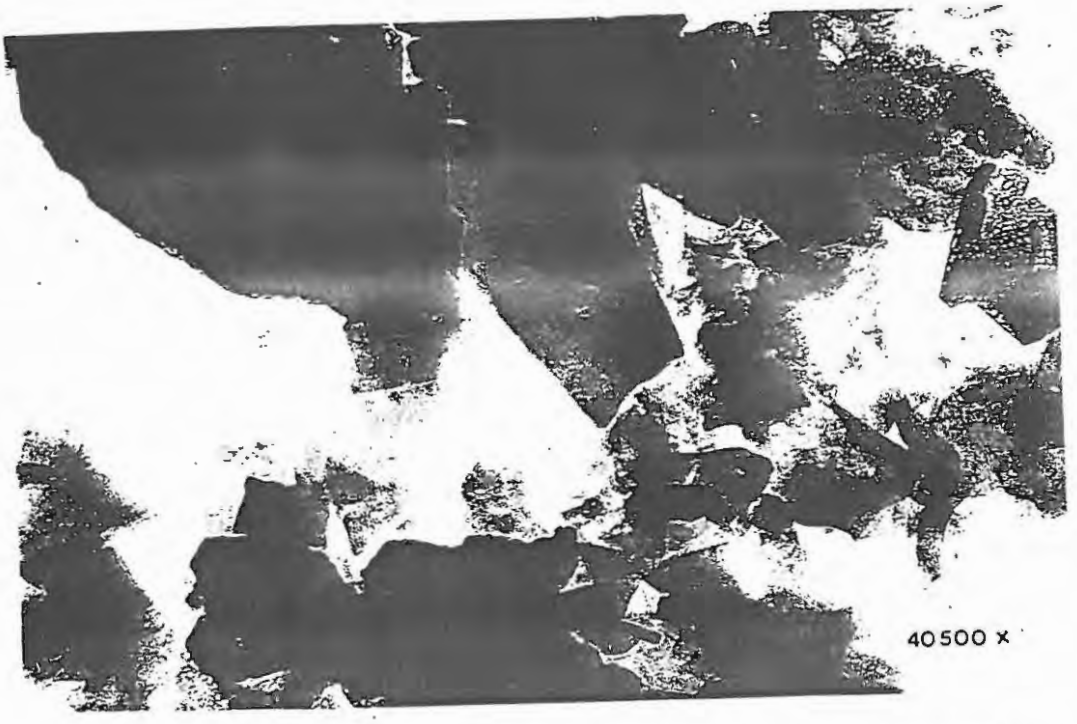

Plate 4.3 An electron photomicrograph of the Crous clay showing small hexagonal plates of kaolinite.

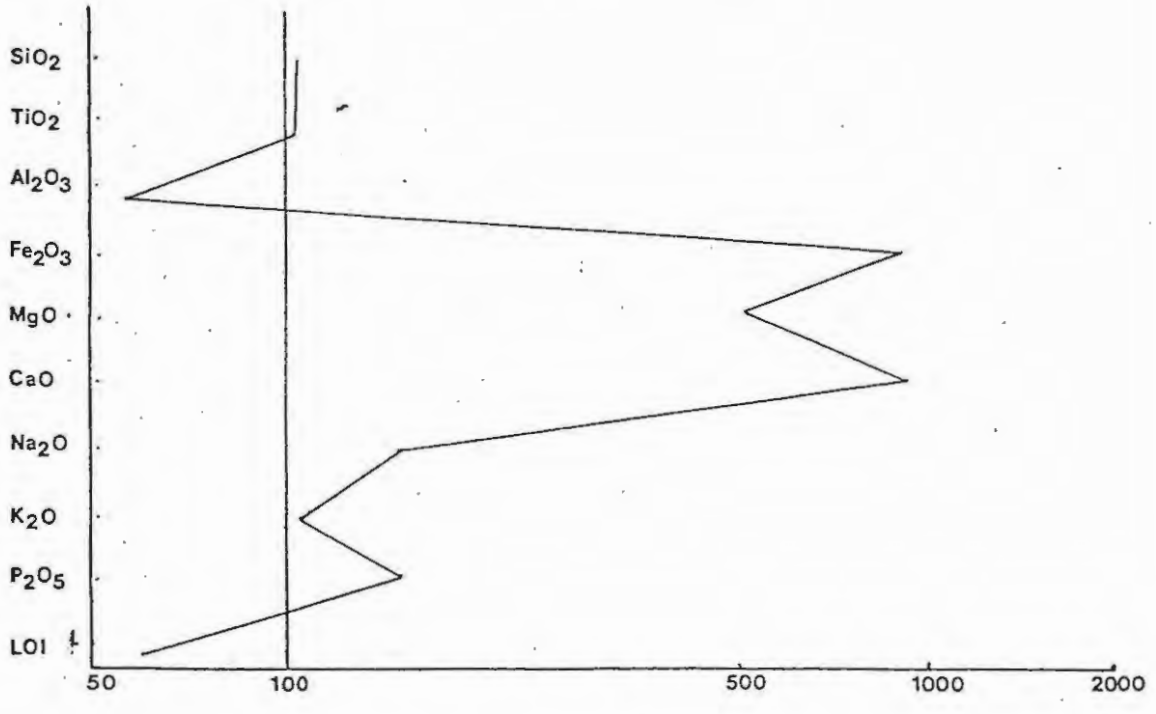

Figure 4.8 Loss/Gain diagram of the Crous clay showing the relative movement of elements.

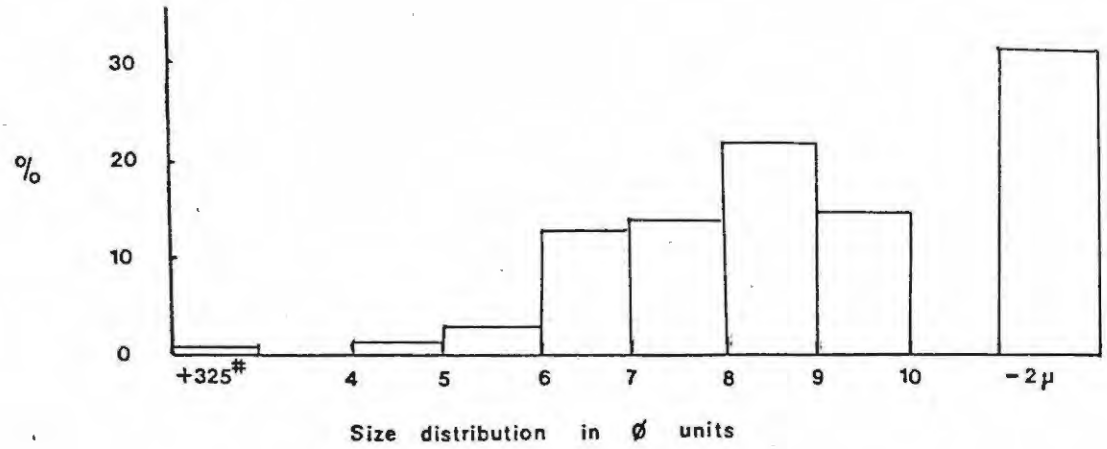

Figure 4.9 A histogram showing the size distribution of the Crous clay

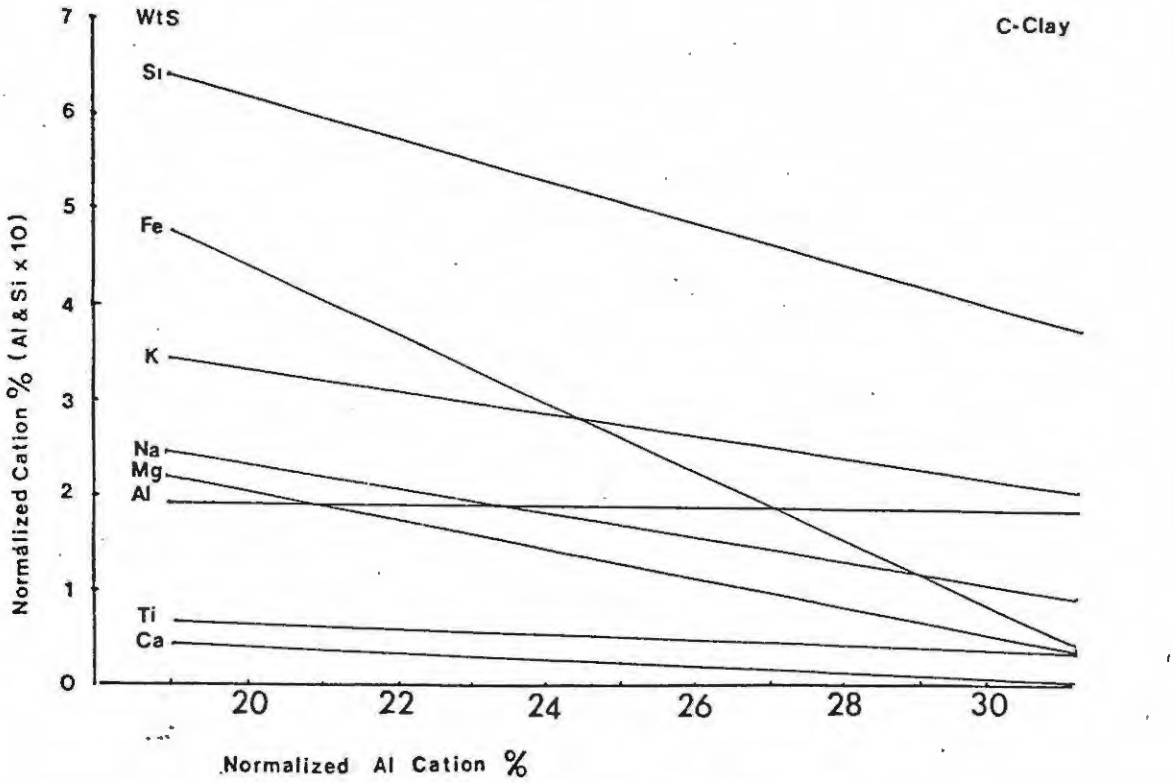

Figure 4.10 Normalized cation % plot for the Crous clay.
Wts - Witteberg Shale, C-ave average of C1, C2 and C3.

A grain size analysis revealed that the Crous clay is almost grit-free. Only 0,5% of the clay is coarser than 325 mesh and 32,5% of the clay is finer than 10 μ. (see figure 4.9).

Quantitative estimates of the mineralogy of the Crous clay were made using the mica convention and the diffraction peak intensities. These estimates are given in the table below:

Table 4.6

Mica Convention		Diffraction Estimates	
Kmica	21,48	Illite	25
Namica	9,60	Kaolinite	35
Clay	37,12	Pyrophyllite	10
Quartz	30,04	Quartz	30
	98,24		100

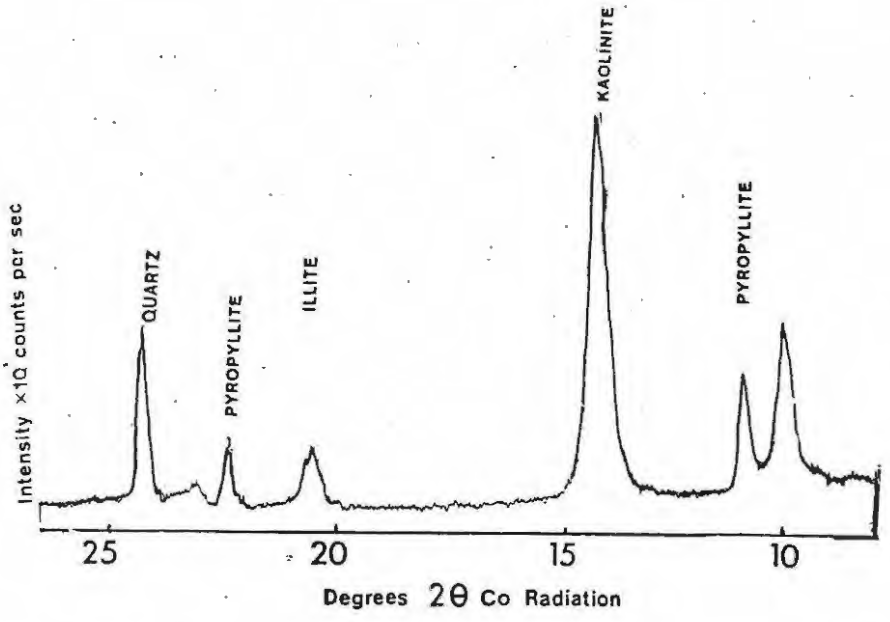

Fig 4·10a Diffraction trace of Crous clay

4. Upper Gletwyn

A total of 5 samples were taken from the Upper Gletwyn deposit starting from just below the silcrete to the base of the deposit. The samples taken showed no visible iron staining and areas showing vein quartz were also avoided. The average analyses of these 5 samples, the Witteberg Shale, the -325 mesh fraction, a suspension fraction and an average of 8 analyses by Eales (1975) are given below:

Table 4.7 Analyses of the Upper Gletwyn clay and related associated parent rocks

	Wts	UG-ave	Eales (1975)	UG-gf	UG-sf
SiO_2	67,34	67,71	67,86	59,39	47,82
TiO_2	0,77	0,69	0,79	0,85	0,37
Al_2O_3	15,73	22,77	21,05	28,66	33,81
Fe_2O_3	6,26	0,97	0,74	0,69	0,95
MnO	0,04	0,01	0,00	0,00	0,00
MgO	1,48	0,29	0,30	0,51	0,83
CaO	0,37	0,05	0,07	0,04	0,09
Ma_2O	1,22	0,14	-	0,04	0,00
K_2O	2,65	1,61	1,78	3,14	4,34
P_2O_5	0,16	0,03	0,08	0,06	0,06
LOI	3,91	6,21	6,66	6,51	10,25
	99,93	100,48	99,33	99,89	98,52
	UG-6	UG-7	UG-8	UG-9	UG-10
SiO_2	70,85	63,85	68,87	66,19	75,48
TiO_2	0,73	0,49	0,71	0,69	0,70
Al_2O_3	19,10	24,89	22,71	22,06	16,77
Fe_2O_3	2,18	0,99	0,52	0,32	0,45
MnO	0,01	0,00	0,00	0,00	0,00
MgO	0,06	0,20	0,34	0,15	0,32
CaO	0,05	0,09	0,05	0,00	0,03
Ma_2O	0,22	0,21	0,21	0,23	0,04
K_2O	0,00	0,88	1,91	0,56	2,13
P_2O_5	0,00	0,10	0,00	0,00	0,01
LOI	7,11	8,12	5,00	9,81	4,33
	100,30	99,82	100,32	100,01	100,25

Wts - Witteberg Shale, UG-ave - average of 5 Upper Gletwyn Clay samples, UG-6- to UG-10 Upper Gletwyn Clay samples taken at 2m intervals UG6 at top and UG10 at base. Ug-gf - Upper Gletwyn - 325 mesh, UG-sf - Upper Gletwyn suspension fraction.

A loss-gain diagram and a Barth plot below (see figure) show a nett loss in alkalis and Fe in the clay relative to the parent rock. The grit-free fraction and especially the suspension fraction show a large gain in K. This is probably due to a higher proportion of fine grained illite.

The diffraction traces showed the clay to consist of kaolinite, illite and quartz. A peculiarity of the diffraction traces of the Upper Gletwyn clay is that the peaks located in the 111, $11\bar{1}$ and 021 regions are not well defined although the electron micrograph shows that the clay consists of very well defined hexagonal plates of kaolinite. It can also be seen from the micrograph that the kaolinite crystals are up to 4 microns in diameter although most crystals are in the order of 2 microns (see plate 4.4).

A grain size analysis (see figure 4.12) shows that 40% of the clay is finer than 10 Ø and that a relatively low grit content of 11% is present although in grain size analysis past grit contents of up to 30% have been found (Eales, 1975).

A semi-quantitative analysis of the Upper Gletwyn clay was done by using the mica convention, the mixing program and the diffraction peak intensities. The results are given in table 4.8.

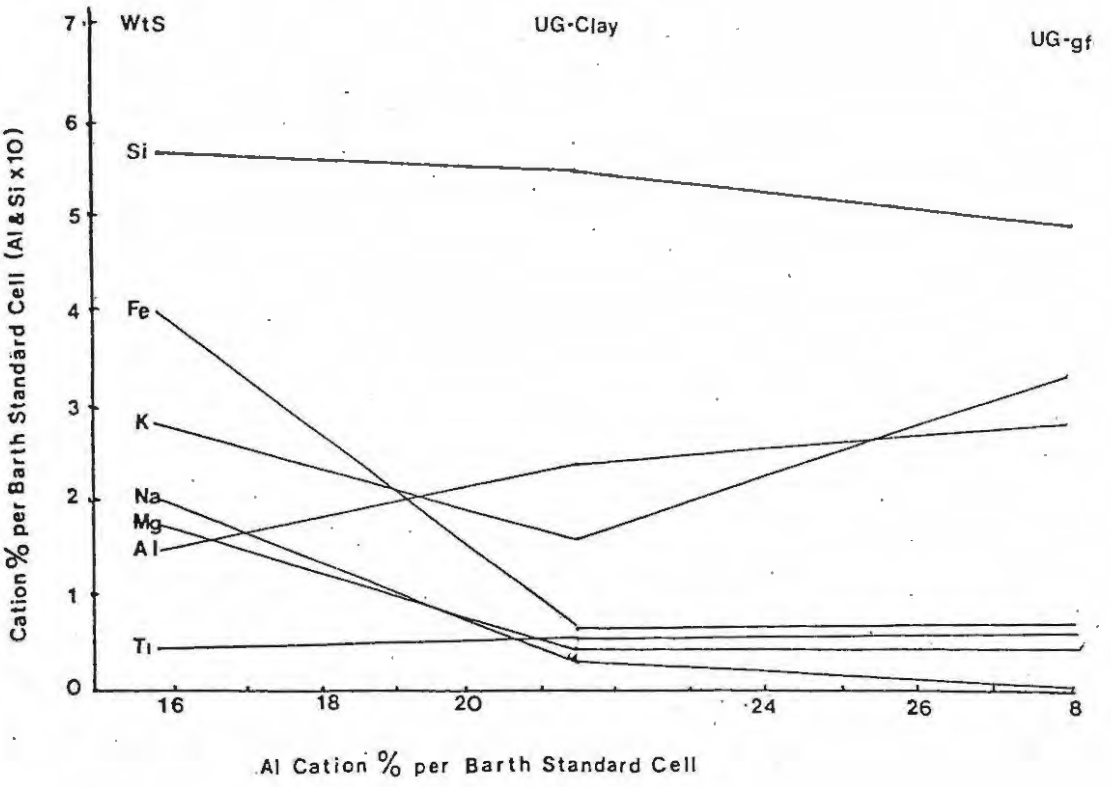

Figure 4.13 Barth Plot of the Upper Gletwyn clay.

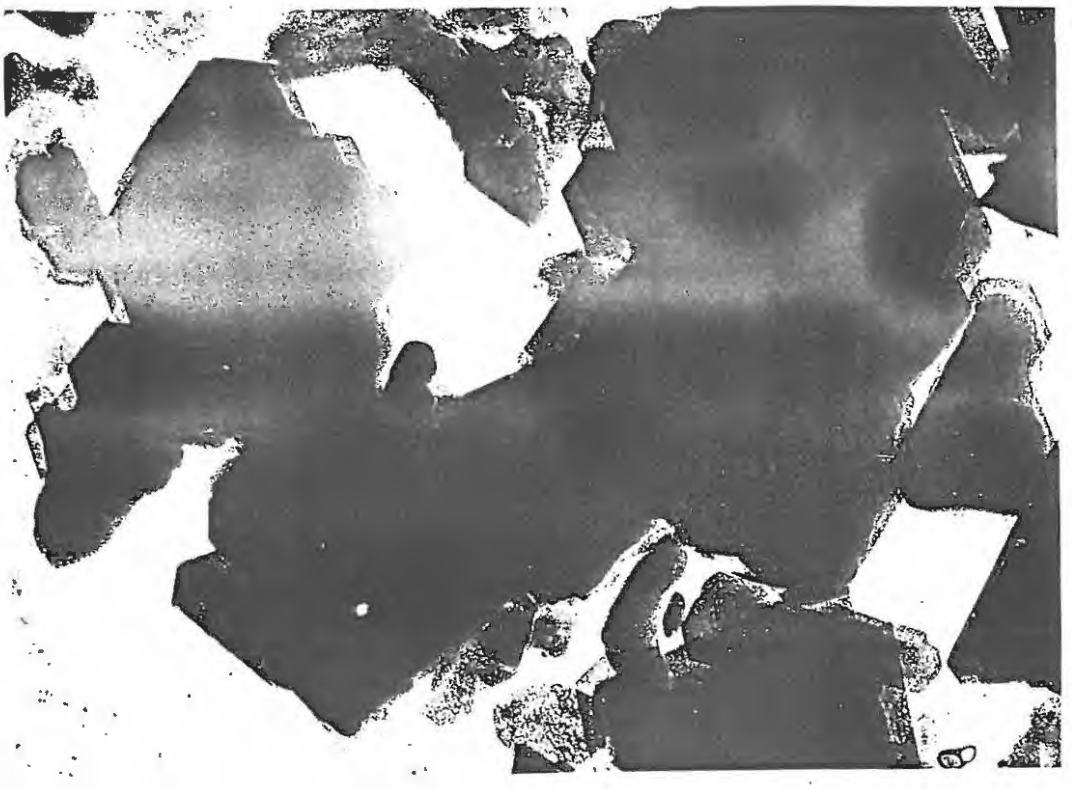

Plate 4.4 An electron micrograph of the Upper Gletwyn clay. Note the large hexagonal crystal of kaolinite.

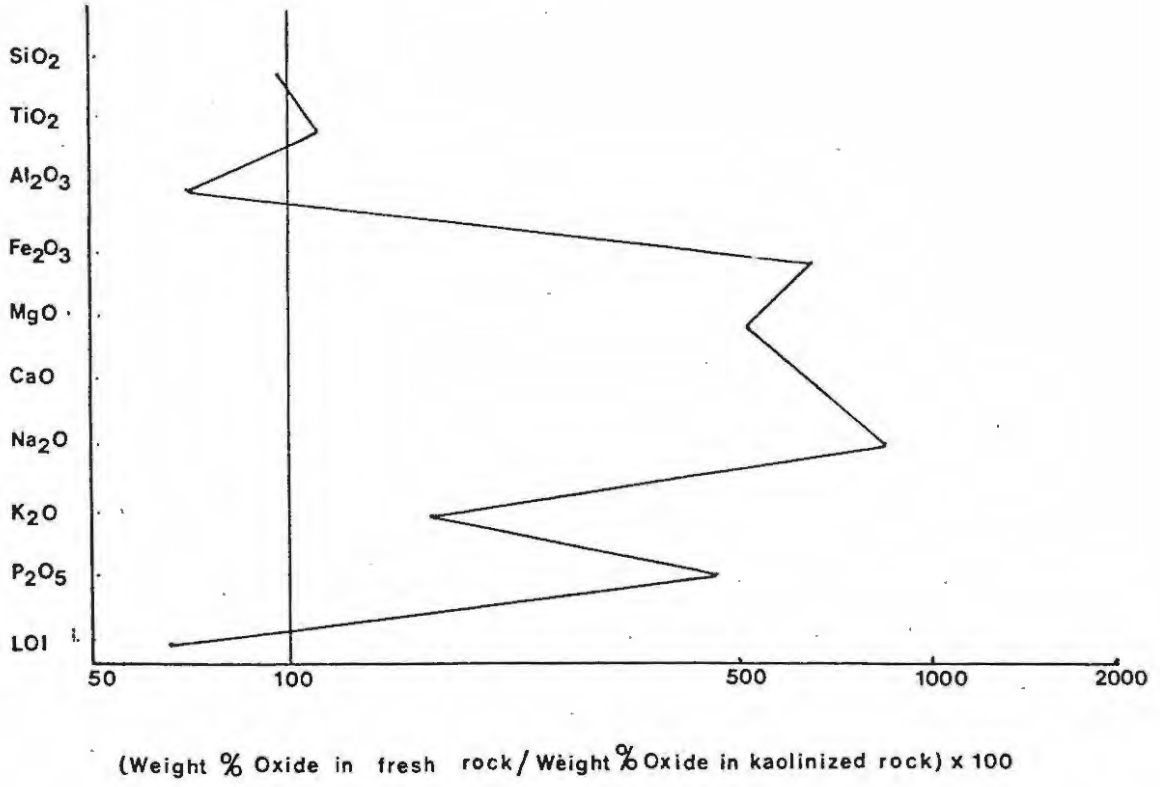

Figure 4.11 Loss/Gain of the Upper Gletwyn clay.

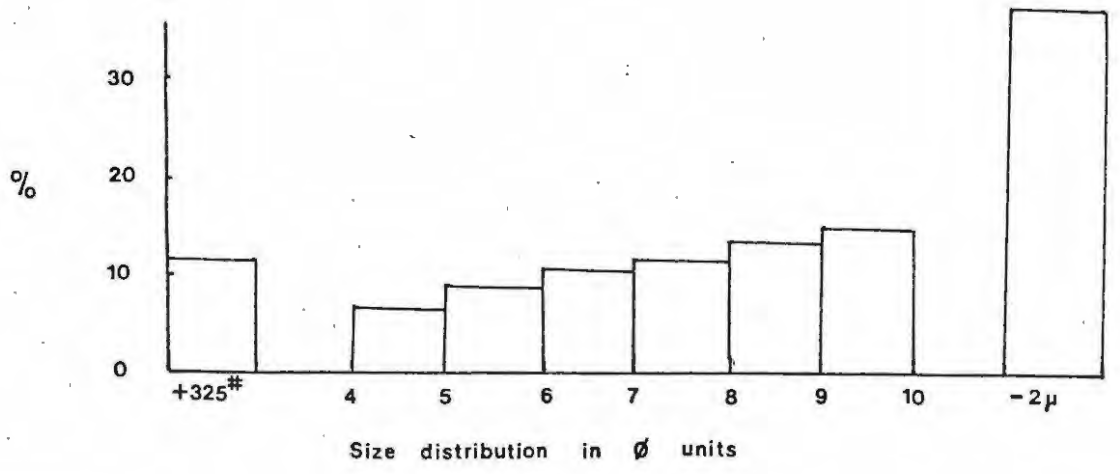

Figure 4.12 Size distribution of the Upper Gletwyn clay sample UG.9. It is apparent that this sample deflocculated particularly well.

Table 4.8

Mica Convention		Mixing Program		Diffraction	
Kmica	13,66	Illite	37,43	Illite	30
Namica	1,76				
Clay	42,56	Kaolite	36,60	Kaolinite	50
Quartz	40,91	Quartz	25,97	Quartz	20
	98,89		100,00		100

Again we can see that the results are in poor agreement with one another.

5. Wallace Deposit

Only one composite sample was taken from the Wallace deposit. The sample was of the stratigraphicaly higher variety of clay. The analysis of this sample, the grit free fraction and the analyses of the two varieties by the National Building Research Institute, CSIR (NBRI) are given below in the Table 4.9.

Table 4.9 Analyses of the Wallace Clay and associated rock

	WtS	W	W-gf	NBRI-1	NBRI-2
SiO_2	67,34	65,84	60,72	59,85	61,25
TiO_2	0,77	0,74	0,90	0,82	1,72
Al_2O_3	15,73	23,25	26,23	28,61	24,61
Fe_2O_3	6,26	0,57	0,68	1,03	1,84
Mno	0,04	0,00	0,00	-	-
MgO	1,48	0,14	0,19	1,24	0,40
CaO	0,34	0,00	0,01	0,93	0,24
Na_2O	1,22	0,22	0,21	0,34	0,18
K_2O	2,65	0,46	0,62	0,58	0,93
P_2O_5	0,16	0,01	0,02	0,00	0,00
LOI	3,91	7,71	9,71	6,44	8,60
	99,93	99,03	99,29	99,84	99,77

Wts - Witteberg Shale, W - Wallace Clay, W-gf - Wallace Clay -325microns, NBRI-1 - National Building Research analysis.

The electron micrograph of the Wallace clay sample shows very well developed hexagonal crystals of kaolinite of up to 4 microns in diameter.

Plate 4.5 Electron photomicrograph of the Wallace clay showing large, well formed hexagonal plates of kaolinite.

The diffraction traces of the Wallace clay show it to consist of Kaolinite, illite and quartz. Distinct peaks are seen in the 111, 110 and 021 regions which ties up with the good crystal perfection shown in the electron micrograph. No other minerals were detected although the NBRI detected some feldspar.

The stratigraphically highest type of Wallace clay is very similar to the Upper Gletwyn clay and the second type is very similar to the Webber clay. A grain size analysis of the Wallace clay shows a grit content of 11,2% and 29% of the clay is finer than 10 Ø. The particle size distribution is the same as that of the Upper Gletwyn clay.

6. Strowan

Ten samples were taken from the Strowan quarry in a series from just beneath the surface, (S1), to the base of the quarry, (S10). These samples were all taken from the eastern face of the quarry. Places with macroscopically visible iron oxide and quartz were avoided. The average of these analyses, Ecca Shale and the NBRI analysis for Kaolin-G are given in the table 4.10.

Table 4.10 Analyses of the Strowan Clay

	DS	DS-w	S-ave	S-gf	Kaolin -G	S-1	S-2	S-3
SiO_2	68,19	67,95	68,29	58,38	66,83	70,65	79,87	71,10
TiO_2	0,50	0,63	0,58	0,64	0,74	0,49	0,43	0,40
Al_2O_3	15,46	16,35	21,24	29,57	21,52	16,74	13,83	20,88
Fe_2O_3	6,02	5,68	0,30	0,16	0,45	0,25	0,12	0,22
MnO	0,05	0,01	0,00	0,00	-	0,01	0,00	0,00
MgO	1,29	0,95	0,40	0,14	0,22	0,37	0,10	0,12
CaO	0,16	0,05	0,31	0,07	0,84	2,38	0,04	0,09
Na_2O	0,34	0,77	0,97	1,02	0,80	0,80	0,52	0,79
K_2O	2,53	3,01	2,17	1,75	2,75	1,65	3,64	1,02
P_2O_5	0,03	0,07	0,06	0,07	0,00	0,03	0,02	0,06
LOI	4,64	4,74	5,86	8,33	6,07	6,77	4,38	6.05
	99,34	100,21	100,18	100,13	100,22	100,11	99,95	100,73

	S-4	S-5	S-6	S-7	S-8	S-9	S-10
SiO_2	70,68	74,13	60,61	58,74	64,512	65,08	67,51
TiO_2	0,51	0,64	0,57	0,63	0,65	0,86	0,62
Al_2O_3	20,11	16,62	27,75	29,34	24,41	20,83	21,87
Fe_2O_3	0,25	0,27	0,22	0,26	0,35	0,69	0,37
MnO	0,00	0,00	0,00	0,00	0,00	0,00	0,00
MgO	0,16	0,21	0,13	0,19	0,24	1,16	0,72
CaO	0,08	0,19	0,07	0,10	0,05	0,04	0,05
Na_2O	1,03	1,59	1,60	0,98	0,81	0,96	0,65
K_2O	1,70	2,02	1,58	2,18	3,26	4,10	3,35
P_2O_5	0,10	0,14	0,05	0,08	0,05	0,04	0,04
LOI	5,67	3,84	7,72	7,67	5,48	5,85	5,14
	100,29	99,65	100,30	100,17	99,81	99,61	100,32

The above abbreviations are as follows:

DS - Ecca Shale, DS-w - Ecca Shale weathered, S-ave - average of 10 Strowan clay samples, S-gf - grit free Strowan clay, Kaolin-G - NBRI Strowan clay analysis, $S1^{-S10}$ at surface to S10 at base of quarry at 2m intervals on eastern face.

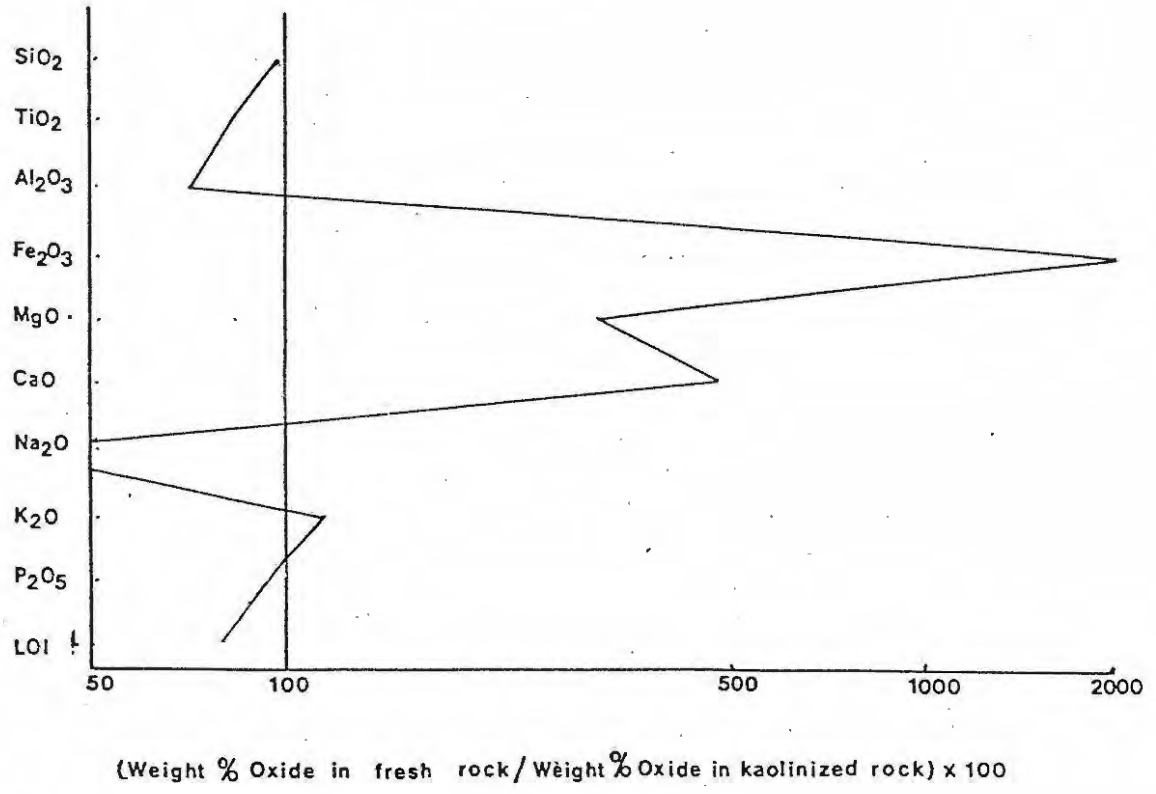

Figure 4.14 Loss/Gain diagram of the Strowan clay.

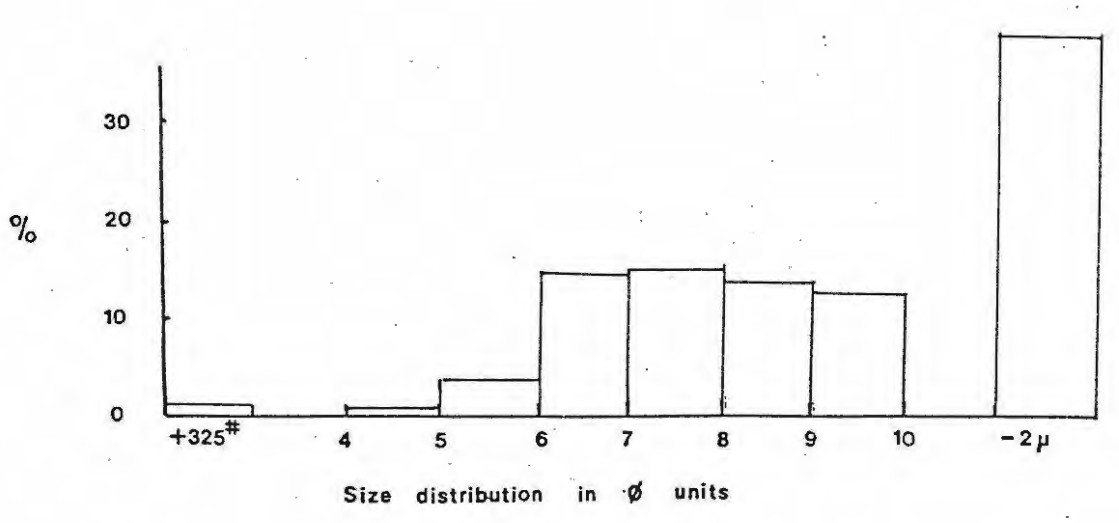

Figure 4.15 Size distribution of the Strowan Clay.

Plate 5.5 An electron micrograph of the Strowan clay. Note the aggregates of hexagonal crystals of kaolinite.

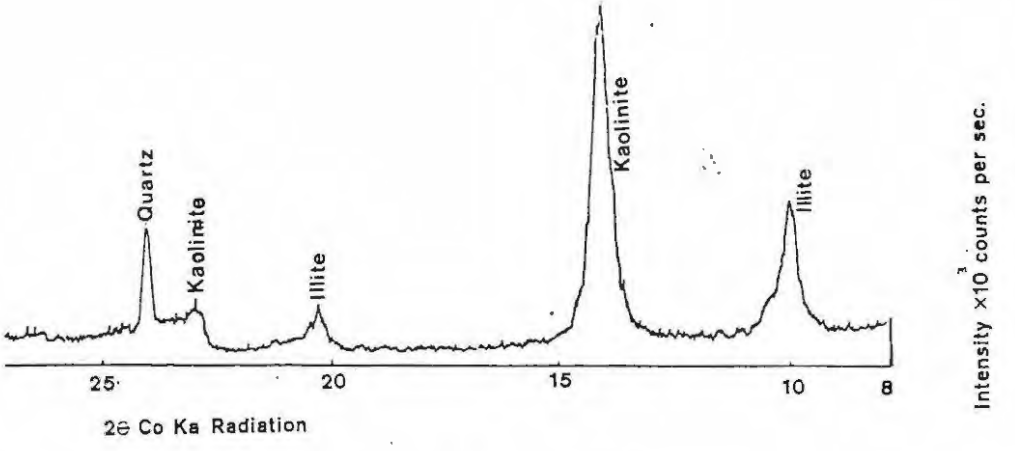

Fig. 4·15a Diffraction trace of Strowan clay

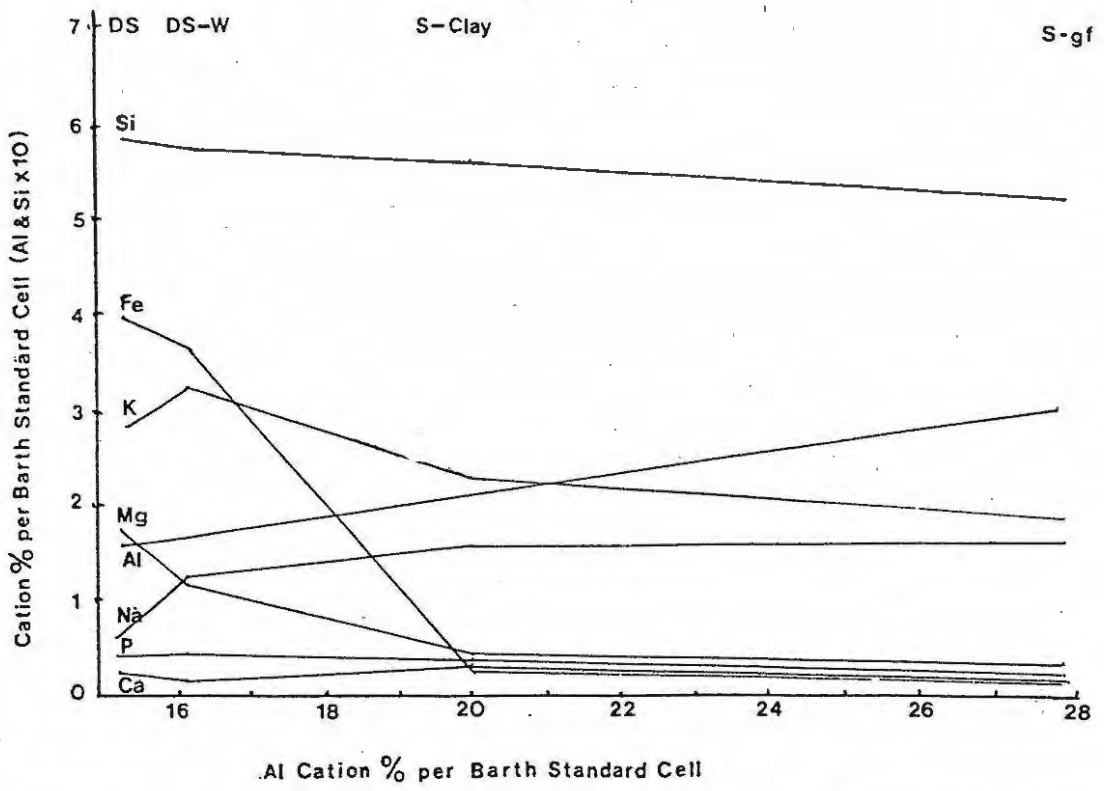

Figure 4.16 Barth Plot of the Strowan clay, DS - Ecca Shale, DS-W - Ecca Shale weathered, S - Strowan, S- - Strowan -325 fraction.

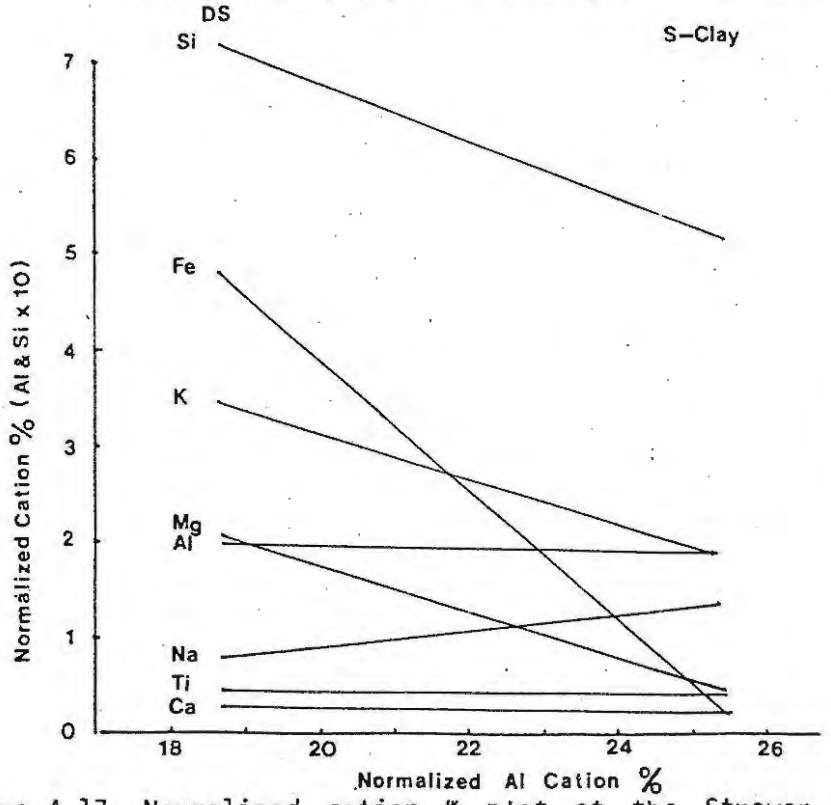

Figure 4.17 Normalized cation % plot of the Strowan clay, ES - Ecca Shale, S-ave - Average of 10 Strowan clay samples.

The electron micrograph of the Strowan clay shows sub-angular platy particles of illite and aggregates of hexagonal kaolinite particles. The diffraction traces of the Strowan clay show the clay to consist of illite, kaolinite and quartz. The kaolinite is not well ordered as is reflected in the diffraction trace and the electron micrograph.

A grain size analysis of the clay shows 1,5% of grit and 38% of the clay finer than 10 μ. This clay, the Coronation clay and the NBRI 'Palmer' clay, which is different to the Palmer deposit are all derived from the Ecca Shales and are in close proximity to one another.

7. Palmer Deposit

Five samples were taken from the Palmer quarries. Two were taken from the Palmer 1 deposit and three were taken from the Palmer 2 deposit. The samples taken were devoid of visible iron oxide and a sample was taken of the 'secondary' clay in the 'ghost fractures'. The analyses of the clay and Dwyka Tillite are given in the table Table 4.11

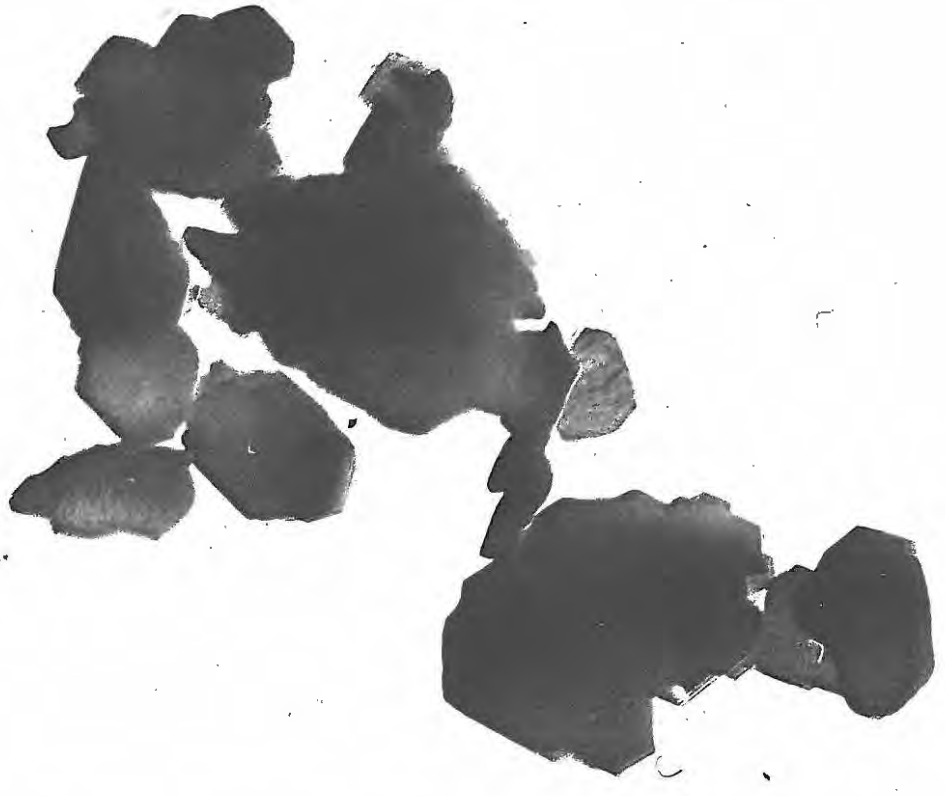

Plate 4.6 An electron micrograph of the Palmer clay. Note the very well formed hexagonal crystals of kaolinite and the 'book' structures at the edge of the crystals in the top left side of the micrograph.

Table 4.11 Analyses of the Palmer clay and Dwyka Tillite

	DT	DT-w	P-ave	P-gf	P-s	Kaolin-GP
SiO_2	67,63	68,83	63,89	62,20	49,30	64,67
TiO_2	0,66	0,66	0,76	0,84	0,13	0,76
Al_2O_3	13,98	14,51	24,87	26,55	37,26	23,99
Fe_2O_3	5,81	5,52	0,43	0,27	0,17	0,61
MnO	0,08	0,05	0,00	0,00	0,00	-
MgO	2,32	1,43	0,22	0,15	0,03	0,32
CaO	1,36	1,03	0,02	0,01	0,01	0,07
Na_2O	2,89	2,52	0,19	0,18	0,20	0,13
K_2O	2,97	3,00	0,50	0,59	0,00	0,76
P_2O_5	0,14	0,11	0,00	0,00	0,00	0,02
LOI	2,11	2,91	8,05	9,34	13,31	8,68
	99,34	100,57	98,38	100,13	100,41	100,01

	P1	P2	P3	P4	P5
SiO_2	66,62	66,36	67,28	66,42	52,78
TiO_2	0,71	0,68	0,70	0,80	0,93
Al_2O_3	22,69	23,39	23,15	22,49	32,61
Fe_2O_3	0,32	0,41	0,31	0,33	0,80
MnO	0,00	0,00	0,00	0,00	0,00
MgO	0,14	0,18	0,12	0,15	0,53
CaO	0,00	0,00	0,00	0,01	0,07
Na_2O	0,18	0,20	0,19	0,20	0,19
K_2O	0,47	0,49	0,49	0,56	3,59
P_2O_5	0,00	0,00	0,00	0,00	0,06
LOI	7,98	8,24	8,08	7,91	8,06
	99,11	99,95	100,32	98,67	99,62

The above abbreviations are as follows:

DT - Dwyka Tillite, DT-w - Dwyka Tillite weathered, P-ave - average of 5 Palmer clay samples, P-gf - grit free Palmer clay, P-s - 'secondary' clay and Kaolin-GP - NBRI analysis of Dwyka Tillite clay, P1 top of Palmer 1 quarry and P2 at base, P3 at top of Palmer 2 quarry and P4 at base, P5 fine fracture filling caly in Palmer 2.

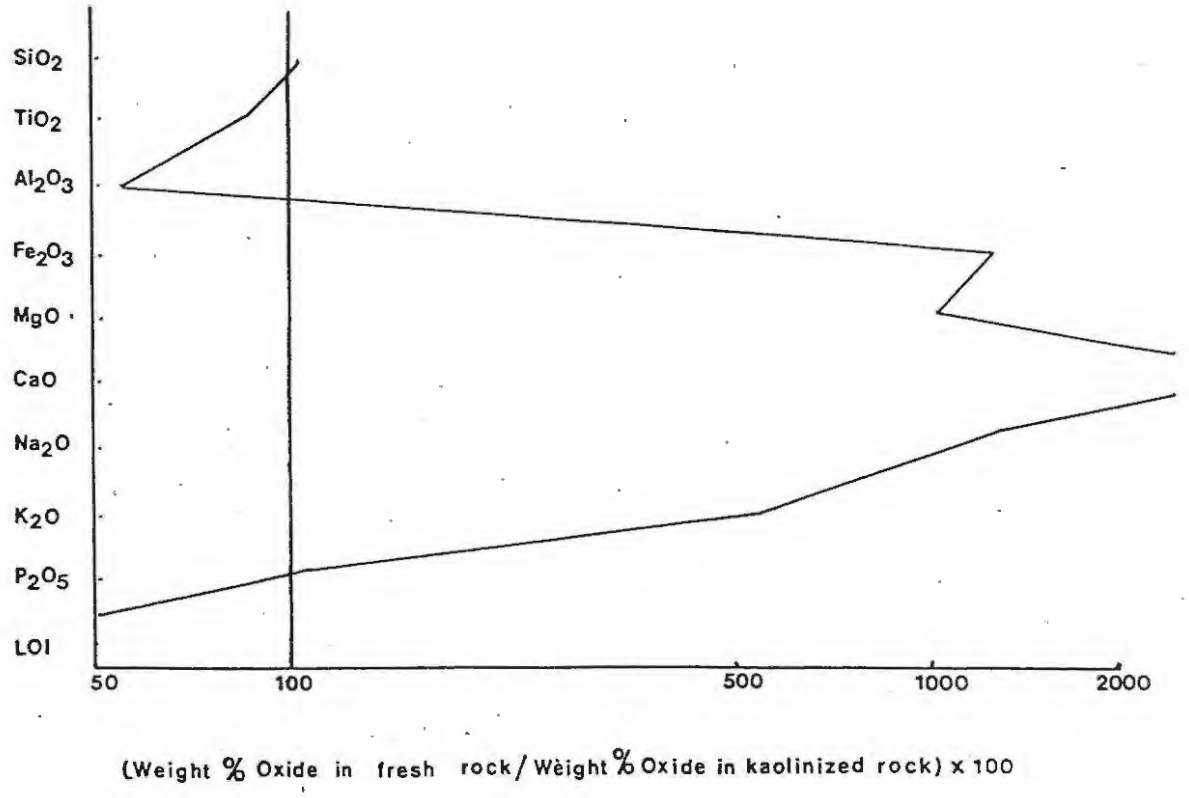

Figure 4.18 Loss/Gain Plot of the Palmer clay.

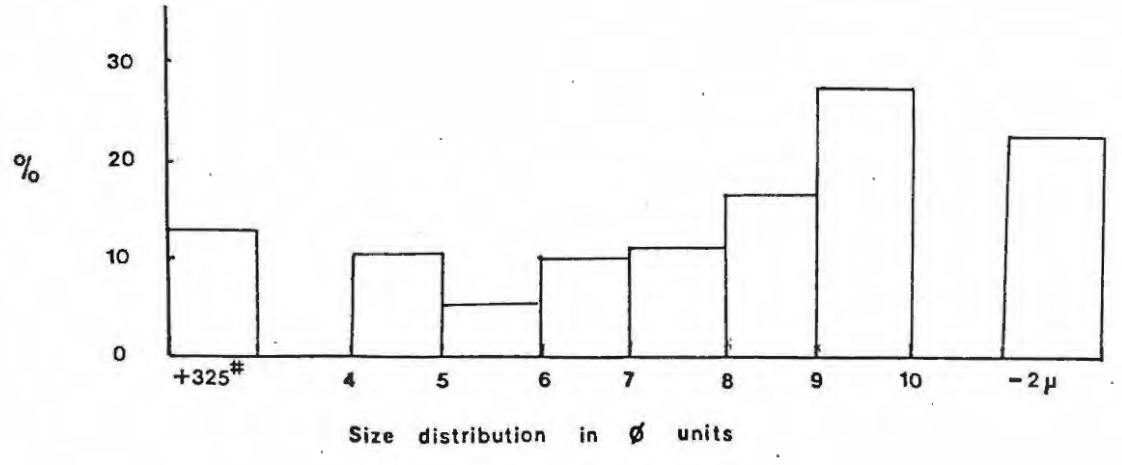

Figure 4.19 Size distribution of the Palmer clay.

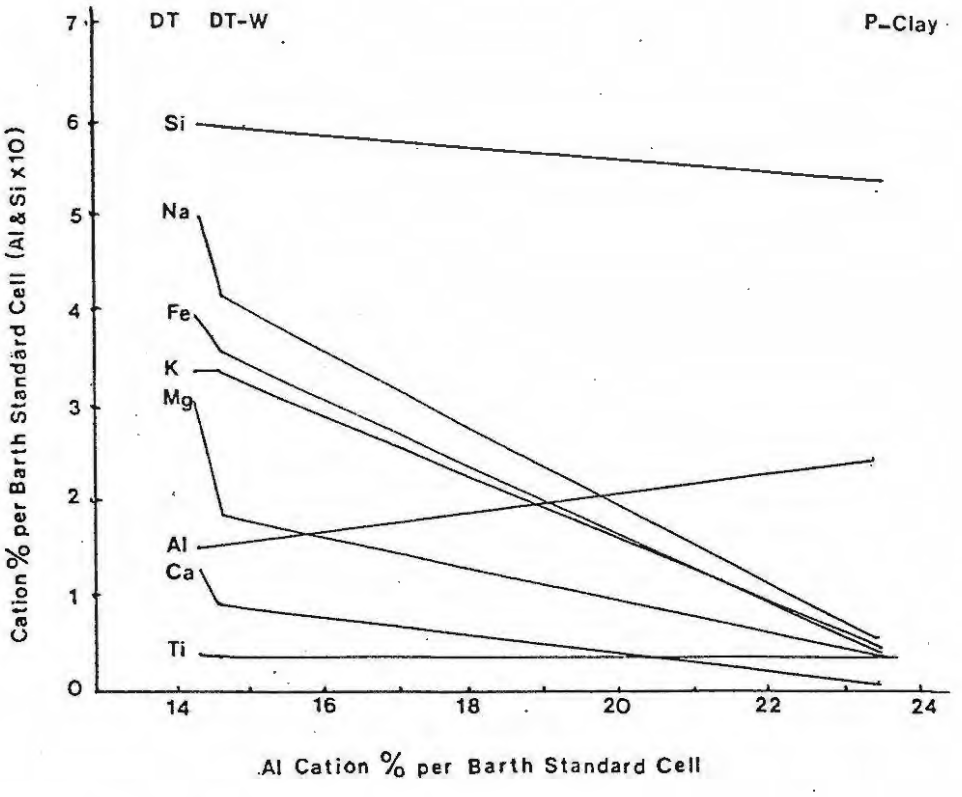

Figure 4.20 Barth plot of the Palmer clay.

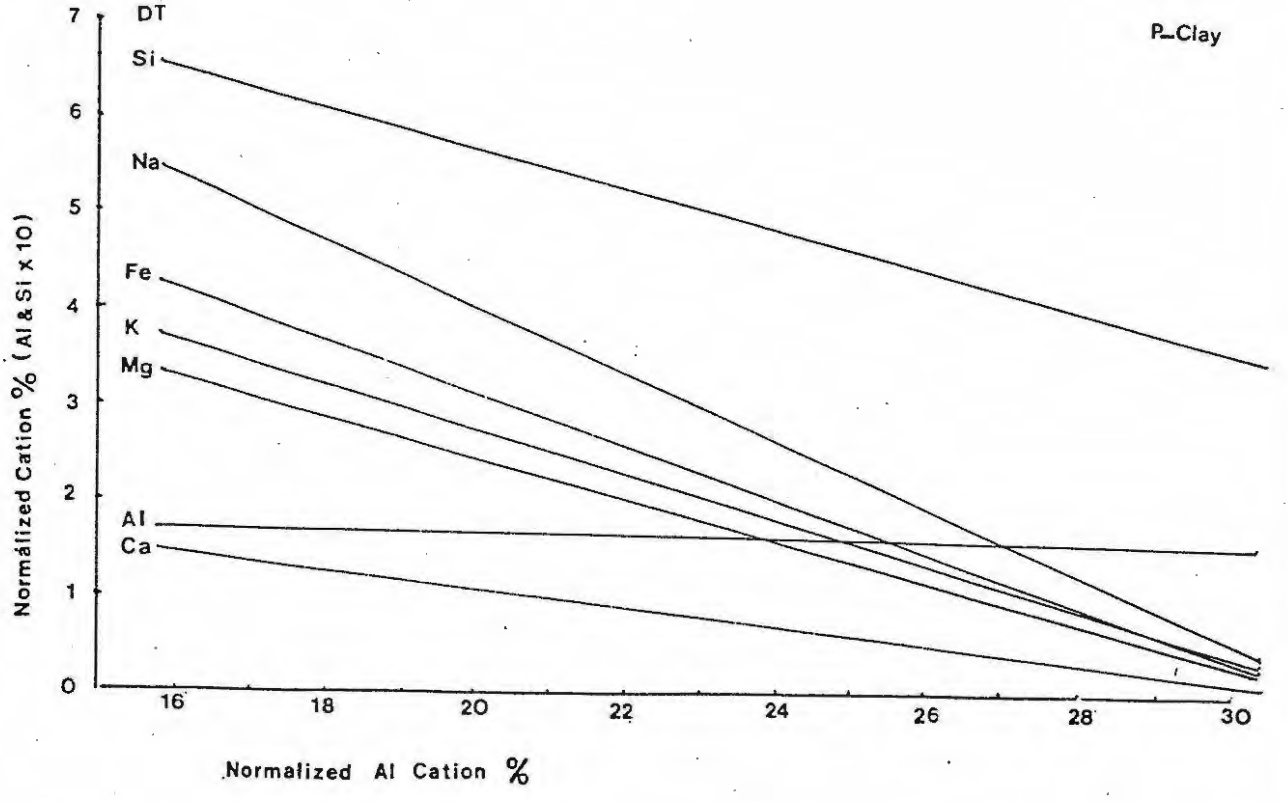

Figure 4.21 Normalized cation percentage plot for the Palmer clay.

Diffraction traces of the clay show that the clay has very good crystallinity. The $11\bar{1}$, $1\bar{1}\bar{1}$ and $02\bar{1}$ peaks are very clearly defined. Quartz, illite and kaolinite are detected but very little illite is present. The P-s trace shows almost no quartz and no illite present in the sample. The analysis of the P-s sample shows that it most closely represents pure kaolinite.

The electron micrograph of the Palmer clay shows very well developed hexagonal crystals of kaolinite up to 3 microns in diameter. Some of the crystals show multiple edges which indicates that the kaolinite grains are stacked directly over one another.

A grain size analysis of the Palmer clay shows a grit content of 13,1% and 21,5% of the clay finer than 10 Ø. A histogram of the grain size analysis is shown in figure 4.19. A loss-gain diagram and a Barth plot are shown in figures 4.18 and 4.20.

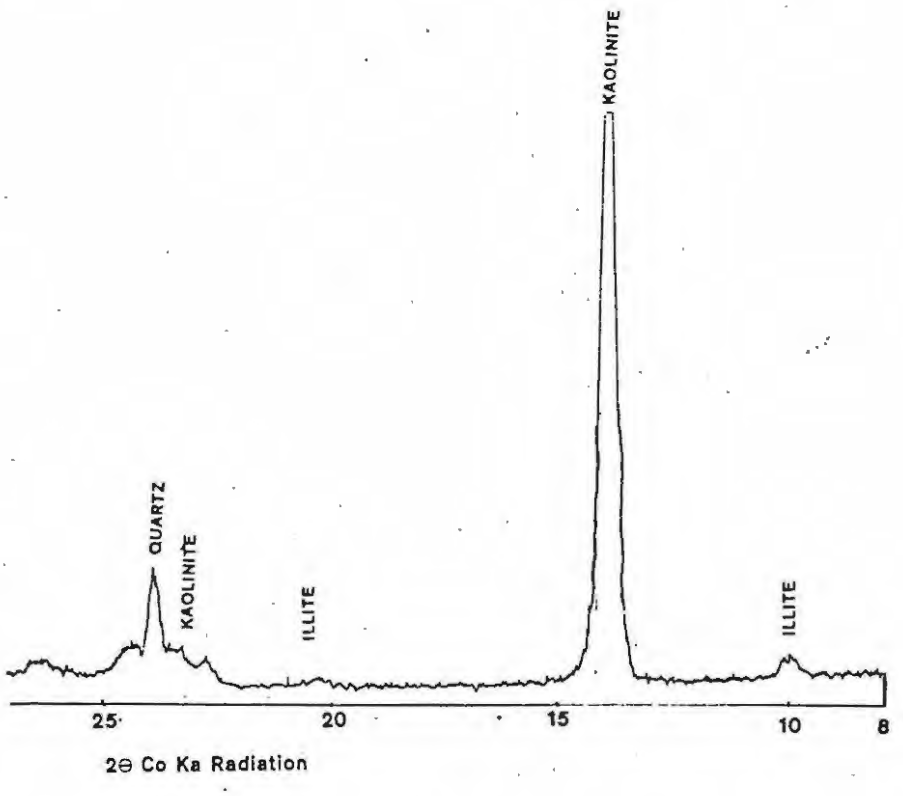

Fig 4.22 Diffraction trace of Palmer clay

There is a correlation between the K_2O concentration and the intensity of the illite 001 peak for most of the clay. An example of this is provided by the UG6, UG7 and Ug9 samples. UG6 has no detectable K_2O and shows no illite 001 peak, UG7 has a relatively low percentage of K_2O, (0,88%), and shows a small illite peak, and UG9 (which has 3,14% K_2O) shows a substantial illite peak.

The grit-free fractions of clay (325 mesh), show an increase in K_2O% relative to crude clay. The suspension fraction (2-4 micron) for the Upper Gletwyn clay shows a larger increase in K_2O%. The increase in K_2O% in the fine fraction is due to the removal of quartz which forms the greatest proportion of the coarse material. The removal of silica in the form of quartz results in a proportional increase in the other elements, notably K_2O and Al_2O_3 which form the greatest proportion of the remaining elements.

K_2O concentrations rarely exceed 3%. Generally higher K_2O concentrations are found in the Coastal Plain deposits which also tend to show higher illite contents. It could therefore be assumed that most of the potassium is incorporated in the illite.

Sodium is of little consequence in the Grahamstown clays and rarely exceeds concentrations of over 1% Na_2O. Total alkalis are usually below 4% in concentration and the clay is consequently quite acceptable to industry which usually requires clay to have less then 5% total alkalis.

2. Alkali earths

Calcium and magnesium are minor elements in the Grahamstown clay, and together rarely exceed 1%. The illustrative plots show that both calcium and magnesium are depleted relative to the parent rack. The absence of magnesium supports the diffraction evidence for absence of chlorite and montmorillonite.

The only sample analysis which shows any appreciable amount of calcium is the S1 sample taken from just below the silcrete in the Strowan deposit. Apparently calcium concentration at the surface used to cause problems with the clay in the initial quarrying operations but is no longer a significant factor. The concentration of calcium at the surface is

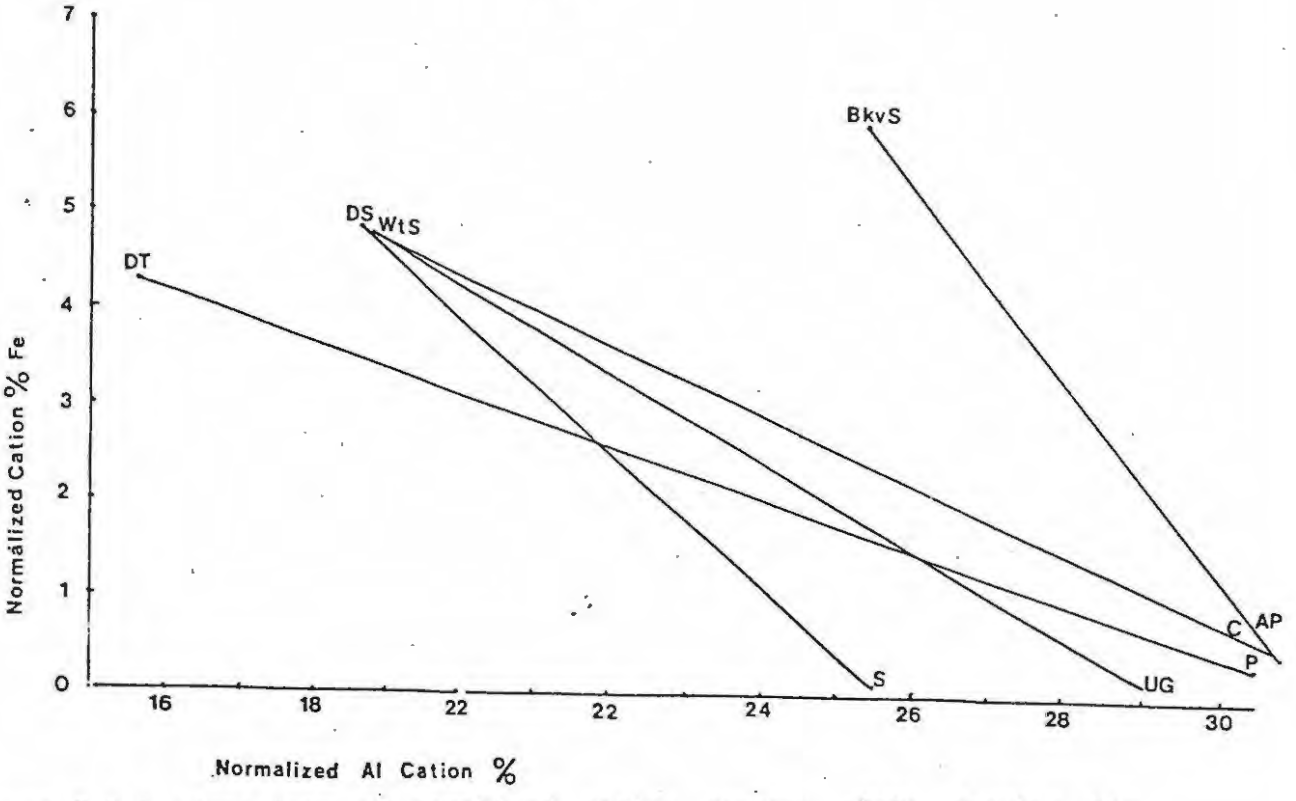

Figure 5.2 A comparison of nomalised cation percent plots showing the relative loss of Fe in parent rock relative to clay. S-Strowan, C-Crous, P-Palmer, UG-Upper Gletwyn, AP-Avenue Park. DT-Dwyka Tillita, ES-Ecca Shale, Wts-Witterberg Shale. BkvS-Bokkeveld Shale

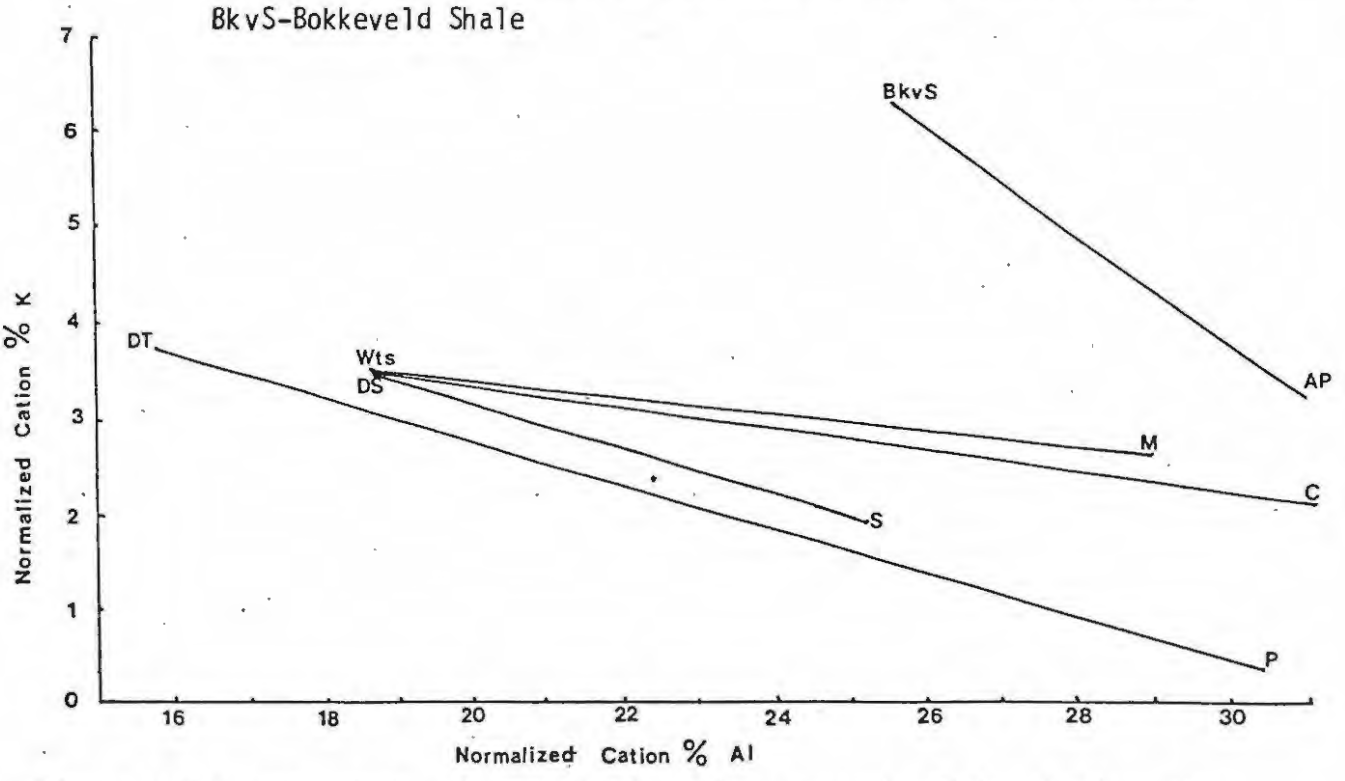

Figure 5.3 A comparison of nomalised cation percent plots showing the relative loss of K in parent rock relative to clay. S-Strowan, C-Crous, P-Palmer, UG-Upper Gletwyn, AP-Avenue Park. DT-Dwyka Tillita, ES-Ecca Shale, Wts-Witterberg Shale. BkvS-Bokkeveld Shale

probably caused by calcium in solution moving to the surface by capillary action and movement of water table, and precipition in the drier environment on evaporation of water.

3. Iron

Iron shows the greatest depletion in the clay relative to the parent rock. This is well illustrated in the loss gain diagrams. Iron appears to be mobilised at an early stage because weathered, but poorly kaolinised Dwyka Tillite shows an apparent loss of iron. This is in disagreement with similar loss-gain diagrams of granites and basalts by Garrels and McKenzie (1971).

There is a slight increase in the concentration of iron with depth. Samples S1 to S9 from the Strowan deposit show this trend. Often the clay just below the surface shows a substantial increase in iron. Examples of this trend are sample S1 from Strowan and UG6 from Upper Gletwyn. The increase of iron at surface indicates that iron has migrated to the surface and precipitated in the same way as Ca.

Iron in the clay is in the form of limonite. The limonite often adheres to the surface of the kaolinite crystals and sometimes forms spherulitic aggregates. These characteristics of the limonite are illustrated in the electron micrographs from Upper Gletwyn (Plate 5.1).

SiO_2/Al_2O_3

A plot of Al_2O_3 against SiO_2 is not very meaningful as SiO_2 plus Al_2O_3 constitute approximately 90% of the clay and as a result increase in SiO_2 shows a sympathetic decrease in Al_2O_3 automatically. What is of note in the change in ratio of SiO_2 to Al_2O_3 for the clay from different deposits and the change in this ratio in the grit free samples. An increase in the SiO_2/Al_2O_3 ratio shows an increase in the amount of free quartz in the clay which can be confirmed by XRD. The general tendancy is for the Peneplane deposits to have a higher proportion of silica relative to the Coastal Plain deposits but on a grit free basis they are all in the same field.

Table 5.1 Trace Element Contents (ppm) in Clay Samples

	Nb	Zr	Y	Sr	Rb	Co	Cr	V	Zn	Cu	Ni	Ce	Nd	La
AP 9	24	240	50	350	226				5	19	6			
AP 10	22	244	58	325	197				9	14	7	160	69	89
AP 16	17	458	107	953	194	1	188	155	9	16	4	305	130	166
AP 19	24	287	62	563	198				2	15	1			
AP 20	27	333	53	527	160							166	70	90
AP 22	24	297	49	449	156	1	99	108						
AP 29	25	352	54	432	141				15	24	8			
UG 6	13	398	10	18	1				3	6	4	25	6	13
UG 7	9	317	20	252	36	1	98	38	3	4	3	296	94	175
UG 8	14	354	34	18	82				5	6	2			
UG 9	14	270	26	103	110	1	86	66	9	3	4	124	65	61
UG 10	13	512	19	47	90				6	2	3			
S 1												92	43	49
S 2									3	6	13			
S 3									13	10	19	75	41	33
S 7									6	11	13	92	45	47
S 8									19	30	5			
S 10									3	5	8			
P 1									3	5	5			
P 2									4	5	11	15	3	2
P 3									3	6	3	36	13	13
P 4									3	3	1			
P 5									3	3	1	20	9	8
M 1									10	23	7	165	82	88
M 2									5	15	4	145	69	74
C 1									6	18	9	129	55	86
C 2									11	20	61	180	84	89
C 3									4	8	3	137	58	79
W 1									5	7	1	131	87	52
D T									76	24	28			
DS									85	45	32			
WS									149	39	70			

Trace element analyses were done on a number of clay samples to determine whether significant trends exist. Trace element analyses have been used in studies of clays by Triplehorn (1970), to show movement of major elements during alteration. The analyses in the present study were done on the same samples prepared for sodium analysis. The standards used for determining the trace element concentrations included the following international rock standards; AGV, GSP, BCR and G. Details of the instrumental settings and method of analysis are given in the Appendix.

Trace element concentrations determined include Niobium, Zirconium, Yttrium, Strontium, Rubidium, Cobalt, Chromium, Vanadium, Zinc, Copper, Nickel, Cerium, Neodinium and Lanthanum.

The only really significant trend in the trace elements is the good correlation of $K_2O\%$ and Rb. This is expected because of the same valencey and similar ion size i.e. K 1.33Å and Rb 1.48Å (see figure 5.4).

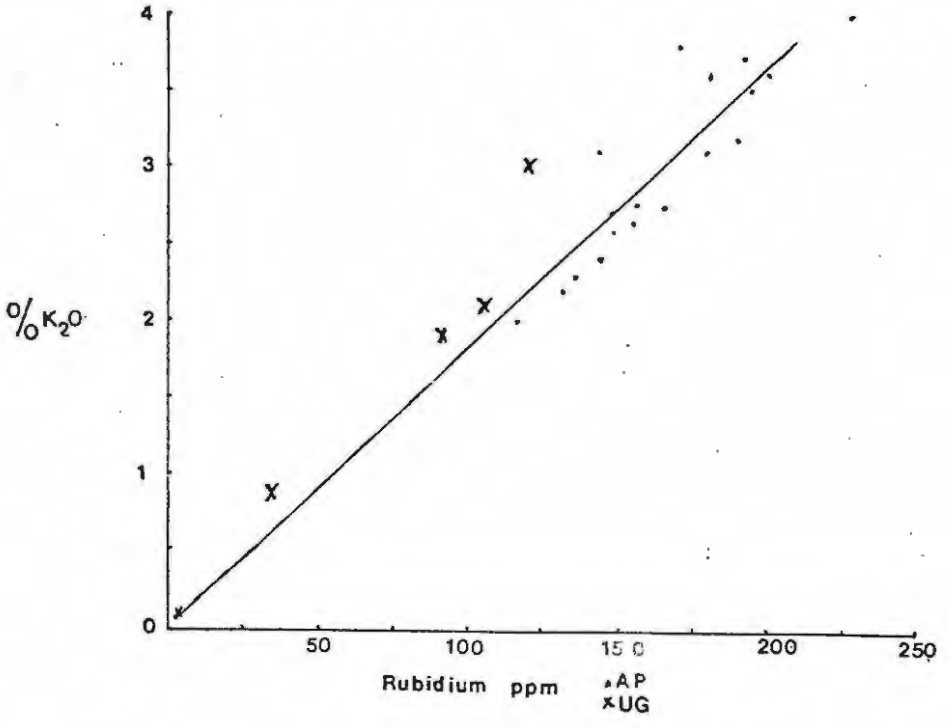

Figure 5.4 $K_2O\%$ and Rubidium PPM for the Avenue Park and Upper Gletwyn Clays.

Mineralogy of the seven deposits

XRD studies show that all the deposits contain kaolinite, illite and quartz and only the Coastal Plain deposits show the presence of pyrophyllite in addition to the other minerals. Limonite is present in all of the clays but cannot be identified by XRD techniques. Electron micrographs however, are able to show lath-like particles of limonite and in some cases spherulitic aggregates of limonite.

The kaolinite of the Coastal Plain deposits is different to that of the Peneplane deposits. Generally the kaolinite crystals of the Coastal Plain are smaller, anhedral and show some disorder. Electron micrographs show the difference in size and morphology quite distinctly and electron diffraction and XRD show the poor order and crystallinity. The kaolinite from the Peneplane deposits is generally of larger crystal size and the crystals are hexagonal plates. The Palmer clay is especially well crystallised and shows good ordering and crystallinity in both the electron diffraction micrographs and the XRD traces.

The Coastal Plain deposits have, in general, a higher proportion of illite than the Peneplane deposits. However, the clay in the lower part of the Wallace deposit also shows a high proportion of illite. Physically, the clay with high illite content is also more plastic.

The quartz content of the Peneplane deposits is also higher then the Coastal Plain deposits and as a result these clays are also more friable and less plastic. However, if the grit-free clay of the Peneplane deposits is compared to the Coastal Plain clay there is no great textural difference.

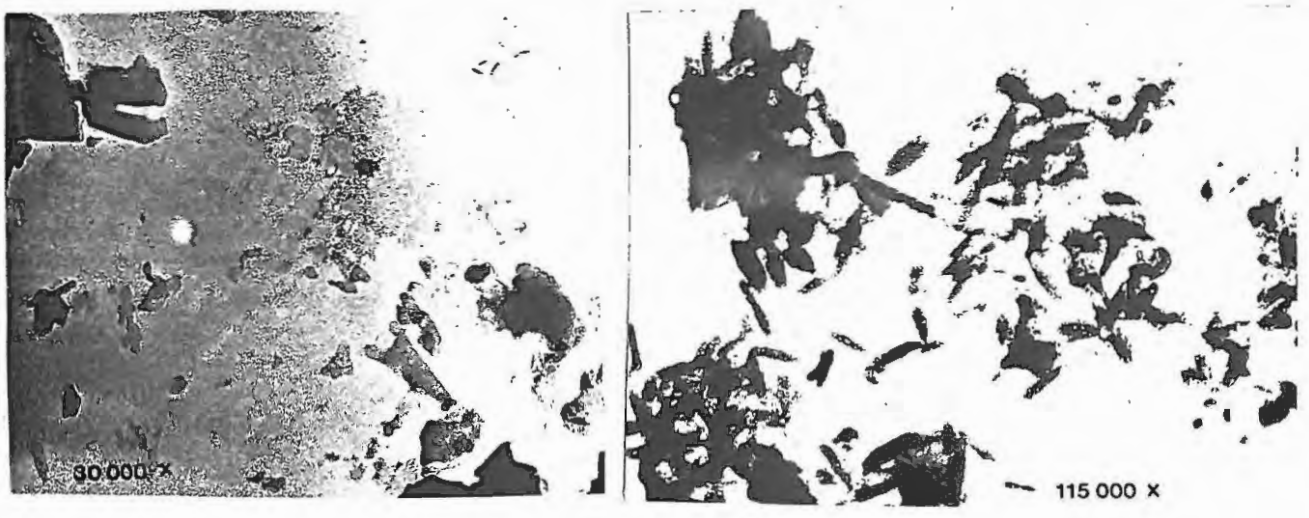

Plate 5-1 Limonite particles in the Avenue Park clay

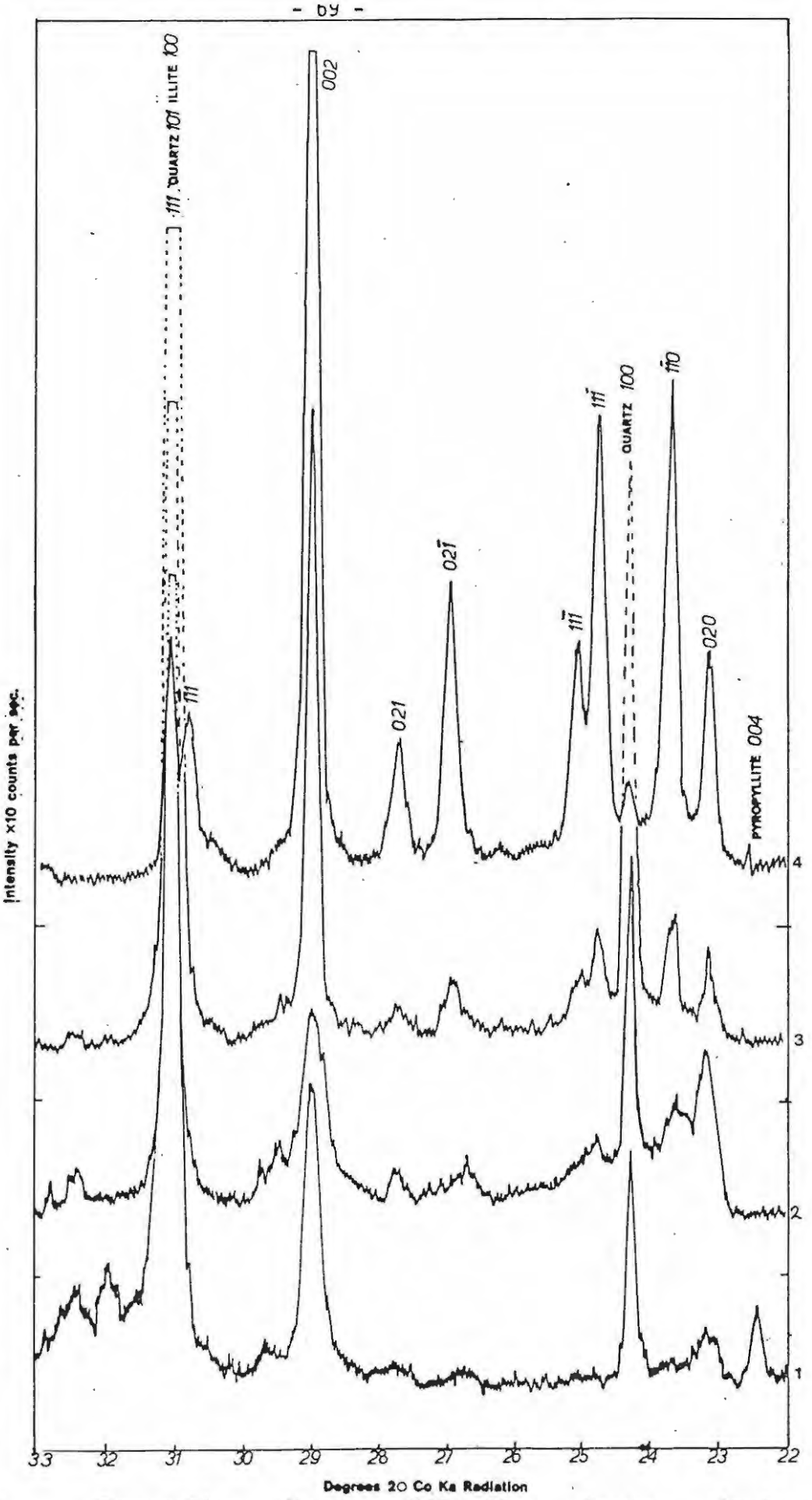

Figure 5.5 Comparative X-ray diffraction traces showing differences in crystallinity and the influence of quartz percentage on diffraction peak intensity. 4) Palmer P3A 3) Palmer 5 2) Strowan 1) Crous. Note: the decrease in intensity of the kaolinite between 4) and 3) because of the quartz dilution factor and the poorer crystallinity of the Strowan 2) and Crous 1) clays.

Figure 5.5 illustrates the differences in crystallinity of the Palmer 'secondary', Palmer, and Strowan and Crous kaolinite. The intensity of the 020, 110, 111 and 021 between the 'secondary Palmer and Palmer clay are affected by the dilution effect of quartz but the ratio of the 110 to 020 is still in the same order. However, in the diffraction trace of the Strowan kaolinite the ratio of the 020 to 110 has reversed and in the Crous kaolinite the 110 reflection has almost disappeared. In addition the 021 and 111 reflections are depressed in the Crous kaolinite relative to the Strowan kaolinite despite the fact that the Strowan clay has a higher quartz content and therefore more dilution.

The electron micrographs of the Palmer and Avenue Park kaolinite, plates 5.2a and 5.3a respectively, with the accompaning electron diffraction photomicrographs, plate 5.2b and 5.3b respectively, illustrate the difference between well ordered, well crystallised kaolinite and poorly ordered, poorly crystallised kaolinite.

The electron diffraction photomicrographs are of the recipricol lattice and therefore the spots closest to the origin have the largest d spacings and the spots furthest from the origin are the smallest d spacings. Magnification is approximately 43,500 times and details of the instrumental conditions and formula to work out d spacings are in the appendix.

The large spots in plate 5.2b are the reciprocal points of lattice d 1.49Å of kaolinite which has an I/Ii of 90 which is the second most intense reflection of kaolinite. The only reflection which is more intense is the d 7,16Å which is the plane 001 which is perpendicular to the beam and cannot be shown.

Plate 5.3b, the electron diffraction photomicrograph of the Avenue Park kaolinite shows multiple reflections which possibly indicates a degree of disorder in the crystal. The particular crystal, as photographed in plate 5.3a, is considerably thinner than the Palmer kaolinite crystal. To photograph this crystal the beam current of the transmission electron microscope had to be turned down otherwise no image could be formed.

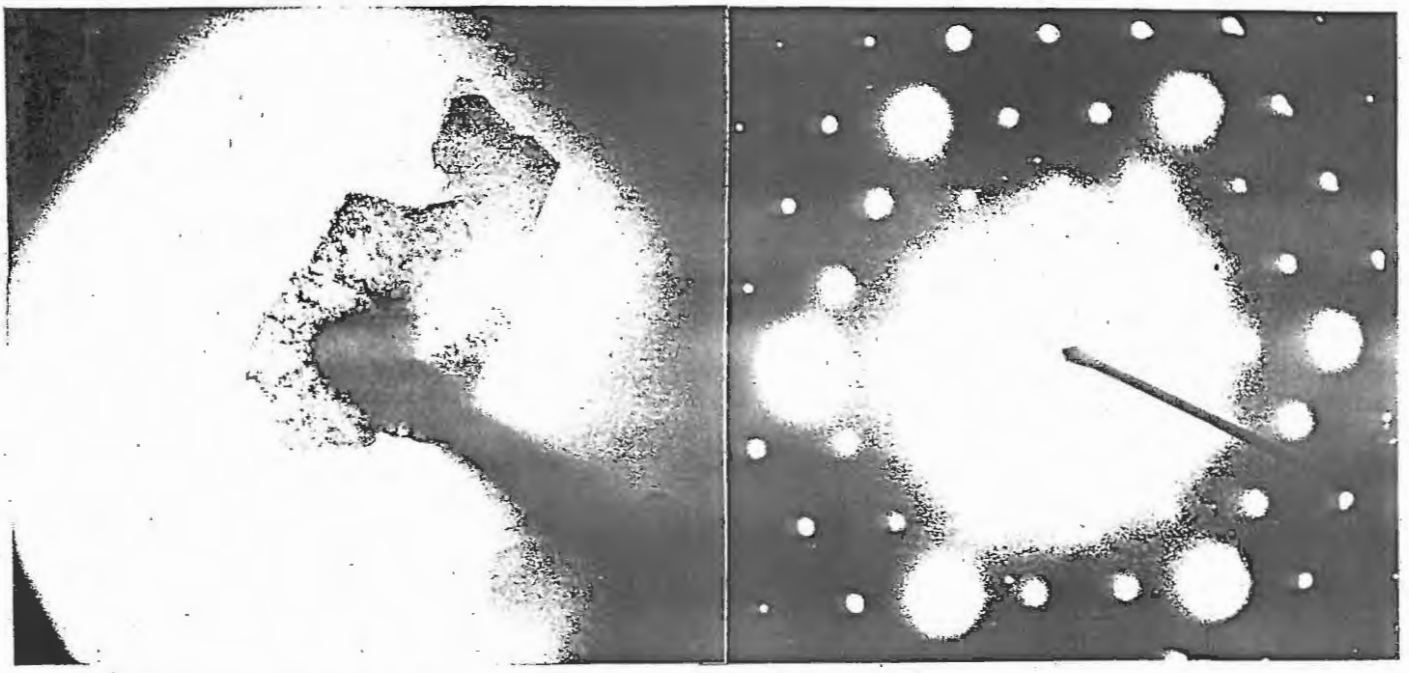

Plate 5.2a & 5.2b Electron micrograph of Palmer Kaolinite crystal and accompaning electron diffraction pattern. The large spots are the 1,49 Å "d" spacing of kaolinite which are the $33\bar{1}$, $3\bar{3}\bar{1}$ and 060 planes.

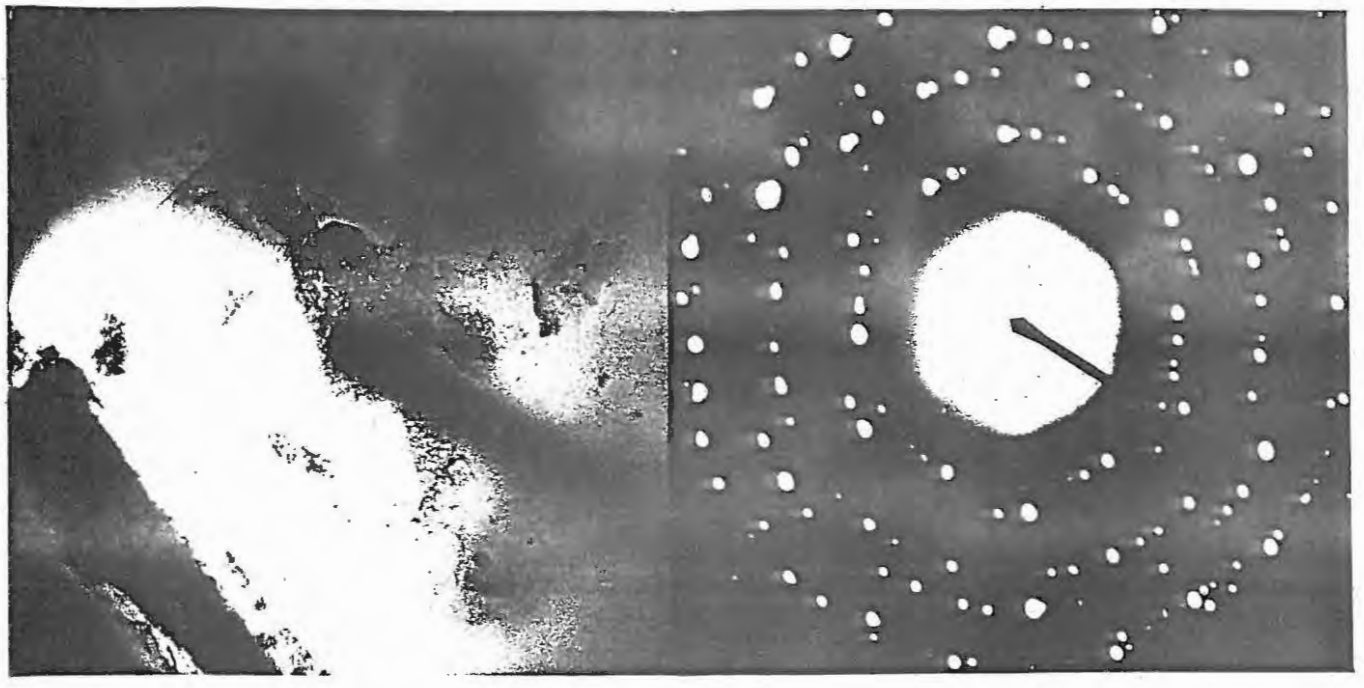

Plate 5.3a & 5.3b Electron micrograph of Avenue Park kaolinite and accompaning electron diffraction patterns.

6. THE GENESIS OF CLAY MINERALS

The dominant minerals in the parent rocks are mica (sericite, illite, muscovite), feldspar (plagioclase, orthoclase, microcline), quartz and some iron oxides and amorphous material. The breakdown of the mica and feldspar and removal of the iron oxide generates the residual material necessary for the formation of the clay minerals. The environmental conditions are important in determining the type of clay mineral formed, the extent or depth of alteration and the solubility of the various cations. A number of factors promote the formation of a clay body and these are summarised by Keller (1970).

A) Removal of Ca, Mg, Fe, Na and K:

1) Precipitation exceeding evaporation
2) Permeable rocks
3) Percolating water
4) Oxidation of FeO to Fe_2O_3 or FeS_2.

B) Addition of H^+:

1) Fresh water
2) Acids, carbonic and organic.

C) High Al:Si:

1) Removal of Si, Na and K silicates and organic compounds
2) High Al concentration and insolubility of Al^{3+}.

The environment under which most atmospheric weathering takes place is oxidising with an oxidation potential of -600 mV and a pH of 4 to 10. Most chemical reactions in weathering take place between minerals and water which may be in the form of ground water and/or interstitial water. Carrol (1970) generalises these interactions as

(atmosphere + biosphere + hydrosphere) + lithosphere = weathered lithosphere + residual materials + dissolved chemical elements.

The most fundamental process of the weathering environment is leaching by rain water and the hydrolysis of the silicates. In the formation of clay bodies the aluminous silicates are of particular importance.

Most often kaolinites are formed over long periods in environments that produce deep weathering, commonly below the ground-water table and below active erosion and denudation (Keller, 1978).

1. Breakdown of Aluminosilicates

The breakdown of aluminosilicates is largely controlled by the hydrogen ion activity and the structure and chemistry of the minerals concerned. The type of bonding and the strength of the bonds are important in determining the mechanism of breakdown and the order of resistance to weathering of the minerals. Bond strengths are determined by ion size, valence and ionic potential of the elements characterising the silicate structure.

Silicates are considered to be the salts of weak acids and strong bases and the reaction of hydrolysis is alkaline. Hydrolytic action between crystal ions and solutions is important in this respect. This hydrolytic action is partly controlled by ion size which determines co-ordination within the crystal. It has also been said that solution, migration, absorption and evolution of ions in a solution depend on their hydration (Millot, 1970). The stronger an ionic field is in water the greater its capacity for hydration will be and the greater its apparent radius in the solvent. The radius of any one ion will therefore change according to the medium it is surrounded by and these relative difference will affect its behaviour in the weathering process. The elements are grouped on the basis of ionic potential by Goldschmidt (1954) see figure 6.1. A comparison of the ionic and hydrated radii of the major elements is shown in table 6.2.

2. Mechanism of Breakdown

There are three common types of bonds to be considered. Firstly, in structures with linked silica tetrahedra the weakest bonds bind the tetrahedra together and, secondly, in structures with two dimensional linkage the weakest bonds bind the bases of the tetrahedra together. Lastly, in structures which are three dimensional frameworks involving both silica tetrahedra and other cations the weakest bond binds the cations that balance the charge of the tetrahedrons (Millot, 1970).

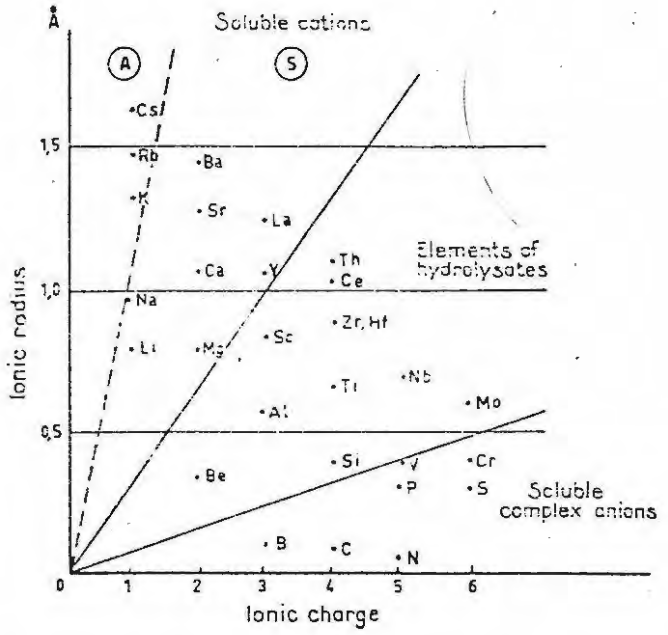

Figure 6.1 Distribution of elements according to ionic potential on the basis of ionic radius as a function of charge. Group 1 have weak ionic potential and remain in solution to high pH; group 2 with intermediate ionic potential which precipitate by hydrolysis in the form of hydroxides at low pH; group 3 have strong ionic potential and form complex anions with oxygen and remain in true ionic solution (after Goldschmidt, 1954).

	Stokes' radii in water Sutra (1946) Å	Ionic radii in crystals Goldschmidt (1926) Å
Al^{3+}	4,57	0,57
Fe^{2+}	3,42	0,83
Mn^{2+}	3,42	0,91
Mg^{2+}	3,45	0,78
Ca^{2+}	3,07	1,06
Na^{1+}	1,83	0,98
K^{1+}	1,24	1,33

Table 6.1 A comparison between ionic radii in water and ionic radii in crystals. Note that K^{+} has a larger ionic radius in a crystal than in solution.

In a system of water in contact with a silicate, for example albite, the oxygens of the albite surface have a negative residual charge which is not completely satisfied. The positive poles of the water molecule saturate the negative surface and weaken the bonds of the alkaline ions in the crystal structure. The exchange of the Na^+ ions of the crystal and the H^+ of the solution takes place (Frederickson, 1951). A second mechanism of hydrolysis is suggested by Devore (1956). This mechanism involves a permutation between the OH^- ions of the solution and the oxygens of the Si-O-Si bonds of the crystal. The Si-OH bonds are stronger than the Si-O bonds and several bonds are converted and the alkali ions in the structure are more weakly bound and therefore available for exchange with H^+. These two mechanisms may work well together and result in the hydrolysis and eventual breakdown of the framework of the crystal structure.

It must be appreciated that with the exchange of H^+ with alkaline ions of the silicate minerals the solution in contact with the minerals cannot remain appreciably acid for long and if this contact is continued the solution must eventually become alkaline. If the solution had to become alkaline, hydrolytic action would eventually cease. It is well known that surface water is always slightly acidic because of reaction with the atmospheric CO_2 and forms weak solutions of carbonic acid. This would therefore supply hydrogen ions as long as rainfall exceeded evaporation. This can be stated thermodynamically as:

$$\frac{(H^+)\ (HCO_3^-)}{(H_2CO_3)} = K_{H_2CO_3} = 10^{-6.4} \text{ at } 25^oC$$

(Garrels and Christ, 1965)

3. Solubility of the Elements

It is important that once the minerals have been hydrolised the elements liberated are able to exist in solution and be removed from the system. Ions with weak ionic potential can exist in true solution to high pH values and include Na, K, Ca and Mg. These ions have relatively large diameters and exert weak fields on hydroxyl ions and form alkaline solutions. K^+ does not go into solution as readily as Na, Ca and Mg because of its greater cation size and because it satisfies the

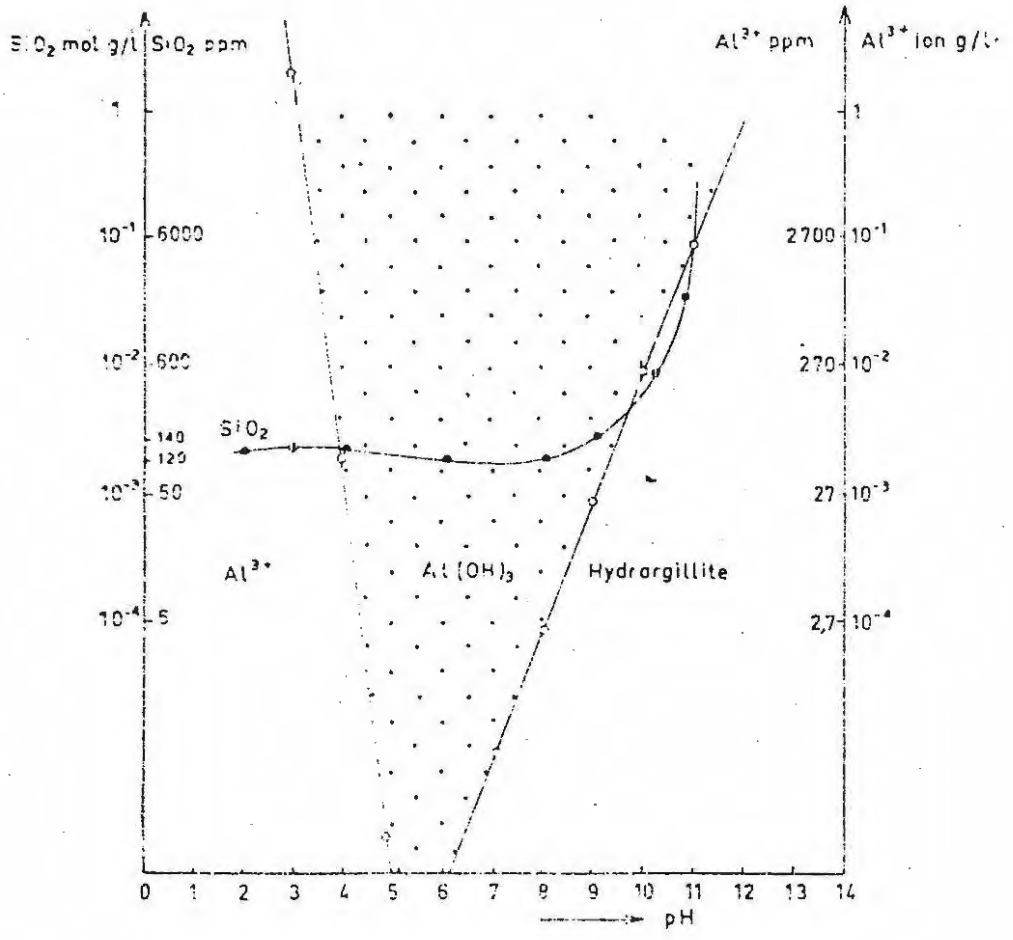

Figure 6.2 Superposed curves of the solubility of silica and alumina as function of pH (after Krauskopf, 1956 and Wey, 1962).

crystallochemical conditions for secondary minerals such as illite. Ions with intermediate ionic potential are precipitated by hydrolysis in the form of hydrosols at low pH values and these include Al, Fe and Si. Ions with strong ionic potential form complex ions with oxygen and exist in true solution and include P and S.

a) Alkalis and Alkali-earths

Indications from the loss-gain diagrams, Barth plots and normalised cation plots are that the order of decreasing solubility of these elements is Ca, Mg, Na and K. This is in agreement with the work of Anderson and Hawkes (1958) and Miller (1961).

b) Aluminium and Silicon

The solubility of Al and Si is very limited and in the presence of either element in solution the solubility of the other is depressed. A concentration of 10 ppm of Al reduces the solubility of silica to 15 ppm at pH 8-9 (Okonoto et al, 1957). Quartz is only slightly soluble but amorphous silica can exist in solution to concentrations of 140 ppm. Dissolved silica exists as silicic acid.

$$SiO_2 + 2H_2O \longrightarrow H_4SiO_4$$

Silicic acid is much weaker than carbonic acid and its first ionisation constant is about a thousand times smaller (Krauskopf, 1967).

$$H_4SiO_4 \longrightarrow H^+ + H_3SiO_4; \quad K_{10}\text{-}9.9$$

This indicates that the solubility of silica will be affected by pH values below 9 and that at values above 9 solubility of silica will increase considerably. pH is not the only factor affecting the solubility of silica. It is also affected by the presence of foreign ions, e.g. NaCl. Aluminium ions are practically insoluble between pH 4 and 8. A solubility diagram for aluminium ions and silica as a function of pH is given below. (see Figure 6.2).

c) Iron

Iron in the ferric state (Fe_2O_3) is particularly insoluble but indications are that iron has been removed from the system to a large degree. The occurrence of iron staining along the bedding and joint planes, root casts and the formation of ferricrete lenses near the surface clearly indicate that iron has migrated. There are three possible ways in which iron could go into solution. It would be expected that most iron in a shale would be in the ferric state but it is possible that during burial diagenesis ferric iron would change to ferrous iron. Ferrous iron is soluble in the hydroxide form and would be able to migrate and then precipitate on contact with a more acid oxidising environment of surface water. A second possibility for the solution and transportation of iron will be in the form of a colloidal hydroxide and a third possibility is that ferric iron forms a complex colloid with silica (Garrels and Christ, 1965). Indications from the photomicrographs of silcrete are that iron has been transported with silica in solution channels and coprecipitated at the surface. (see Plates 8.1 & 8.2).

4. Neoformation or Transformation

The crystallisation of kaolinite is poorly understood. The mineral can be crystallised from a solution phase intermediate between the parent minerals and the daughter kaolinite (neoformation) or it can be formed by the hydrolysis of a parent mineral via a secondary intermediate mineral to daughter kaolinite without a solution phase (transformation), Millot (1970).

It is known that kaolinite can be formed from feldspars. Feldspars are framework silicates and represent a network of chains and not sheets as in the phyllosilicates. The feldspar structure would therefore have to be broken down before a layer silicate could crystallise. A careful investigation of felspathic rocks in the Southern Appalachians region of the U S A was made by Sand (1956). He found that K-felspar altered to vermicular kaolinite through an intermediate stage of secondary mica until all the feldspar in the most highly leached regions was altered to kaolinite. In support of this scheme is the observation that completely leached, hydrated muscovite has the same ratio of Al:Si:H_2O as

kaolinite. The mechanism of transfer from a 2:1 structure to a 1:1 type was not explained.

Several authors have put forward theories as to the crystallisation of kaolinite. Garrels (1971) has two schemes for the formation of kaolinite from feldspars. One is the hydrolysis of K-feldspar and transformation to K-mica and then kaolinite and the second is from plagioclase to montmorillonite and then kaolinite. Nash and Marshall (1956) show a scheme of cation exchange and reorganisation of the structures without any specific intermediates. Carrol (1970) supports a cation exchange theory with the observation that sericite is often absent as an alteration product of feldspar. She suggests that the K^+ ions are removed from the interstitial position in silica tetrahedra and the alumina octahedra where they bind the two layers together. The K^+ is subsequently removed from the central binding position and the two layers become independent and kaolinite is formed.

Experimentation by other authors has shown other intermediates. Henley et al. (1961) found albite to react with water to form beidellite and then kaolinite. Oberlin and County (1970) found that albite under acid attack and in the presence of silicic acid transformed to boehmite and then to kaolinite.

Keller (1978) made a careful study of kaolinisation of feldspars from granites in Missouri and Georgia, U S A. He states that "the argillic transition was not a solid state transformation or replacement, but that a solution in reaction with the solid phases intervened". He showed that kaolinite crystallised directly from solution.

Mica may also form the parent material for kaolinisation. The transformation of a mica to kaolinite or illite is a more simple process. K^+ is leached or exchanged with H^+ from its interstitial binding position in the mica structure which results in a hydromica, illite or sericite, depending on the degree of hydration. To form kaolinite from a hydromica would involve removing the remaining K^+ which would cause the tetrahedral and octahedral layers to dissociate. The remaining structure would be a 1:1 type of kaolinite. The actual mechanism of this dissociation is not known (Millot, 1970).

7. PYROPHYLLITE AND KAOLINITE STABILITY

It has been seen that pyrophyllite is present in all the Coastal Plain deposits but absent from the peneplane deposits. Almost all known deposits containing pyrophyllite are located in low-grade metamorphic terrains and in fact the presence of the mineral is used as an indicator for temperature and pressure conditions during metamorphism, Hemley et.al (1961).

Much experimental data on the temperature of formation of pyrophyllite has been published.

Table 7.1

		Temperature	Pressure and Starting Materials
Roy and Osborn	(1954)	405°C ± 10	2 Kb nat K + 2 Q
Winkler	(1957)	420 ± 5	2 Kb nat K + 2 Q
Carr et al.	(1960)	355 ± 8	2 Kb Nat K + amorphous Si
Carr	(1963)	340	2 Kb Nat K + amorphous Si
Carr et al.	(1960)	414 ± 7	2 Kb Nat K + 2 Q
Aramaki et al.	(1963)	405 ± 10	4 Kb Glass K
Hemley and Jones	(1964)	350	1 Kb Nat K + Nat Q + Nat Py
Althaus	(1966)	390	2 Kb
Velde and Kornprobst	(1969)	311 ± 8	2 Kb Glass
Thompson	(1970)	345 ± 10	2 Kb Nat K + Nat Q + Nat Py
Reed and Hemley	(1966)	300	1 Kb
Eberl and Hower	(1974)	345 ± 5	2 Kb Nat K + 2 Q

The above abbreviations are Nat K - Natural Kaolinite, Q - Quartz, Nat Py - Natural Pyrophyllite. These are the starting materials used to form pyrophyllite and the pressures are given in Kilobars.

It can be seen from the above table that there are large discrepancies in the experimental data for the upper stability limits for pyrophyllite. Thompson (1970) suggests that some of the authors do not consider their stability limits to represent equilibrium for a quartz-kaolinite bearing system. Eberl and Hower (1974) performed synthesis experiments using gels as starting materials and found that stability of kaolinite was affected by the Si:Al ratio and the presence of alkalis. Henley and Jones (1964) showed that kaolinite stability in the Na_2O-K_2O-Al_2O_3-SiO_2-H_2O system depended on the ratio of

alkali to hydrogen ion activity. Catalysts also appear to have a large influence on temperature stability ranges for kaolinite.

Hen and Lind (1974) synthesised well crystallised material of kaolinitic nature at 25°C in a solution of queratin which is an organic flavine. The formation of kaolinite and pyrophyllite at low temperature in nature may be catalysed by the presence of organic compounds.

Discrepancies in the basal 'd' spacings of synthetic and natural pyrophyllite were noticed by Rosenberg (1974). He suggested that substitution of Al^{3+} and H^{+} for Si^{4+}, and Al^{3+} and $(OH)^{-}$ for Si^{4+} and O^{2-} in pyrophyllite could account for these discrepancies and concluded that this solid solution could explain differences in the thermal stability ranges of pyrophyllite.

Kaolinite, quartz and pyrophyllite were found to coexist in shales in Utah, U S A , by Zen (1961). He suggested that the coexistence was an equilibrium relationship and that the kaolinite represented a retrograde metamorphic product of pyrophyllite. He also indicated that kaolinite and quartz were more stable than pyrophyllite in normal environmental conditions.

Tzusuki and Mizatani (1971) showed that sericite changed to kaolinite and then to pyrophyllite in an acidic solution at 260°C. They were unable to explain why kaolinite produced from sericite and not natural kaolinite was liable to be altered to pyrophyllite at these temperatures. They suggest that the paragenesis may not represent equilibrium and that the stability field of pyrophyllite may extend to much lower temperatures.

The use of thermodynamics and Gibbs free energy values can help explain the paragenesis of minerals at 25°C and 1 bar.

1) $3KAlSi_3O_8 + 2H^+ + 12H_2O \longrightarrow Al_3Si_3O_{10}(OH)_2 + 2K^+ + 6H_4SiO_4$
K-feldspar $Gf^0 = -20704{,}74$ Mica K/cal

2) $2KAl_3Si_3O_{10}(OH)_2 + 2H^+ + 3H_2O \longrightarrow 3Al_2Si_2O_5(OH)_4 + 2K^+$
Mica $Gf_o = -12{,}75$ Kaolinite

3) $Al_2Si_2O_5(OH)_4 + 2H_2SiO_4 \longrightarrow Al_2Si_4O_{10}(OH)_2 + 5H_2O$
Kaolinite $Gf_o = -8{,}44$ Pyrophyllite

The level of confidence placed on the values obtained is not great because the free energy values for the formation of pyrophyllite show large systematic discrepancies depending on the nature of the reaction used, (Haas and Holdaway 1973) . There may also be errors in the kaolinite values (Zen, 1969). There are also discrepancies in the values obtained using different starting materials for the reactions, for example the values for SiO_2 crystal, SiO_2 amorphous and silicic acid are different. Thermodynamics is usually applied to an idealised state, the equilibrium state and gives an indication as to the direction of the reaction. Tzusuku and Mizatani (1971) prefer to use kinetics to explain the alteration processes because it is a disequilibrium open system.

It will probably only be possible to explain the occurrence of pyrophyllite in the Grahamstown clay which is definitely a residual, surface deposit with no signs of high temperature or metamorphism once fixed values for the stability of the kaolinite, pyrophyllite and quartz system are established and more confidence placed on the Gibbs Free Energy values for kaolinite and pyrophyllite. The reason for the pyrophyllite occurring only in the Coastal Plain deposits will be even more difficult to explain because of the close proximity, similar lithology in the case of the Witteberg Shale, and very similar chemistry, relative to the Peneplane deposits.

It would seem impossible that metamorphism, if there was any, would restrict itself to an altitude over a distance of 25km longitudinally and would not affect any of the adjacent country rock.

8. THE GENESIS OF THE GRAHAMSTOWN CLAY DEPOSITS

Regional study, field evidence and laboratory work done indicate the mode of genesis of the clay deposits and their associated minerals.

Regionally it can be seen from the map and the contour overlay that all of the known deposits occur at two specific altitudes and are associated with the two planes, the Coastal Plain at 500 m and the Grahamstown Peneplane at 630 m. These two planes were developed at different geological times according to Haughton (1968). The Peneplane was developed during the Miocene and the Coastal Plain in the late Tertiary. The two plains are associated with well developed silcrete horizons especially where the silcrete is underlain by clay. Silcrete is also found on the Witteberg Quartzite slopes but it is not as well developed. Smale (1973) described a number of silcrete occurrences in Australia which have a massive nature at surface and grade into a mottled zone which includes ferricrete lenses and is underlain by a bleached clay. The Upper Gletwyn deposit essentially shows the same features as the Australian terrain described by Smale (1973). The only difference between the Australian deposits and the Grahamstown type found at Upper Gletwyn is that there are two silcrete horizons in the latter. A change in base level at the edge of the Grahamstown Peneplane could have resulted in the incision of the peneplane and erosion of the silcrete. During this time the other silcrete horizon could have developed at the Coastal Plain level and secondary silcrete levels beneath the Peneplane.

In support of the co-development of the silcrete and the clay is evidence of solution channels and colloform growth rings in the silcrete as shown in the photomicrographs. Also in support of this co-development is the evidence of the Australian deposits which were thought to have developed under semi-arid conditions in flat lying areas with fluctuations in the water table due to spasmodic rainfall.

Chemically we can see from the loss-gain diagrams, normalised cation percentage and Barth plots that Al remains essentially stable and that the alkali and alkali-earths are removed at an early stage in the alteration process and are followed by iron at a later stage in the weathering process. This order of movement of elements out of the rock and minerals and into the surrounding ground water follows the sequence

of hydrolysis by acid surface water, solution of the elements and an increase in alkalinity. The increase in alkalinity would assist the solution of silica and iron especially during a dry period when no fresh surface water would be added to the system. This alkaline ground water would then be drawn by evaporation and capillarity to the surface and precipitate its solution load on contact with the more acid environment encountered (see plate 8.1 and 8.2).

The presence of iron-oxide along the joint and bedding surfaces and the presence of ferricrete lenses at surface are evidence of precipitation of iron in contact with acid surface water. Likewise the presence of silcrete, colloform structures in the silcrete and quartz in fracture zones show that silica has also been precipitated on contact with a more acid environment.

The differences in the crystallinity within deposits and also between deposits are probably due to kaolinisation of different minerals. Indications are that when the parent rock has a substantial proportion of feldspar crystallinity of the kaolinite is better developed. Examples of this are the Palmer deposits which show very well defined crystals in the electron micrographs and sharp reflections in the 111, $1\bar{1}1$ and 021 diffraction trace. This is further supported in that kaolinite formed from feldspar is crystallised from solution and not by transformation. It is probable that not all of the kaolinite formed in the deposit is by crystallisation from solution but that a substantial proportion is formed by a process of transformation of existing phyllosilicates. A transformation process may well explain the poor crystal perfection and aggregation of crystals shown in the electron photomicrographs and low crystallinity index in the diffraction traces.

Genetically it is most difficult to explain the presence of pyrophyllite in the Grahamstown deposits and why it is only present in the Coastal Plain deposits. We have seen that there is no evidence of metamorphism, major faulting or hydrothermal activity in the area because if there was, the kaolinite could be explained as a retrograde metamorphic product of the remaining pyrophyllite. Thermodynamics cannot adequently explain the occurrence as it is usually applied to the equilibrium state whereas alteration processes are not in equilibrium and should be expressed in terms of space and time on a kinetic basis which in geological time scales is almost impossible. A possible explanation for the occurrence

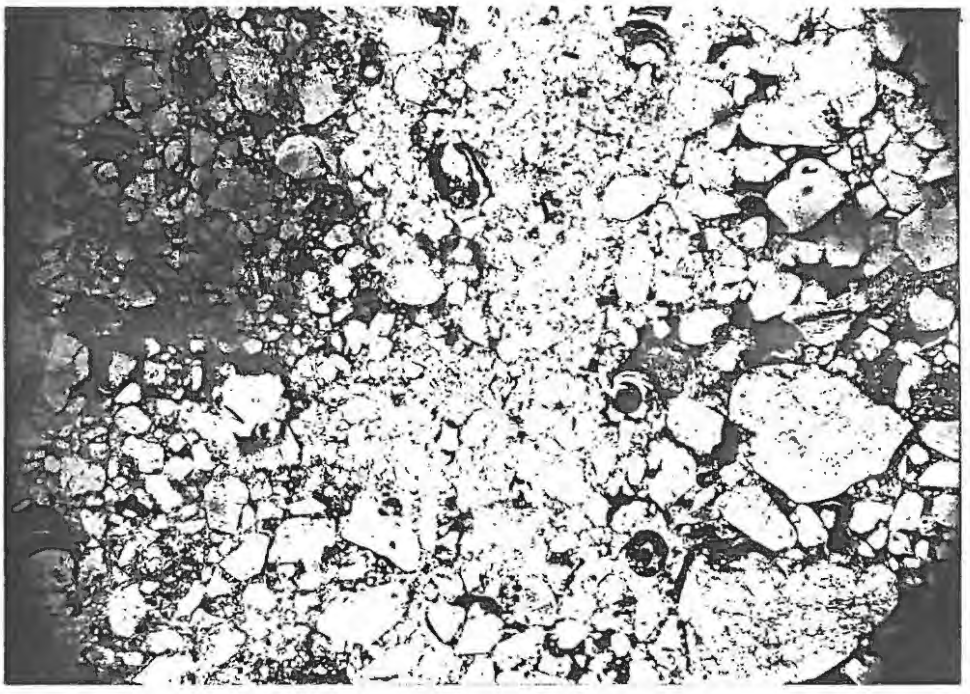

Plate 8.1 Photomicrograph of the silcrete from Upper Gletwyn. Note the solution channels and mosaic of interlocking grains of quartzitic material. This type is known as a 'terrazzo-type' (Smale, 1973).

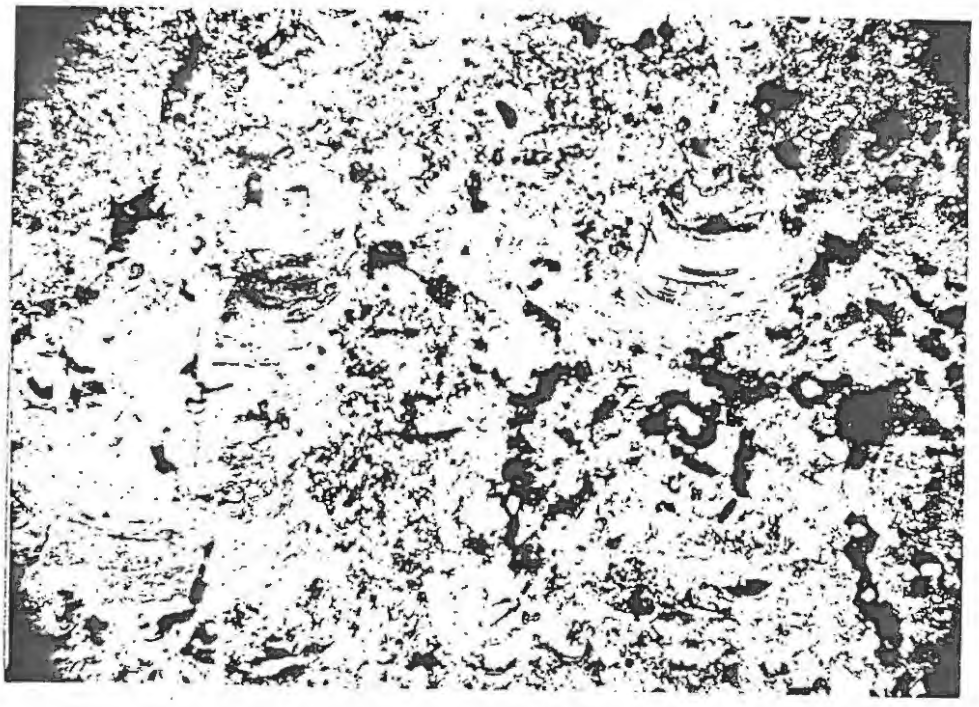

Plate 8.2 Photomicrograph of silcrete from Upper Gletwyn. Note that this type has a fine-grained matrix of cryptocrystalline quartz and shows distinct colloform structures of iron oxide, quartz and leucoxene. This type is known as the Klipheuwel type (Smale, 1973).

of pyrophyllite is that it is a transformation product of illite in which the K^+ in the interstitial binding position is removed and the binding force of K^+ is replaced by van der Waal's forces which would result in a structure and a chemical formula of pyrophyllite. This would not satisfactorily explain the absence of pyrophyllite from the Peneplane deposits. It is possible that the geologic and chemical environment during the formation of the Coastal Plain deposits and the Peneplane deposits was different and that an organic catalist was active during the formation of the Coastal Plain deposits.

9. ECONOMICS

In 1972 the world consumption of Kaolin was in the region of 3 million tons and the projected figure for the year 2000 is 10 million tons (Cooper 1971). South African production is small in terms of world production but the growth in production is far greater than for the rest of the world. Local production has trebled in the past 10 years and will probably continue to grow at this fast rate with increase in industrialisation. Some statistics on South African local sales, extracted from the South Africa Department of Mines Quarterly Information circulars, are listed below in table 9.1:-

Table 9.1

	Local Sales 1000 Metric tons	Sales Value '000 Rand	Price per ton Rand Crude	Price per ton (Rand) Milled	Price per ton (Rand) Washed
1971	44,8	290	-	-	-
1972	47,5	296	-	-	-
1973	48,4	393	-	-	-
1974	59,4	634	4,22	10,93	30,53
1975	59,0	929	4,71	7,99	33,32
1976	55,0	1,394	6,56	13,56	38,89
1977	61,2	1,506	7,36	22,45	42,92
1978	113,6	2,136	9,06	36,95	60,25
1979	118,1	2,394	8,38	43,00	70,48
1980	130,9	3,499	11,62	47,90	85,86
1981	132,8	4,384	12,62	50,87	108,93

From the above figures we can see that the price of kaolin is steadily increasing, in fact between 1974 and 1981 the price of crude kaolin has almost trebled but is still dismally low relative to the milled price. The price increase mainly reflects the inflation figure for the time period.

We have already seen that the bulk of the clay mined in the Grahamstown area is exported to the Transvaal in a crude, unmilled and unwashed form. It would seem obvious that local producers should refine their product before selling, but there are several restricting factors. Rail

tariffs for crude materials are considerably lower than for refined or semi-finished products; refining would require capital outlay and some degree of expertise; a large local water supply would be needed if material was to be washed; cheap power would be required and the marketing and distribution grip of a few large corporations on clay production in South Africa would have to be broken.

It would seem impossible to achieve any degree of success but with the Government's new dispensation for rural areas and policy of decentralisation, capital and subsidy on rail tariffs and power costs should become available. The local water supply capacity has just been increased and thus the major stumbling blocks could be overcome.

Farm producers are at present using primitive quarrying techniques and wasting a good percentage of the mineable material. This is partially due to lack of expertise and partially due to the low price of crude clay which does not allow for any degree of sophistication.

Besides the primary producers there are only a few relatively small industries using the local clays. These include the brickworks which use the clay for the manufacture of bricks, roofing and flooring tiles and the local potteries of which there are three, but only one of any great importance.

The clays which show the greatest economic potential are the Crous clay because of its good plasticity, pyrophyllite content and low grit, and the clay derived from the Dwyka Tillite because of the percentage of kaolinite, whiteness and large ore reserves.

In conclusion we might reproduce a quote from Mountain (1931).

> "The conditions under which the clays were formed are somewhat unique, and the enormous reserves of white clay suitable for pottery represent an asset which Grahamstown should realise. Unfortunately, the geographical position of Grahamstown is on two accounts unsatisfactory. She is far from the coal-fields and coal is consequently dear, and she is rather far from the biggest markets and transport costs are high. In spite of these drawbacks, however, tiles, pipes and even bricks are marketed throughout the Union, and Johannesburg is one of the principle buyers at the present time".

APPENDIX

A. CHEMICAL ANALYSIS BY XRF SPECTROMETRY

1. Sample Preparation

a) The bulk samples were homogenised by a hand crushing and splitting process until a split of approximately 100 g split was obtained. 10 g of the material was ground in an agate motar and pestle to -300 mesh and then heated in an oven at 102°C for 8 hours to remove any hygroscopic water present. Approximately 6 g was weighed out and pressed in a die at a pressure of 15 tons/sq. in. to form a bakelite-boric acid-backed briquette. The remainder of the ground material was accurately weighed into a Vitreosil crucible and heated at 1000°C for 10 hours in a muffle furnace. The crucible was then removed and cooled in a desiccator and accurately reweighed. The difference in weight was taken as the loss of ignition (LOI) figure. 0.2800 g $\pm$ 0,0001 g of the ignited material was weighed out and to this 1.5000 $\pm$ 0.0001 g of preheated Johnson and Mathey 105 Spectroflux and 0.0200 g of NH_4NO_3 was added. The mixture was heated in a Pt/Au crucible over a bunsen flame until completely fused. The fused bead was cast onto a graphite disc on a hot plate kept at 230°C and lightly stamped with a plunger. The resultant fusion disc was then placed on an asbestos hot plate kept at 170°C and annealed for 7 hours in accordance with the Norrish and Hutton (1969) method.

b) Instrumental Conditions on Philips PW 1410 X-Ray Spectrometer

Sample	Fusion Disc									Briquette
Element	Si	Ti	Al	Fe	Mn	Mg	Ca	K	P	Na
Generator kV/mA	50/40	50/40	50/40	50/40	50/40	50/40	50/40	50/40	50/40	50/40
Tube	Cr	Cr	Cr	Cr	Cr	Cr	Cr	Cr	Cr	Cr
Counter	Flow	Flow	Flow	Flow	Flow	Flow	Flow	Flow	Flow	Flow

Collimator	C	F	C	F	C	F	F	F	C	C
	PET	LiF	PET	LiF	LiF	LiF	TLAP	LiF	Ge	TLAP
Crystal		200		200	200	200		200		
Time(secs)	40	10	40	20	40	200	10	10	20	200
Position				Ka lines for all elements						
Al-Filter	Out	Out	Out	Out	In	Out	Out	Out	Out	Out

c) Standards and correction procedure

The standards used were the international rock standards AGV-1, GSP-1, BCR-1, G-2, NIM-N, NIM-P, NIM-G and NIM-D. Corrections were made for matrix effects, deadtime, position factors and spectral line interference and working curves calculated using the major element calibration program written by Dr. J.S. Marsh of the Rhodes University Geology Department. Corrections, concentration calculations, cation percentages and Barth Standard Cell calculations were done using the Geology Department major element program.

d) Errors in detection The following averages are statistically derived:

SiO_2	0,077(Ave. LLD)	0,28(Ave.abs.error)	0,48(Ave.% error)
TiO_2	0,10	0,02	3,74
Al_2O_3	0,057	0,12	0,82
Fe_2O_3	0,023	0,01	0,79
MnO	0,027	0,02	9,54
MgO	0,117	0,12	1,70
CaO	0,014	0,04	1,46
Na_2O	0,020	0,05	1,78
K_2O	0,007	0,02	0,77
P_2O_5	0,031	0,02	6,47

Ave.LLD- average lower limits of determination
Ave.abs. error-average absolute error
Ave.% error-average percentage error

2. Trace element determinations using X-ray fluorescence spectrometry

a) Sample preparation was exactly the same as that for sodium analysis in the major element analysis.

b) Instrumental Conditions on the Philips PW1410 X-ray sepctrometer.

Element	Sr	Rb	Zr	Y	Nb	Zn	Cu	Ni	Co	Cr	V	La	Ce	Nd.
Generator KV/mA	55/40					50/40			50/40					
Tube	Tungsten													
Counter	Flow					Flow + scintillation								
Crystal	LiF 220													
Counting Time	200 seconds on peak.													

c) Standards and correction procedure.

The standards used were the international rock standards AGV, GSP, BCR and G. Corrections were made for mass absorption using Heinrich's values. Interferance standards using 'Specpure' silicon and the element were used for interference of Yttrium on Niobium, Strontium on Zirconium and Rubidium on Yttrium. The blank used for the Zinc-Copper-Nickel analysis was P5A, a sample from the Palmer quarry because the 'Specpure' silica normally used for making a blank has 6-8 ppm Cu.

d) Errors in detection. All values ppm.

	Average lower limits of detection	Average absolute error
Sr	1,4	0,7
Rb	1,4	0,45
Y	1,4	0,44
Zr	1,5	0,55
Nb	1,55	0,45
Zn	1,5	0,65
Cu	2,3	6,5
Ni	1,6	0,7
Co	3,0	0,8
V	4,0	1,2

Cr	2,7	1,3
ha	6,0	1,5
Ce	11,5	2,9
Nd	6,5	1,6

Lower Limit of detection: $LLD = \frac{6}{Ip/m} \times \sqrt{\frac{Ib}{T}}$

Ip = peak intensity
Ib = background
T = total counting time
m = counts per second per % of element

B. MINEROLOGICAL ANALYSIS BY X-RAY DIFFRACTION

a) Sample Preparation

The samples for X-ray diffraction (XRD) were prepared in three different ways from homogenised bulk samples.

(i) Normal standard back-mounting Philips sample holders of clay where the clay is pressed into a aluminium frame from the surface not to be X-rayed.

(ii) Suction -onto- membrane filter, method of Cubitt and Davis (1976), using the minus 325 mesh fraction which had been previously ultrasonically dispersed and deflocculated in 0,1.N solution of sodium hexametaphosphate.

(iii) Powder press method by placing the sample in a die and pressing it at 15 tons/sq. in. into a bakelite-boric acid-backed bricquette.

The Philips mounts were used for quick scans of the clay. The membrane filter sample mounts were used for determining crystallinity of the kaolinite and accurate peak location determinations. The power press samples were used for comparisons of the mineralogy of the clays.

b) Instrumental Condition on the Philips PW 1050/25 vertical goniometer diffractometer.

A sealed Xenon counter was used in combination with a Cobalt tube, Chromium filter and appropriate divegence slits. The generator was set at 40KV and 30mA and the scan speed of the goniometer at 1^{o} 2θ per minute. Peaks were identified using the ASTM tables assuming that Cobalt Ka radiation is 1,79 Å and the Bragg formula $n\lambda = 2d \sin \theta$.

C. TRANSMISSION ELECTRON MICROSCOPY

1. Morphology

a) Sample Preparation

Samples for transmission electron microscopy (TEM) were first deflocculated in a 0,1N solution of sodium hexmetaphosphate and allowed to stand overnight. The sample was then shaken and after a minute the suspension fraction was pipetted out into a vial. The material was then diluted until only faintly milky in appearance. A small fraction was then pipetted out onto a transmission grid and the excess water allowed to dry.

b) Instrument

The clays were examined in a Jeol 100 CS transmission electron microscope at an accelerating voltage of 80 KV and magnifications of ± 40,000, times.

2. Electron Diffraction

Transmission electron diffraction was done on the same samples as the morphological inspection. The electron diffraction involves inserting a small diffraction aperture in the position of the intermediate image. The camera length was set at 83 cms and an accelerating voltage of 80 KV was used. The enlargement factor on the diffractograms is 1.5 times.

The basic formula for deriving the d spacing from the diffractograms is as follows.

$$\overset{o}{dA} = \frac{\sqrt{1500}}{\dfrac{KV \times \text{Camera length (cm)} \times \text{Enlargement factor}}{\text{Radius (cms)} \times 100}}$$

$\sqrt{\frac{1500}{KV}}$ (Kilovolts) determines the wavelength of the electron beam.

A tilt and rotate facility is available on the sample holder so it is not difficult to align the sample perpendicular to the beam.

5. SIZE ANALYSIS

Approximately 100 g of homogenised clay sample was dried at 102°C and then reweighed to exactly 100 g. The sample was then ultrasonically dispersed and screened through a 325 mesh nylon gauze. The two resultant fractions were then dried at 102°C and then weighed accurately. The +325 fraction was taken to be the grit content of the clay. 10 g of the -325 fraction was weighed and deflocculated with 0.1 N sodium hexmetaphosphate in a litre measuring cylinder. The suspension was allowed to stand overnight and was then vigorously shaken. Withdrawals of 20 ml were made at depths and times calculated by the following formula (Folk, 1968):

$$T \text{ min} = \frac{\text{Depth in cm}}{1500 \text{ A } d^2 \text{ mm}}$$

A = 3.75 which is a density factor for quartz and clay at 24°C.
T min = time in minutes.

Each fraction was dried at 102°C and then weighed accurately. Corrections were made for the mass of deflocculent. The values obtained were plotted on histograms in phi units (Ø),
i.e. 1 Ø = 500 microns, 2 Ø = 250 microns, etc.
All samples were done in duplicate and the average values taken.

ACKNOWLEDGEMENTS

I wish to thank the Council for Scientific and Industrial Research for their financial assistance and therefore making it possible for this study to be done.

I would also like to express my appreciation to Professor H.V.Eales for his guidance, Dr J.S. Marsh for his assistance in the X-ray fluroscence work and data processing, and Mr R. Cross of the Electron Microscopy Unit, Rhodes University for his help in obtaining the electron micrographs and electron diffraction micrographs.

REFERENCES CITED

ADAMS, J. (1918) : The manufacture of ceramic ware in the Union. S.Afr. Jouranl of Industries, 1, No 9, p 772.

ALEXANDER, L.E. & KLUG, H.O. (1954) : X-ray Diffraction procedures. John Wiley and Sons Inc. New York.

ALTHAUS, E. (1966) : Der stabilitaetsbereich des pyrophyllits unter dem

ANDERSON, D.S. & HAWKES, H.E. (1958) : Relative solubility of the common elements in weather of some schist and granite areas. Geochim. Cosmochim Acta 14, p 204-211.

ARAMAKI, S. & ROY, R. (1963) : A new polymorph of Al_2O_3 and further studies in the system Al_2O_3 -SiO_2 H_2O. Am. Mineralogist, 48, p 1322-1347.

BAILEY, S.W. (1963) : Polymorphism of the kaolin minerals. Am. Mineralogist, 48, No 11, p 1196-1209.

BLIGNAUT, J.J.G. (1928) : Clays derived from the Lower Dwyka Shales. Unpublished M.Sc. thesis, Rhodes University.

BOSAZZA, V.L. (1946) : The petrography and petrology of South African clays. Lund Humphries & Co. London.

BRINDLEY, G.W. (1946) : The structure of kaolinite. Miner. Mag., 27, p 242-253.

BRINDLEY, G.W. & ROBINSON, K. (1946) : Randomness in the structures of kaolinite. Clay Minerals, Trans. Faraday, Soc. 42B, p 198-205.

BRINDLEY, G.W. (1951) : X-ray identification and crystall structures of clay minerals. Miner. Soc. Great Britain, Monograph, London.

BRYAN, W.B., FINGER, L.W. & CHAYES, F (1969) : Estimating proportions in petrographic mixing equations by least-squares approximation. Science, 163, p 926-927.

CARR, R.M. & FYFE, W.S. (1960) : Synthesis fields of some aluminium silicates Geochim, Cosmochim, Acta, 21, p 99-109.

CARR, R.M. (1963) : Synthesis fields of some aluminium silicates: further studies. Geochim. Cosmochim. Acta, 27, p 133-135.

CARROL, D. (1970) : Clay Minerals: A guide to their x-ray identification. Geol. Soc. Am. Special Paper, No 126, p 80.

COOPER, J.D. (1971) : Mineral facts and problems. U.S. Bureau of Mines, Bull. 650.

CUBITT, J.M. (1975) : A regression technique for the analysis of shales by x-ray diffractometry. Journ. Sed. Pet., 45, No 2, p 546-553.

CUBITT, J.M. & DAVIS J.C. (1976) : Preparation of shales for x-ray diffraction analysis by a suction-onto-membrane filter method. Unpub.

DEER, W.A., HOWIE, R.A. & ZUSSMAN, J. (1962) : Rock Forming Minerals. Sheet Silicates Vol. III, Longmans, London.

DEER, W.A., HOWIE, R.A. & ZUSSMANN, J (1968) : An introduction to the rock forming minerals. Longman Ltd, London.

DE KIMPE, C.R., GASTUCHE, M.C. & BRINDLEY, G.W. (1961) : Ionic co-ordination in alumino-silicates in relation to clay mineray formation. Am. Mineralogist, 46, p 1376-1381.

DE KIMPE, C.R. (1969) : Crystallisation of kaolinite at low temperatures from an alumino-silica gel. Clays Clay Miner., 17, p 37-38.

DEVORE, G.W. (1956) : Surface chemistry as a chemical control on mineral association. Journ. Geol., 64, p 31-55.

EALES, H.V. (1962) : Report on Grahamstown clay deposits. Unpub.

EALES, H.V. (1975) : Report on chemistry of clay deposits on the farm 'Upper Gletwyn', property of messrs SAPPI Ltd. Unpub.

HEN, J.D. & LIND, C.J. (1974) : Kaolinite synthesis at 25°C. Science, 184, p 1171-1173.

EBERL, D. & HOWER, J. (1975) : Kaolinite synthesis: The role of the Si/Al and Alkali?H^+ ratio in hydrothermal systems. Clays Clay Miner., 23, p 301-309.

FOLK, E.L. (1968) : Petrology of sedimentary rocks.

FRANKEL, J.J. & KENT, L.E. (1937) : Grahamstown surface quartzites (silcretes). Trans. Geol. Soc. S. Afr., 40, p 1-42.

FREDERICKSON, A.F. (1951) : Mecanisme de l'alteration. Bull. Geol. Soc. Am., 62, p 221-231.

GARRELS, R.M. & CHRIST, C.L. (1965) : Solutions, minerals and equilibrium. Harper & Raw, New York.

GARRELS R.M. & MC KENZIE, F.T. (1971) : Evolution o f sedimentary rocks. W.W. Norton & Co.

GOLDSCHMIDT, V.M. (1954) : Geochemistry. Muir, A. Oxford.

GRIFFITHS, P. & RADFORD, C. (1965) : Calculations in ceramics. McLaren and Sons Ltd, London.

GRIM, R.E., BRAY, R.H. & BRADY, W.F. (1937) : The mica in argillacious sediments. Am. Miner., 22, p 813.

GRIM, R.E. (1962) : Applied clay mineralogy. McGraw-Hill, New York.

GRIM, R.E. (1968) : Clay mineralogy. McGraw-Hill, New York.

GRUNER, J.W. (1932) : The crystal structure of kaolinite. Z. Krist., 83, p 75-88.

HAAS, H & HOLDAWAY M.J. (1974) : Equilibria in the system Al_2O_3-SiO_2-H_2O involving the stability limits of pyrophyllite and thermodyranic data of pyrophyllite. Am. J.Sci., 274, p 825-828.

HAUGHTON, S.H. (1969) : Geological history of Southern Africa. Geol. Soc. S.Afr.

HEN, J.D. & LIND, C.J. (1974) : Kaolinite synthesis at 25°C. Science, 184, p 1171-1173.

HEMLEY, J.J., MEYER, C. & RICHTER, D.H. (1961) : Some alteration reactions in the system Na_2O-Al_2O_3-SiO_2-H_2O. Geol. Surv. Res. Prof. Paper 424-D No 408.

HEMLEY, J.J. & JONES, W.R. (1964) : Chemical aspects of hydrothermal alteration with emphasis on hydrogen metasomatism. Econ. Geol., 59, p 538-569.

HINKLEY, D.N. (1965) : Variability in the values among Kaolin deposits of the coastal plain of Georgia, South Carolina. Clays and Clay Miner., 13, p 229.

KELLER, W.D. (1970) : Environmental aspects of clay minerals. Journ. Sed. Pet., 40, No 3 p 788-854.

KELLER, W.D. (1978) : Kaolinisation of felspar as displayed in scanning electron microscope. Geology, 6, p 184-188.

KRAUSKOPF, K.B. (1965) : Dissolution and precipitation of silica at low temperatures. Geochim. Cosmochim. Acta, 10. p 1-22.

KRAUSKOPF, K.B. (1967) : Introduction to geochemistry. McGraw-Hill, New York.

MILLER, J.P. (1961) : Solutes in small streams draining single rock types. Sangue de Cristo Range, New Mexico U.S. Geological Survey Water Supply Report No 535-F p 23.

MILLOT, G. (1970) : Geology of clays. Masson et C_{ie}, Paris.

MOUNTAIN, E.D. (1931) : The Grahamstown ceremic industry. S. Afr. Journ Sci., 28, p 135-139.

MOUNTAIN, E.D. (1946) : The Geological Sheet No 126 Geol.Surv. S.Afr.

MOUNTAIN, E.D. (1975) : The geology of the Upper Dwyka stage in Grahamstown. Trans. Geol. Soc. S.Afr., 78, p 161-165.

MURRAY, H.H. & LYONS, S.C. (1956) : Correlation of paper, coating quality with degree of crystalline perfection of kaolinite. Clays Clay Miner., 4, p 31-40.

MURRAY, H.H. & SMITH, J.M. (1973) : The geology and mineralogy of Grahamstown, South Africa, kaolin deposit. Abs. Clay Miner. Conf. Program, No 22, p 48.

NASH, V.E. & MARSHALL, C.E. (1956) : The surface reactions of silicate minerals. Reactions of felspar surfaces with salt solution. Missouri Univ. agr. Ex. Stat. Research Bull, No 614, p 36.

NORRISH, K. & HUTTON, J.T. (1969) : An accurate x-ray spectograph method for the analysis of a wide range of geological samples. Geochim. Cosmochim. Acta, 33. p 431-453.

OBERLIN, A. & COUNTY, R. (1970) : Condition of kaolinite formation during alteration of some silicates by water at 200°C. Clays Clay Miner., 18, p 347-356.

OKONOTO, G., OKURA, T. & GOTO, K. (1957) : Properties of silica in water. Geochim. Cosmochim. Acta, 12, p 123-132.

PEARSON, M.J. (1978) : Quantitative clay mineralogical analyses from the chemistry of 8 sedimentary rocks. Clays Clay Miner, 26, p 423-433.

RANGE, K.J. RANGE, A. & WEISS, A. (1969) : Fire-clay type kaolinite or fire-clay mineral? Experimental classification of kaolinite-halloysite minerals. Proc. Int. Clay Conf., Tokyo, 1, p3-13.

REED, B.L. & HENLEY, J.J. (1966) : Occurrence of pyrophyllite in the Kekiktuk Conglomerate, Brooks Range, Northeastern Alaska, U S Geol. Surv. Prof. Paper, No 550C, p 162-166.

ROY, R. & OSBORN, E.F. (1954) : The system Al_2O_3-SiO_2-H_2O. Am. Mineralogist, 39, p 853-885.

ROSENBERG, P.E. (1974) : Pyrophyllite solid solutions in the system Al_2O_3-SiO_2-H_2O. Am. Miner., 59, p 254-259.

SAND, L.B. (1956) : On genesis of residual kaolins. Am. Miner., 41, p 28-40.

SCHMIDT, E.R. (1976) : Mineral resources of the Republic of South Africa. 5th Ed. Editor C.B. Coetzee, Government Prinmter, Rep. of S.A.

SCHWARZ, E.H.L. (1919) : Report on the Grahamstown Brickfields. Rhodes University

SMALE, D. (1973) : Silcretes and associated silica diagenesis in South Africa and Australia. Journ. Sed. Pet., 43, p 1077-1087.

SOUTH AFRICAN COMMITTEE FOR STRATIGRAPHY (SACS), (1980) : Stratigraphy of South Africa. Part I (Comp. L.E. Kent Lithostratigraphy of the Republic of South Africa, South West Africa-Namibia, and the Republics of Bophutahtswana, Transkei and Venda: Hardb. geol. Surv. S.Afr., 8.

SUTRA, G. (1946) : Surla dimension des ions electrolytiques. Journ.Chim. Phys. p 190-326.

THOMPSON, A.B. (1970) : A note on kaolinite-pyrophyllite equilibrium. Am. Journ. Sci., 268, P 454-458.

TILL, R. & D.A. SPEARS (1969) : The determination of quartz in sedimentary rocks using an X-ray diffraction method. Clays Clay Miner., 17, p 323-327.

TRIPLEHORN, D.M. (1970) : Clay mineral diagenesis in Atoka (Pennsylvanian) sandstones, Crawford County, Arkansas. Journ.Sed Pet., 40, No 3, p 838-847.

TZUSUKI, Y. & MIZATANI, S. (1971) : A study of rock alteration process based on kinetics and hydrothermal experiments. Contr. Miner. and Pet., 30, p 15-33.

VELDE, B. & KORNPROBST, J. (1969) : Stabilite des silicates d'alumine hydrates. Contr. Miner. and Pet., 21, p 63-74.

WEAVER, C.E. & L.D. POLLARD (1973) : Developments in sedimentology Elsevier, Amsterdam.

WINKLER, H.G.F. (1957) : Experimentelle Gesteinsmetamorphose. Geochem. cosmochim. Acta, 13, p 42-69.

ZEN, E-AN (1961) : Mineralogy and petrology of the system Al_2O_3-SiO_2-H_2O in some pyrophyllite deposits of North Carolina. Am. Miner., 46, p 52-66.

ZEN, E-AN (1969) : Free energy of formation of pyrophyllite from hydrothermal data. Values, discrepancies and implications. Am. Miner., 54, p 1592-1606.

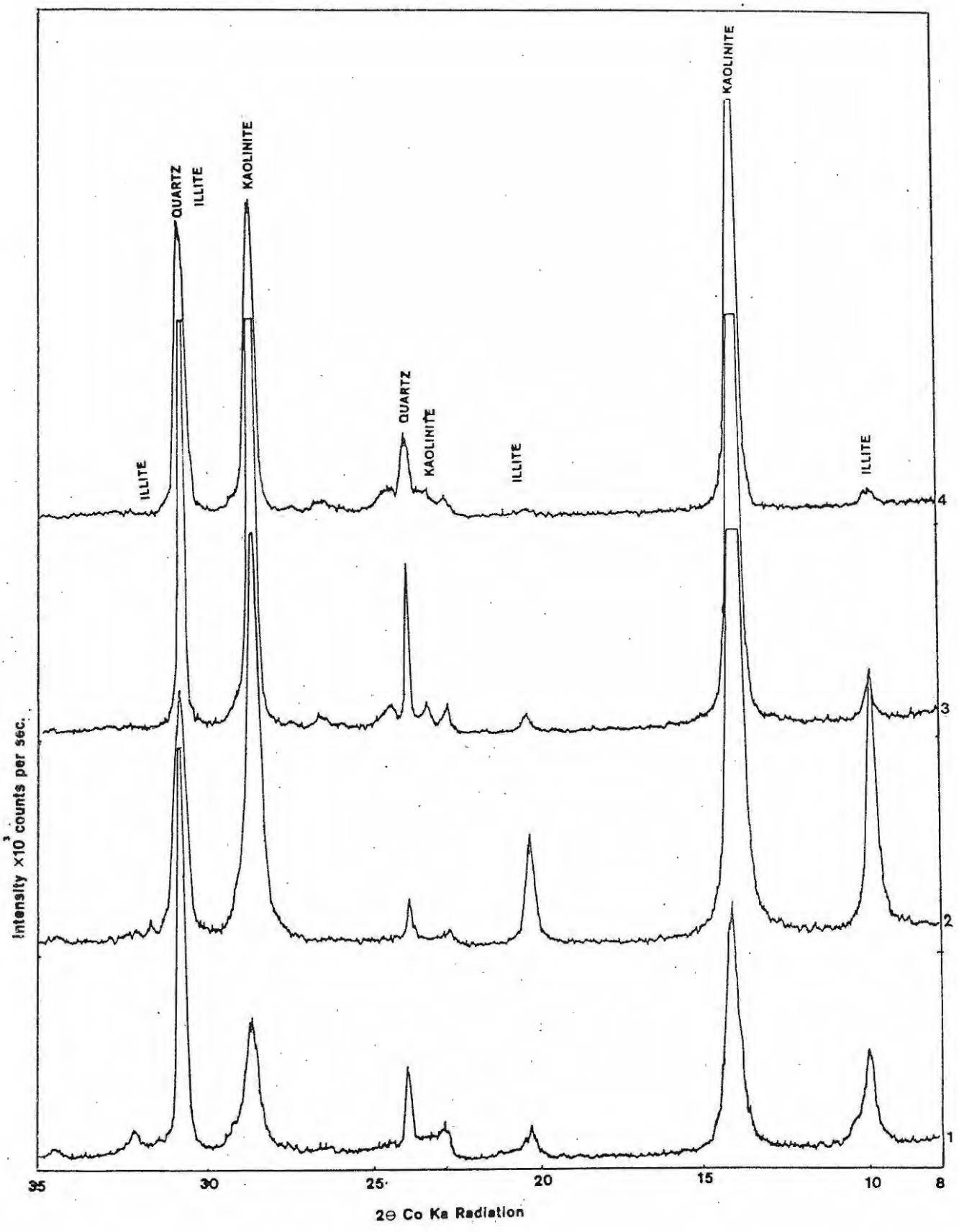

Appendix Fig. 1 Comparative X-ray diffraction traces of the four Grahamstown Peneplane clay deposits. 1) Strowan 2) Wallace 3) Upper Gletwyn 4) Palmer. All samples are of the raw clay prepared by the powder press method.

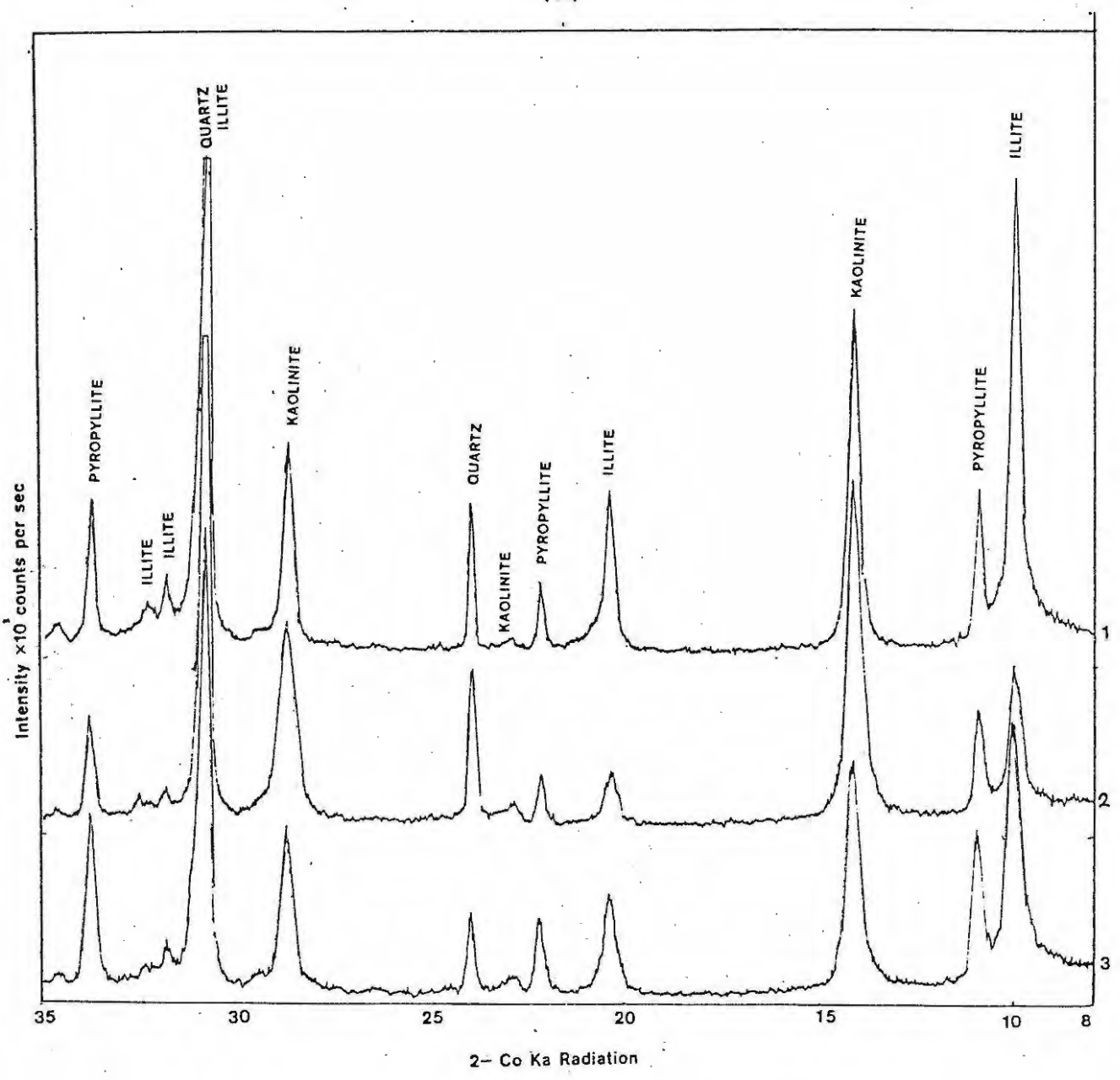

Appendix Fig. 2 Comparative X-ray diffraction traces of the three Coastal Plain clay deposits. 1) Melrose 2) Crous 3)Avenue Park All samples are of raw clay prepared by the powder press method.

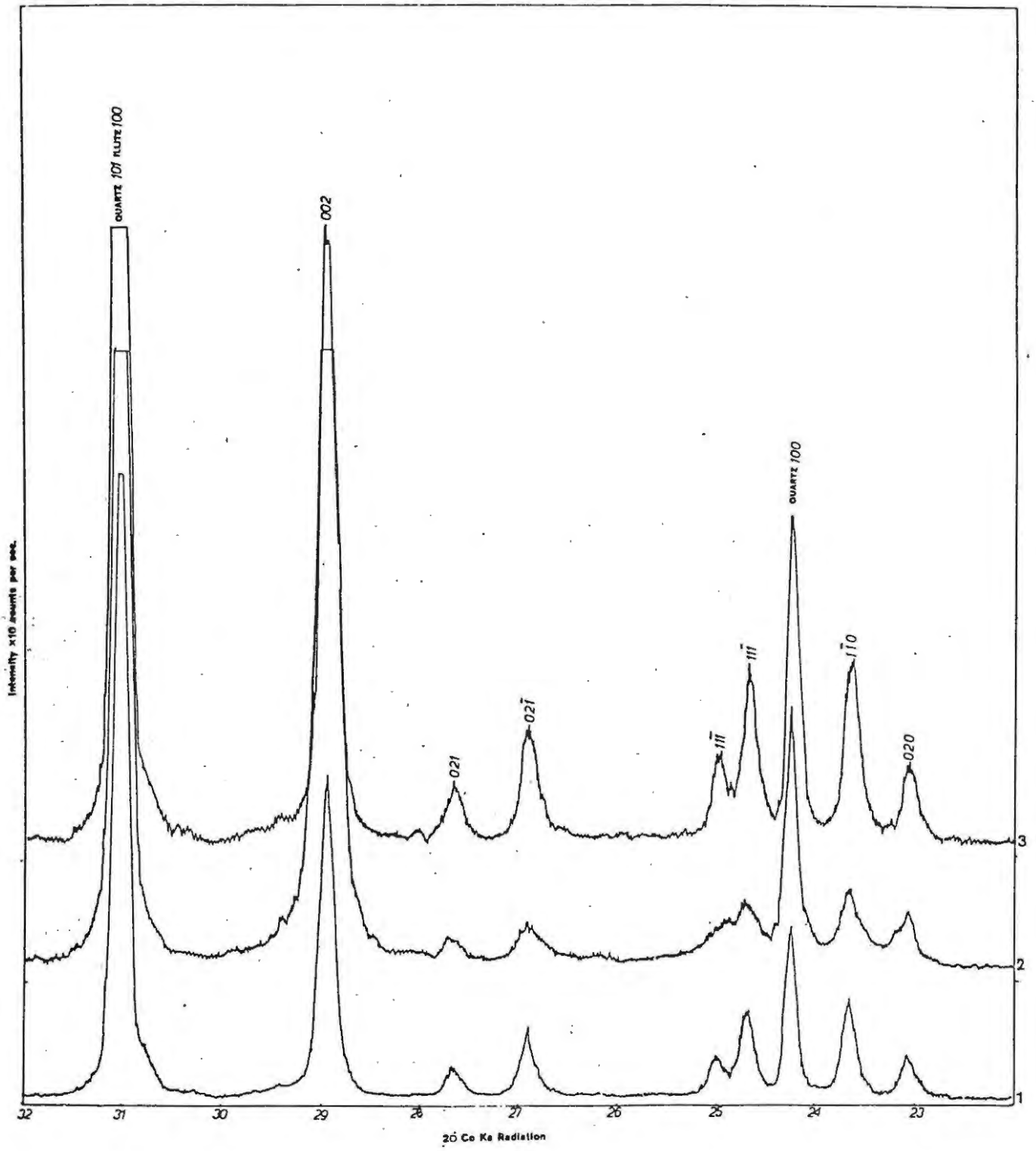

Appendix Fig. 3 Comparative X-ray diffraction traces of the Peneplane clays showing differences in crystallinity and similar quartz percentages. Samples were prepared by the suction-onto-membrane filter method. All indices are for kaolonite unless otherwise indicated. 1) Upper Gletwyn 2) Wallace 3) Palmer.

GEOLOGICAL MAP OF THE GRAHAMSTOWN AREA

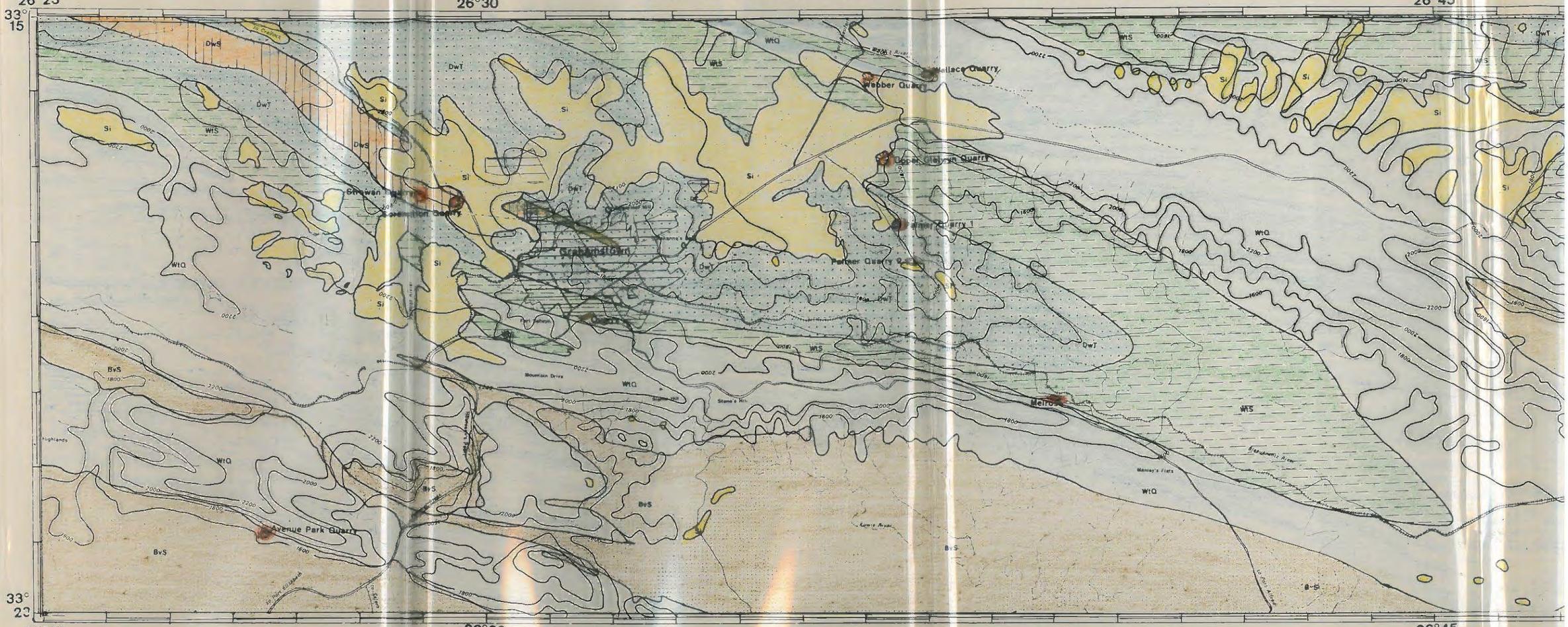

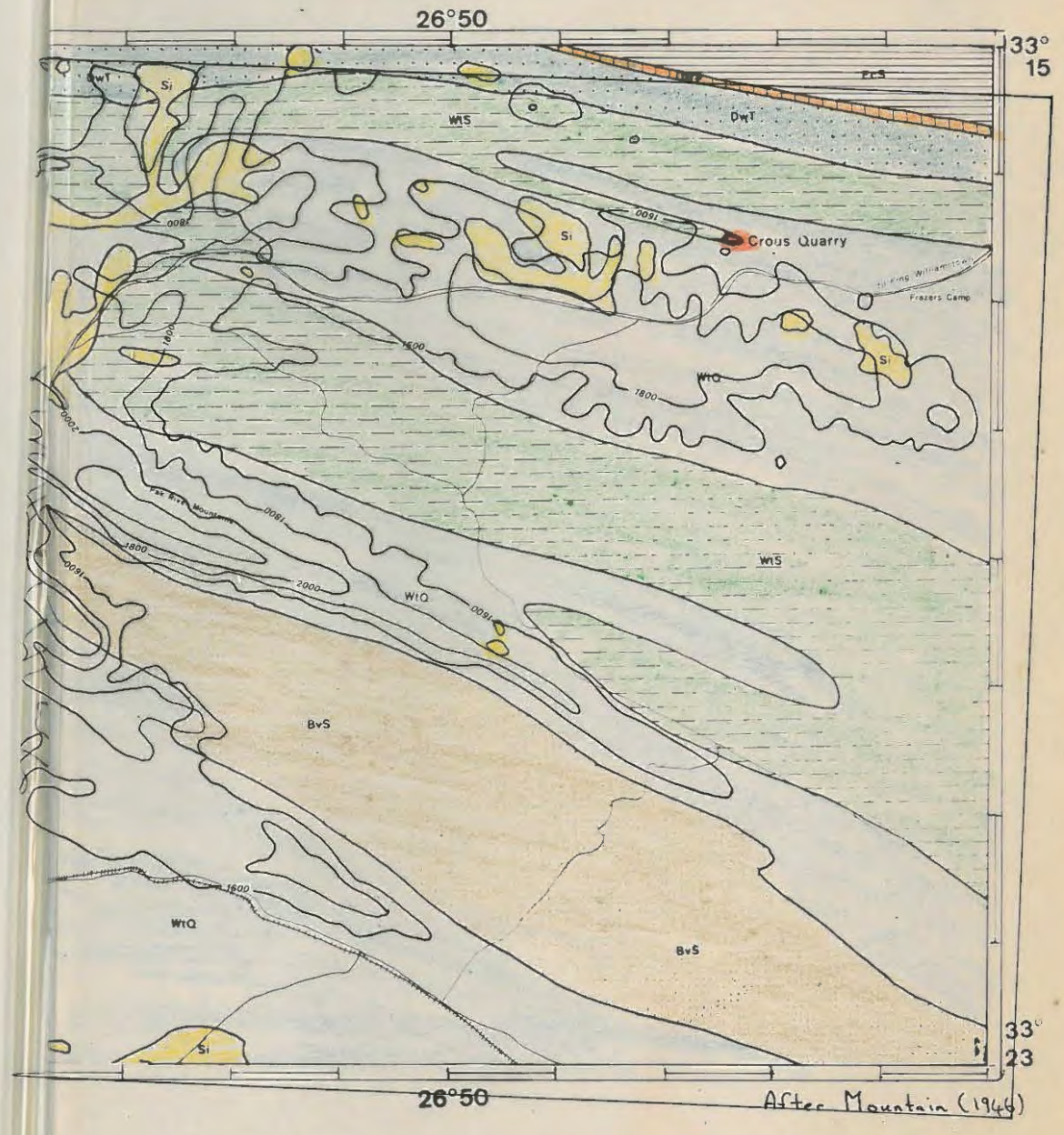

After Mountain (1968)